CONRAD - A Combined Hydrodynamics-Condensation/Vaporization Computer Code

R.R. Peterson, J.J. MacFarlane, G.A. Moses

January 1986
(revised July 1988)

UWFDM-670

FUSION TECHNOLOGY INSTITUTE

UNIVERSITY OF WISCONSIN

MADISON WISCONSIN

CONRAD - A Combined Hydrodynamics-Condensation/Vaporization Computer Code

R.R. Peterson, J.J. MacFarlane, G.A. Moses

Fusion Technology Institute
University of Wisconsin
1500 Engineering Drive
Madison, WI 53706

http://fti.neep.wisc.edu

CONRAD - A COMBINED HYDRODYNAMICS-CONDENSATION/VAPORIZATION

COMPUTER CODE

Robert R. Peterson

Joseph J. MacFarlane

Gregory A. Moses

Fusion Technology Institute
Nuclear Engineering and Engineering Physics Department
1500 Johnson Drive
University of Wisconsin-Madison
Madison, Wisconsin 53706

(Revised July 1988)

TABLE OF CONTENTS

1. INTRODUCTION

The behavior of gases under intense heating by x-rays and ions is a topic of interest to several areas of applied physics. A system of computer codes has been under development at the University of Wisconsin for a number of years that simulates the behavior of gases under such conditions. The main application of these codes has been to study the gases in Inertial Confinement Fusion (ICF) target chambers. The earlier codes, FIRE [1,2] and MF-FIRE [3], addressed the absorption of x-rays and ions in a single species gas and the subsequent hydrodynamic motion and radiant heat transfer. The CONRAD code is the latest in this series and has several new capabilities. The most important of these capabilities is the ability to model the transfer of the heat, momentum, and mass between the central gas and a surrounding condensed region. The condensate can be vaporized by the x-ray and thermal radiation from the cavity, and later recondense back onto the chamber wall. Mass transfer is an important feature for ICF because the condensation of vaporized material may limit the repetition rate of the target chamber. Another addition to CONRAD is the ability to have two regions in the gas with different species, something that has allowed the study of novel target chamber designs [4].

The FIRE code [1,2] was developed to simulate the response of a gas to the x-rays and ionic debris emanating from an exploding inertial confinement fusion target. The code computes target x-ray attenuation and ion slowing down in gases. It also computes the gas response using a one-dimensional plasma-hydrodynamics model with the major energy transfer mechanism being radiative transfer. This radiative transfer can be modeled in three different ways. The first is a two temperature (2-T) approximation where the plasma and radiation are characterized by their own unique temperatures, $T_p(r,t)$ and

1

$T_R(r,t)$. The radiation temperature is treated as a "color temperature" for purposes of the opacity determination, and is not necessarily related to the fourth root of the radiation energy density [2]. The radiation energy density is the quantity that is actually transported. The second method is similar to the first but in this case the temperature is assumed to be the fourth root of the energy density. The third option of treating the radiation in a multi-frequency group approximation has been added in the MF-FIRE code [3], the latest version of FIRE.

This document describes the physical models and assumptions and the numerical techniques that have been used in CONRAD. The design of the code, which is modular, is discussed, including descriptions of each subroutine and common block variable. Tables of input variables, along with default values, are presented and sample calculations are provided.

2. GENERAL APPROACH

CONRAD simulates the energy deposition within an ICF target chamber, the growth and radiative emission from the microfireball, the vaporization and hydromotion of the first wall material, and the recondensation of that material back onto the wall. The chamber environment is divided into three regions consisting of two materials: 2 non-mixing vapor regions consisting of non-condensable and condensable materials, and a condensed (solid or liquid) region. Before the target explodes, the cavity is filled with a non-condensable gas that is surrounded by a thin condensed layer. The condensed region vaporizes as it absorbs energy from target x-rays, radiation from the microfireball, and debris ions.

Two vaporization models are used in CONRAD. In one model, Lagrangian cells of the condensed region undergo hydrodynamic motion as they are vaporized, and move toward the center of the cavity. No mass is exchanged between mass cells. Energy is transported from the vapor/condensate interface to the back of the condensed region by conduction. As the radiant emission from the microfireball subsides and the temperature at the vapor/condensate interface decreases, material recondenses back onto the chamber wall. In the second model, mass and energy from the condensed region are transferred to the Lagrangian vapor cells already in the cavity. Periodically, a rezoning procedure is used to redistribute mass and energy within the cavity. These models are described in detail in Section 5.

3. TARGET ENERGY DEPOSITION

3.1 X-Ray Deposition

CONRAD assumes exponential x-ray attenuation, which should be adequate for most target x-ray spectra [5]. As the code is presently written, gases composed of only one element can be used to attenuate the x-rays. A table of attenuation coefficients for elements with atomic numbers ranging from 1 to 100 and x-ray energies ranging from 0.01 to 1000 keV are provided with the CONRAD code [6].

The initial x-rays that are photo-absorbed by the gas reduce the number of bound electrons available to interact with subsequent x-rays, so the attenuation coefficient decreases as x-rays are deposited. A method of modifying the photoelectric attenuation coefficient of the gas to account for increasing ionization has been developed for the CONRAD code [5]. By counting the number of electrons ejected from each electron shell as the x-rays are

3

deposited, the contribution to the photoelectric attenuation coefficient from each shell can be reduced by an amount proportional to the number of missing electrons. Additionally, the number of electrons lost due to the initial gas temperature is included even though this effect is usually very small. Although simple, this model does at least give the correct attenuation for the limiting cases of a completely neutral and completely ionized atom. The accuracy of this model at intermediate levels of ionization has not been determined. In this version of the code, the model for computing the reduction in photoelectric absorption can only be used with neon, argon, xenon, lithium, carbon, beryllium, oxygen, silicon, helium or nitrogen gas. To extend the model to other gases, the number of electrons in each shell of the neutral atom and the energies of the K, L, and M shells must be added to the EDATA subroutine.

The x-rays emitted by the target can be assumed to be Planckian or an inputted multigroup spectrum. In either case, the code divides the x-ray spectrum into energy groups. The x-rays in each group are then attenuated as if they were monoenergetic.

This code is written to treat the incident x-rays as either an instantaneous or time-dependent source. In both cases, the x-rays are treated as having an infinite propagation speed.

3.2 Ion Deposition

Target debris ions transfer energy and momentum to the background gas by collisions. Debris ions exploding from the target into the background plasma are highly ionized and have a velocity much greater than the thermal velocity of the background plasma. The mean ionization of the debris ions decreases as they undergo ion-electron, ion-neutral, and ion-ion collisions until they

4

eventually reach a state of equilibrium with the surrounding plasma. The rate at which ions transfer their momentum and energy to the background is calculated by the stopping power expression:

$$S = \frac{1}{N_{bg}} \left[\left(\frac{dE}{dx}\right)_{fe} + \left(\frac{dE}{dx}\right)_{be} + \left(\frac{dE}{dx}\right)_{nucl} \right] \qquad (3.1)$$

where $\left(\frac{dE}{dx}\right)$ is the kinetic energy lost by a debris ion as it traverses a distance dx through a background medium of density N_{bg}. The 3 terms on the right hand side of Eq. (3.1) represent (from left to right) the contributions from collisions with free electrons, bound electrons, and nuclei of the background plasma.

The free electron contribution to the stopping power is given by [7]:

$$\left(\frac{dE}{dx}\right)_{fe} = \left(\frac{\omega_p q_1 e}{v_1}\right)^2 G(y^2) \, \ln \Lambda_{fe} \qquad (3.2)$$

where

$$G(y^2) = erf(y) - \frac{2}{\sqrt{\pi}} e^{-y^2}$$

and

$$\omega_p = \left(\frac{4\pi e^2 n_e}{m_e}\right)^{1/2}$$

is the plasma frequency. y is the ratio of the debris ion velocity v_1 to the mean electron velocity, $<v_e>$, $erf(y)$ is the error function. q_1 is the debris ion charge state, e is the electron charge, n_e is the electron density, and m_e

5

is the electron mass. The Coulomb logarithm is given by

$$\Lambda_{fe} = (0.764 \, v_1)/(\omega_p b_{min})$$

where

$$b_{min} = a_0 \max\left[q_1\left(\frac{v_1}{v_0}\right)^2, \frac{v_1}{2v_0}\right]$$

a_0 is the Bohr radius, and v_0 is the Bohr velocity (= 2.2×10^8 cm/s). At high temperatures, the background plasma is highly ionized and the stopping power is dominated by the free electron term. Under these conditions, the stopping power is proportional to q_1^2.

Inelastic scattering with bound electrons and elastic nuclear scattering are important at low temperatures. The nuclear contribution can be written as [7]:

$$\left(\frac{dE}{dx}\right)_{nucl} = C_1 \epsilon^{1/2} \exp\{-45.2(C_2\epsilon)^{0.277}\} \tag{3.3}$$

where

$$\epsilon = E/A_1 \,(\text{MeV/amu})$$

$$C_1 = (4.14 \times 10^6 \text{MeV cm}^2\text{g}^{-1}) \frac{\rho_2}{A_2^2} \left(\frac{A_1 A_2}{A_1 + A_2}\right)^{3/2} \left(\frac{(Z_1 Z_2)^{1/2}}{Z_1^{2/3} + Z_2^{2/3}}\right)^{3/4}$$

and

$$C_2 = \left(\frac{A_1 A_2}{A_1 + A_2}\right)(Z_1 Z_2)^{-1}(Z_1^{2/3} + Z_2^{2/3})^{-1/2}$$

6

The subscripts 1 and 2 refer to the debris ion and background plasma, respectively. A, Z, and ρ represent the atomic weight, atomic number, and mass density, respectively.

The bound electron contribution is calculated using one of two theories, depending on the debris ion velocity. Lindhard-Scharff theory [8] is valid when the debris ion velocity is small compared to the orbital velocity of the bound electrons. In this case, the bound electrons are treated as a "cloud", as opposed to point charges. The expression for the Lindhard-Scharff stopping power is:

$$\left(\frac{dE}{dx}\right)_{LS} = (3.84 \times 10^{-18} \text{ keV cm}^{-1})N_2 \frac{Z_1^{7/6}Z_2^*}{[Z_1^{2/3} + (Z_2^*)^{2/3}]^{3/2}} \left(\frac{E_1}{A_1}\right)^{1/2} \qquad (3.4)$$

where E_1 is the debris ion kinetic energy in keV, and Z_2^* is the average number of bound electrons per nucleus. At low velocities, the rate at which the debris ions lose their energy is proportional to their velocity. When the debris ion velocities are large compared to the electron orbital velocities, the bound electrons can be treated as point charges, and Bethe theory is used to determine the debris ion energy loss rate. The expression for the Bethe stopping power is [7]:

$$\left(\frac{dE}{dx}\right)_{Bethe} = \left(\frac{\omega_p q_1 e}{v_1}\right)^2 \left[\ell n\left[\frac{2m_e v_1^2}{<\Phi_2>(1-v_1^2/c^2)}\right] - \left(\frac{v_1}{c}\right)^2\right] \qquad (3.5)$$

where $<\Phi_2>$ is the average ionization potential of the background plasma. To ensure a smooth transition between the 2 models, we interpolate to get the total bound electron stopping power:

7

$$\left(\frac{dE}{dx}\right)_{be} = \begin{cases} \left(\frac{dE}{dx}\right)_{LS} & v_1 < v_L \\[2ex] (1-f)\left(\frac{dE}{dx}\right)_{LS} + f\left(\frac{dE}{dx}\right)_{Bethe}, & v_L \leq v_1 \leq v_B \\[2ex] \left(\frac{dE}{dx}\right)_{Bethe} & v_1 > v_B \end{cases} \qquad (3.6)$$

where $v_L = Z_1^{2/3} v_o$ and $v_B = 3 Z_1^{2/3} v_o$ and $f = (v_1 - v_L)/(v_B - v_L)$.

When the stopping ranges are comparable to or larger than the dimensions of interest (e.g., the fireball), the time-dependence of the debris ions' charge states must be computed to accurately determine the energy deposition. In CONRAD, we consider the following reactions in calculating the rate of change in the mean ionization: collisional ionization and recombination, radiative recombination, and recombination due to charge exchange with the background plasma. The debris ion ionization populations are computed by solving the coupled set of rate equations:

$$\frac{dN_q}{dt} = = N_{q-1} n_e C_{q-1} + N_{q+1} \left(n_e^2 \alpha_{q+1}^{coll} + n_e \alpha_{q+1}^{rad} + N_{bg} v_1 \sigma_{cx,q+1}\right) \qquad (3.7)$$

$$- N_q \left(n_e C_q + n_e^2 \alpha_q^{coll} + n_e \alpha_q^{rad} + N_{bg} v_1 \sigma_{cx,q}\right)$$

where N_q is the number of ions in the qth ionization state, N_{bg} is the background plasma number density, and $\sigma_{cx,q}$ is the charge exchange cross section. C_q α_q^{coll}, and α^{rad} represent the collisional ionization, collisional recombination, and radiative recombination rate coefficients, respectively. Expressions for these quantities are given in Reference [9]. Eq. (3.7)

8

neglects charge exchange reactions in which the debris ions increase with charge. To properly include these reactions, CONRAD would have to also track the time-dependence of the background plasma ionization populations; something it is not currently set up to do. This can cause the debris ion charge states to fall to anomalously low values. This will be discussed in more detail below.

To calculate the charge exchange reaction rates, we use the classical cross sections given by Knudson et.al. [10]:

$$
\sigma_q = \pi a_0^2 q_1
\begin{cases}
\frac{1}{2} Z_2^{2/3} \left[\left(\frac{\alpha v_a}{v_0}\right)^{-2} - (\beta Z_2)^{-2} \right], & v_1 < \alpha v_a \\[2em]
\frac{8}{3} \xi^{-7} \left[\left(\frac{Z_2^{2/3}}{8} \xi^7\right)^{3/5} - \left(\frac{\alpha v_a}{v_0}\right)^3 \right] \\[1em]
\quad + \frac{1}{2} Z_2^{2/3} \left[\left(\frac{Z_2^{2/3}}{8} \xi^7\right)^{-2/5} - (\beta Z_2)^{-2} \right], & \alpha v_a < v_1 < \beta Z_2 v_0 \\[2em]
\frac{8}{3} \xi^{-7} \left[(\beta Z_2)^3 - \left(\frac{\alpha v_a}{v_0}\right)^3 \right], & v_1 > \beta Z_2 v_0
\end{cases}
\tag{3.8}
$$

where $\xi = q_1^{-2/7}(v_1/v_0)$, $v_a = v_0(<\Phi_2>/13.6 \text{ eV})^{1/2}$, $\beta Z_2 = Z_2^{2/3} + \alpha v_a/v_0$, and α is an adjustable parameter.

Values for α were found by fitting Eq. (3.8) to experimental data for ion-neutral charge exchange reactions [10]. The selected values for α are: 0.25 for H, 0.40 for He, 0.46 for Ar, and 0.54 for Xe. Values for other atoms are obtained by simple interpolation. The agreement between the calculated and experimental cross sections is reasonably good, suggesting the scaling laws used by Knudson et al. are reliable for a wide range of projectile ions.

When the background plasma is ionized, the charge exchange cross sections decrease dramatically when the debris ion kinetic energy is not large enough to overcome the Coulomb repulsion energy. To model this effect, we use a low velocity cutoff for the cross sections of ion-ion charge exchange reactions that is based on the results of calculations by Hyman et al. [11]. The cutoff velocity is given by:

$$v_{crit} = 6 \times 10^5 \text{ cm/s } q^{2/7} (\Phi_2/13.6) \tag{3.9}$$

When the background plasma is ionized and the debris ion velocity is less than the cutoff velocity, the charge exchange cross section is zero in CONRAD; otherwise, the Knudson values are used.

4. GAS DYNAMICS HYDRODYNAMIC MOTION

4.1 Hydrodynamic Motion

The equations solved by the CONRAD code for the central gas region are written in the Lagrangian coordinate system, i.e. the equations describe a point that moves with the local fluid velocity. The advantage of this coordinate system is that the mass flux is zero, so the conservation equations are simplified considerably. The code can automatically choose a suitable Lagrangian mesh from the vessel geometry and dimensions input by the user if desired. Either planar, cylindrical, or spherical coordinates can be assumed. The units used by the CONRAD code are

length - cm

time - second

mass - gram

speed - cm/s

energy- Joule

temperature - eV

pressure   - J/cm^3 = MPa

charge - esu

Figure 4.1 illustrates the index system used to denote spatial boundaries. The Lagrangian mass of each zone, $m_{0_{j-1/2}}$, is defined by integrating

$$dm_0 = \rho(r) \, r^{\delta-1} \, dr \qquad (4.1)$$

from boundary j to j+1, where ρ is the mass density and r is the spatial coordinate. The symbol δ denotes planar ($\delta=1$), cylindrical ($\delta=2$), or spherical coordinates ($\delta=3$). The Lagrangian mass is a constant for each zone, so it is a convenient replacement for the product $\rho(r)r^{\delta-1}dr$ when writing the conservation equations in finite difference form. The average Lagrangian mass of two zones, m_{0_j}, will appear in the finite difference form of the equation of motion, and is defined as

$$m_{0_j} = \frac{\left(m_{0_{j+1/2}} + m_{0_{j-1/2}}\right)}{2} . \qquad (4.2)$$

and

11
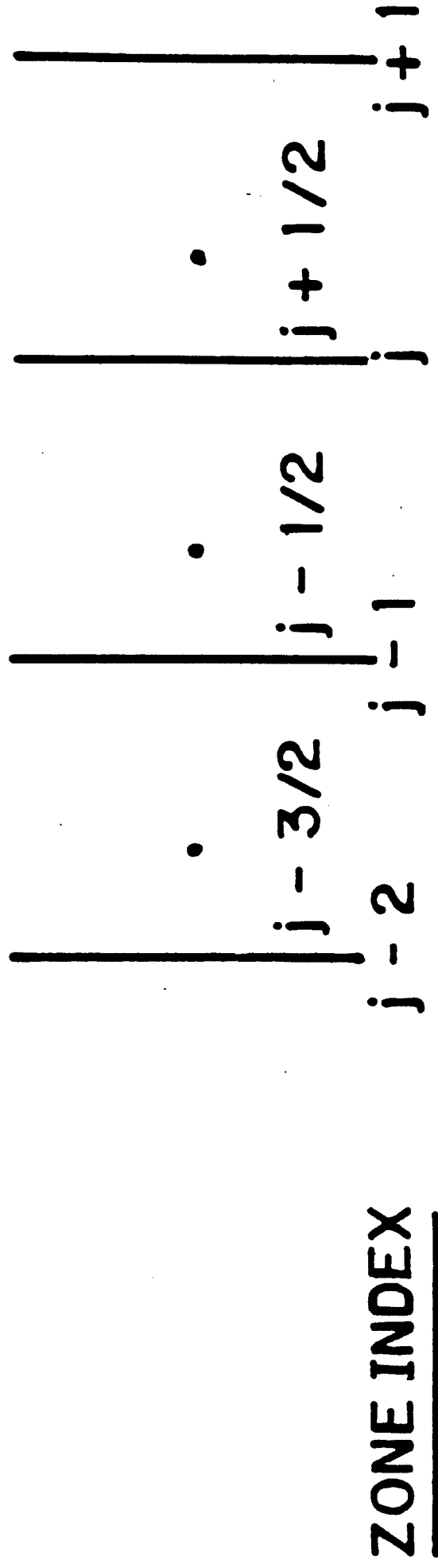
Figure 4.1. Index system for spatial zones in central region.

$$\Delta m_{o_j} = m_{o_{j+1/2}} - m_{o_{j-1/2}} \quad .$$

In Lagrangian coordinates, the equation of motion is

$$\frac{\partial u}{\partial t} = -V \frac{\partial}{\partial r} (P + q) - \frac{V}{V_d} \frac{\partial u_{dr}}{\partial t} \quad , \tag{4.3}$$

where: V is the specific volume of the gas,

V_d is the specific volume of the debris,

u is the radial velocity of the gas,

u_{dr} is the radial velocity of the debris,

P is the sum of the gas and radiation pressure,

q is the artificial viscosity [12],

and where it has been assumed that $V_d \gg V$. The explicit, finite difference form of Eq. (4.3) that is solved by the CONRAD code is

$$\frac{u_j^{n+1/2} - u_j^{n-1/2}}{\Delta t^n} = - \frac{(r_j^n)^{\delta-1} [\Delta P_j^n + \Delta q_j^{n-1/2}]}{\Delta m_{o_j}} + \frac{1}{G \Delta m_{o_j}} \frac{\Delta MOM_j^n}{\Delta t^n} \quad , \tag{4.4}$$

where: $G = 1$ for $\delta=1$ (planar coordinates),

$G = 2\pi$ for $\delta=2$ (cylindrical coordinates),

$G = 4\pi$ for $\delta=3$ (spherical coordinates),

and ΔMOM_j^n is the momentum lost by the debris during Δt^n. The superscript n is the time index. The terms in brackets are defined as

$$\Delta P_j^n = P_{j+1/2}^n - P_{j-1/2}^n \quad \text{and} \quad \Delta q_j^{n-1/2} = q_{j+1/2}^{n-1/2} - q_{j-1/2}^{n-1/2} \quad . \tag{4.5}$$

13

The artificial viscosity is a function of the zone specific volume, so to make Eq. (4.4) explicit, Δq_j is evaluated at $t^{n-1/2}$. The artificial viscosity used is

$$q_{j-1/2}^{n-1/2} = 0 \qquad \qquad \text{for } \dot{V}_{j-1/2}^{n-1/2} > 0 \ ,$$

$$= \frac{\sqrt{2} \ (u_j^{n-1/2} - u_{j-1}^{n-1/2})}{V_{j-1/2}^{n-1/2}} \qquad \text{for } \dot{V}_{j-1/2}^{n-1/2} < 0 \ . \qquad (4.6)$$

The quantity $\dot{V}$ is the time rate of change of the specific volume.

The gas pressure, P_P, is computed from the perfect gas law,

$$P_{P_{j\pm1/2}}^n = 1.602 \times 10^{-19} \ (1 + Z_{j\pm1/2}^n) \ast n_{P_{j\pm1/2}}^n \ast T_{P_{j\pm1/2}}^n \ , \qquad (4.7)$$

where: Z is the charge state of the gas,

n_P is the number density of gas atoms,

T_P is the gas temperature.

The radiation pressure, P_R, is computed from the radiation energy density, E_R, by

$$P_{R_{j\pm1/2}}^n = \frac{1}{3} \ (E_R)_{j\pm1/2}^n \ , \qquad (4.8)$$

where the radiation energy density has been assumed to be isotropic. Although in some instances the radiation field may not be isotropic, the radiation pressure is very small compared to the gas pressure for the temperature and densities of interest here, so the assumption of an isotropic radiation field does not affect the gas motion.

After solving Eq. (4.4) for $u_j^{n+1/2}$, the new radii are computed from

$$r_j^{n+1} = r_j^n + u_j^{n+1/2} \Delta t^{n+1/2} \quad . \tag{4.9}$$

New specific volumes and other quantities are then computed in preparation for the next time step.

To evaluate the momentum imparted by the target debris, CONRAD computes the rate of energy loss by the debris ions using the stopping power model described in Section 3.2. The debris ions can consist of up to 4 elements, and the initial energy and flux distributions are input in histogram form. The maximum number of ion groups (i.e., the number of elements times the number of energy groups times the number of time bins) is 4000. The total momentum deposited in a gas zone is the sum of the contributions from each ion group. In finite difference form, the momentum imparted by the debris ions is:

$$\Delta MOM_j^n = \sum_{k(j)} \Delta m_{d,k}^n (u_{dr,k}^{n+1/2} - u_{dr,k}^{n-1/2})$$

where $\Delta m_{d,k}^n$ is the debris mass in the kth ion group, and the quantities $u_{dr,k}^{n+1/2}$ are the radial velocities of the kth group before and after the time step, Δt_n. The summation is over all groups in the jth zone. The speed and position of each ion group are updated using the stopping rate, (dE_k/dr).

4.2 Energy Transfer in Vapor

4.2.1 Two-Temperature Option

Because of the high temperatures encountered in the gas (up to hundreds of eV), thermal radiation can be the dominant energy transport mechanism. The CONRAD code uses flux limited diffusion to model radiation transport. The

absorption and emission of thermal radiation are strongly temperature dependent, so the radiation diffusion equation is solved simultaneously with the plasma temperature equation. The equations solved by the CONRAD code are

$$C_v \frac{\partial T_P}{\partial t} = \frac{\partial}{\partial m_0} \left(r^{\delta-1} K_P \frac{\partial T_P}{\partial r} \right) - P_P \dot{V} - \left(\frac{\partial E_P}{\partial V} \right)_T \dot{V} - q\dot{V} + \omega_R E_R - \omega_P T_P + S \quad (4.10\text{-}a)$$

$$V \frac{\partial E_R}{\partial t} = \frac{\partial}{\partial m_0} \left(r^{\delta-1} K_R \frac{\partial E_R}{\partial r} \right) - \frac{4}{3} E_R \dot{V} \qquad - \omega_R E_R + \omega_P T_P \quad (4.10\text{-}b)$$

where: C_v is the specific heat at constant volume,

K_P is the gas thermal conductivity,

K_R is the radiation thermal conductivity,

ω_R is the radiation absorption coefficient,

ω_P is the radiation emission coefficient,

S is the rate that internal energy is added by the debris.

To simplify the notation in the finite difference equations that follow, the time index of quantities evaluated at $t^{n+1/2}$ will be omitted. In fully implicit finite difference form, Eqs. (4.10-a) and (4.10-b) are

$$C_{v_{j-1/2}} \frac{T_{P_{j-1/2}}^{n+1} - T_{P_{j-1/2}}^{n}}{\Delta t^{n+1/2}} = \frac{1}{\Delta m_{0_{j-1/2}}} \left[\frac{r_j^{\delta-1}}{\left(\frac{\Delta r}{K_P} \right)_j} \left(T_{P_{j+1/2}}^{n+1} - T_{P_{j-1/2}}^{n+1} \right) \right.$$

$$\left. - \frac{r_{j-1}^{\delta-1}}{\left(\frac{\Delta r}{K_P} \right)_{j-1}} \left(T_{P_{j-1/2}}^{n+1} - T_{P_{j-3/2}}^{n+1} \right) \right] - \left[P_{P_{j-1/2}} + \left(\frac{\partial E_P}{\partial V} \right)_{T_{j-1/2}} \right] \dot{V}_{j-1/2} \quad (4.11\text{-}a)$$

$$- q_{j-1/2} \dot{V}_{j-1/2} + \omega_{R_{j-1/2}} E_{R_{j-1/2}}^{n+1} - \omega_{P_{j-1/2}} T_{P_{j-1/2}}^{n+1} + S_{j-1/2}^{n}$$

16

and

$$V^{n+1/2}_{j-1/2} \frac{E_{R_{j-1/2}}^{n+1} - E_{R_{j-1/2}}^n}{\Delta t^{n+1/2}} = \frac{1}{\Delta m_{o_{j-1/2}}} \left[\frac{r_j^{\delta-1}}{\left(\frac{\Delta r}{K_R}\right)_j + \frac{\Delta E_{R_j}}{F_{R_j}}} (E_{R_{j+1/2}}^{n+1} - E_{R_{j-1/2}}^{n+1}) \right.$$

$$\left. - \frac{r_{j-1}^{\delta-1}}{\left(\frac{\Delta r}{K_R}\right)_{j-1} + \frac{\Delta E_{R_{j-1}}}{F_{R_{j-1}}}} (E_{R_{j-1/2}}^{n+1} - E_{R_{j-3/2}}^{n+1}) \right] - E_{R_{j-1/2}}^{n+1} \frac{4}{3} \dot{V}_{n-1/2} \qquad (4.11\text{-b})$$

$$- \omega_{R_{j-1/2}} E_{R_{j-1/2}}^{n+1} + \omega_{P_{j-1/2}} T_{P_{j-1/2}}^{n+1} \quad .$$

The denominators of the terms in square brackets represent the resistance per unit area to thermal and radiative diffusion between zone centers. For instance,

$$\left(\frac{\Delta r}{K_P}\right)_j = \frac{1}{2} \left(\frac{r_{j+1} - r_j}{K_P^+} + \frac{r_j - r_{j-1}}{K_P^-} \right) \quad , \qquad (4.12)$$

and so on for $\left(\frac{\Delta r}{K_P}\right)_{j-1}$, $\left(\frac{\Delta r}{K_R}\right)_j$, and $\left(\frac{\Delta r}{K_R}\right)_{j-1}$. Equations (11-a) and (11-b) can be written in matrix form as

$$\underline{\underline{a}}_{j-1/2} (\underline{\theta}_{j-1/2}^{n+1} - \underline{\theta}_{j-1/2}^n) = \underline{\underline{a}}_j (\underline{\theta}_{j+1/2}^{n+1} - \underline{\theta}_{j-1/2}^{n+1}) - \underline{\underline{a}}_{j-1} (\underline{\theta}_{j-1/2}^{n+1} - \underline{\theta}_{j-3/2}^{n-1})$$

$$(4.13)$$

$$- \underline{\underline{\gamma}}_{j-1/2} \underline{\theta}_{j-1/2}^{n+1} - \underline{\underline{\omega}}_{j-1/2} \underline{\theta}_{j+1/2}^{n+1} + \underline{b}_{j-1/2}$$

17

where

$$\underline{\underline{\alpha}}_{j-1/2} = \begin{bmatrix} C_{v_{j-1/2}} & 0 \\ & \\ 0 & V_{j-1/2} \end{bmatrix} \frac{\Delta m_{o_{j-1/2}}}{\Delta t^{n-1/2}} \quad,$$

$$\underline{\underline{a}}_j = \begin{bmatrix} r_j^{\delta-1}/(\Delta r/K_P)_j & 0 \\ & \\ 0 & r_j^{\delta-1}/((\Delta r/K_R)_j + \Delta E_{R_j}/F_{R_j}) \end{bmatrix} \quad,$$

$$\underline{Y}_{j-1/2} = \begin{bmatrix} (\partial P_P/\partial T_P)_{j-1/2}\dot{V}_{j-1/2} & 0 \\ & \\ 0 & 4\dot{V}_{j-1/2}/3 \end{bmatrix} \Delta m_{o_{j-1/2}} \quad,$$

$$\underline{\underline{\omega}}_{j-1/2} = \begin{bmatrix} \omega_P & -\omega_R \\ & \\ -\omega_P & \omega_R \end{bmatrix}_{j-1/2} \Delta m_{o_{j-1/2}} \quad,$$

$$\underline{\beta}_{j-1/2} = \begin{bmatrix} -q_{j-1/2}\dot{V}_{j-1/2} + S_{j-1/2}^n \\ \\ 0 \end{bmatrix} \Delta m_{o_{j-1/2}} \quad,$$

and

$$\underline{\theta}_{j-1/2}^{n+1} = \begin{bmatrix} T_{P_{j-1/2}}^{n+1} \\ \\ E_{R_{j-1/2}}^{n+1} \end{bmatrix} \quad.$$

18

A more compact matrix equation can be written by redefining the coefficients as follows:

$$\underline{\underline{A}}_{j-1/2} = \underline{\underline{a}}_j \quad ,$$

$$\underline{\underline{B}}_{j-1/2} = \underline{\underline{\alpha}}_{j-1/2} + \underline{\underline{a}}_j + \underline{\underline{a}}_{j-1} + \underline{\underline{\gamma}}_{j-1/2} + \underline{\underline{\omega}}_{j-1/2} \quad ,$$

$$\underline{\underline{C}}_{j-1/2} = \underline{\underline{a}}_{j-1} \quad ,$$

$$\underline{D}_{j-1/2} = \underline{\underline{\alpha}}_{j-1/2} \underline{\theta}^n_{j-1/2} + \underline{\beta}_{j-1/2} \quad .$$

With these redefinitions, Eq. (4.13) becomes

$$-\underline{\underline{A}}_{j-1/2} \underline{\theta}^{n+1}_{j+1/2} + \underline{\underline{B}}_{j-1/2} \underline{\theta}^{n+1}_{j-1/2} - \underline{\underline{C}}_{j-1/2} \underline{\theta}^{n+1}_{j-3/2} = \underline{D}_{j-1/2} \quad . \tag{4.14}$$

If JMAX is the number of zone boundaries, then Eq. (4.14) represents a JMAX by JMAX tridiagonal matrix equation that has two by two matrices for elements. If the coefficients of Eq. (4.14) are evaluated at t^n, it can be solved by Gaussian elimination. Solutions can be shown to be of the form [13]

$$\underline{\theta}^{n+1}_{j-1/2} = \underline{\underline{E}}_{j-1/2} \underline{\theta}^{n+1}_{j+1/2} + \underline{F}_{j-1/2} \quad , \quad \text{for } 1 \leq j < JMAX$$

$$\tag{4.15}$$

$$\theta^{n+1}_{JMAX+1/2} = \text{BOUNDARY CONDITIONS} \quad , \quad \text{for } j = JMAX \quad .$$

The $\underline{\underline{E}}$ matrix and $\underline{F}$ vector can be related to known quantities by decreasing the spatial index of Eq. (4.15) by one, and substituted into Eq. (4.14). One

19

finds that

$$\underline{E}_j = (\underline{\underline{B}}_{j-1/2} - \underline{\underline{C}}_{j-1/2} * \underline{\underline{E}}_{j-3/2})^{-1} * \underline{A}_{j-1/2} \quad ,$$

and   (4.16)

$$\underline{F}_{j-1/2} = (\underline{\underline{B}}_{j-1/2} - \underline{\underline{C}}_{j-1/2} * \underline{\underline{E}}_{j-3/2})^{-1} * (\underline{D}_{j-1/2} + \underline{\underline{C}}_{j-1/2} * \underline{F}_{j-3/2})$$

for $1 \le j < JMAX$, and

$$\underline{\underline{E}}_{1/2} = (\underline{\underline{B}}_{1/2})^{-1} * \underline{\underline{A}}_{1/2} \quad ,$$

$$\underline{F}_{1/2} = (\underline{\underline{B}}_{1/2})^{-1} * \underline{D}_{1/2} \quad ,$$

for j=1. To solve Eq. (4.15), a sweep is made from the first zone out to the wall to evaluate $\underline{\underline{E}}$ and $\underline{F}$, and then back to the center to evaluate the components of the $\underline{\theta}^{n+1}$ vector.

The expression for the thermal conductivity of the plasma, κ_p, that is used in the CONRAD code is the theoretical expression developed for electrons' interaction with stationary ions [14]. The theoretical expression includes an experimentally determined constant to prevent κ_p from diverging as the average ionization state approaches zero. The expression is

$$\kappa_p = 20 \ (\frac{2}{\pi})^{3/2} \ \frac{T_p^{5/2}}{\sqrt{m_e} \ e^4 \ (Z + 4) \ \ln \Lambda} \quad ,$$ (4.17)

where: e   is the electron charge,

m_e is the electron mass,

$\ln \Lambda$ is the Coulomb logarithm.

To save computational effort, the Coulomb logarithm is computed from a curve fit that has an accuracy better than 10% for $\ln \Lambda$ greater than 5. In finite difference form, the thermal conductivities are

$$\kappa_{P_j}^{\pm} = \frac{1.22 \times 10^2 \, T_{P_j}^2 \, T_{P_{j\pm1/2}}^{1/2}}{(4 + Z_{j\pm1/2}) \, \ln \Lambda_{j\pm1/2}} \, , \qquad (4.18)$$

The T_P^2 terms are evaluated at the zone boundaries rather than the zone centers to enhance the numerical accuracy of the solution.

The expression for the radiation conductivity that is used in the 2-T option is a frequency averaged value. If the radiation mean free path is much smaller than the gradients in the radiation energy density, then the frequency dependent radiation flux, q_{R_ν}, is given by [15]

$$q_{R_\nu} = \frac{- \ell_\nu(T_p)c}{3} \frac{\partial E_{R_\nu}}{\partial r} \, , \qquad (4.19)$$

where: ℓ_ν is the frequency dependent radiation mean free path,

       E_{R_ν} is the frequency dependent radiation energy density,

       c   is the speed of light.

The frequency averaged conductivity is arrived at by integrating Eq. (4.19) over frequency. The frequency dependence of ℓ_ν is known from theoretical models of radiation absorption, but in general the frequency dependence of E_{R_ν} is not known prior to solving the frequency dependent radiation transport equations. For the 2-T radiation diffusion model used in the CONRAD code, there are two options for estimating E_{R_ν}. In the first option the frequency dependence of E_{R_ν} is assumed to be a dilute Planckian, that is

$$E_{R\nu} = \varepsilon V \frac{8\pi h\nu^3}{c^3} \frac{1}{\exp\left(\frac{h\nu}{T_R}\right) - 1} \quad , \tag{4.20}$$

where ε is a proportionality factor and T_R is the radiation temperature. The radiation temperature is defined so as to reflect the temperature of the gas that emitted the radiation occupying the point of interest. The radiation temperature at a point is evaluated by averaging the temperature of the transported radiation, the temperature of the emitted radiation, and the temperature of the radiation already present. In finite difference form, this average is

$$T_{R_{j+1/2}}^{n+1} = \frac{W_1 * T_{R_{j-1/2}}^{n+1/2} + W_2 * T_{R_{j+3/2}}^{n+1/2} + W_3 * T_{P_{j+1/2}}^{n+1/2} + W_4 * T_{R_{j+1/2}}^{n+1/2}}{W_1 + W_2 + W_3 + W_4} \quad 1 \leq j < \text{JMAX} \tag{4.21}$$

where the weighting functions are defined as

$$W_1 = \left(\frac{q_R r^{\delta-1} \Delta t}{\Delta m_0}\right)_{j-1/2}^{n+1/2} \qquad \text{if } q_{R_{j-1/2}} > 0$$
$$= 0 \qquad \text{if } q_{R_{j-1/2}} < 0 \tag{4.22}$$

$$W_2 = 0 \qquad \text{if } q_{R_{j+3/2}} > 0$$
$$= \left(\frac{q_R r^{\delta-1} \Delta t}{\Delta m_0}\right)_{j+3/2}^{n+1/2} \qquad \text{if } q_{R_{j+3/2}} < 0 \tag{4.23}$$

$$W_3 = (\omega_P T_P \Delta t)_{j+1/2}^{n+1/2} \tag{4.24}$$

$$W_4 = (E_R)_{j+1/2}^{n+1/2} \quad . \tag{4.25}$$

In the second option the radiation temperature is simply computed as

$$T_R = (\frac{E_R c}{4\sigma})^{1/4} \quad .$$

where σ is the Stefan-Boltzmann constant. The frequency averaged radiation flux across zone boundaries is represented by q_R in Eqs. (4.22) and (4.23), which after integrating Eq. (4.19) over frequency can be written as

$$q_R = - \frac{\ell(T_p, T_R) c}{3} \frac{\partial E_R}{\partial r} \quad , \tag{4.26}$$

where

$$\ell(T_p, T_R) = \frac{15}{4\pi^4} \int_0^\infty \ell_\nu(T_p) \frac{U^4 e^{-U}}{(1 - e^{-U})^2} \, dU \quad , \tag{4.27}$$

and

$$U(T_R) = \frac{h\nu}{T_R} \quad . \tag{4.28}$$

Equation (4.27) defines the Rosseland mean free path (including spontaneous emission [15]), and is a function of the plasma density, the local plasma temperature, and the local radiation temperature. From Eq. (4.26), the frequency averaged radiation conductivity can be written in finite difference form as

$$K_{R_j}^{\pm} = 10^{10} \, V_{j\pm1/2} \, / \, \sigma_{R_{j\pm1/2}} \tag{4.29}$$

where $\sigma_{R_{j\pm1/2}}$ is the Rosseland opacity (cm^2/g).

If the Rosseland mean free path is larger than the spatial zoning, then radiation may stream from zone to zone without being absorbed. In this case the diffusion model overestimates the radiation flux, and must be modified

with a flux limiter. This flux limiter has been included in Eq. (4.11-b) where it is referred to as F_{R_j} and $F_{R_{j+1}}$. The maximum radiation flux, cE_R, occurs when the radiation intensity of free streaming radiation approaches complete anisotropy. If the radiation intensity is completely isotropic, then the flux limit is $cE_R/4$. This latter expression is used in the CONRAD code. In finite difference form, the flux limit is

$$F_j = 3.75 \times 10^9 \left[(E_R)_{j+1/2}^{n+1/2} + (E_R)_{j-1/2}^{n+1/2} \right] \qquad 1 \leq j < JMAX$$

$$\tag{4.30}$$

$$F_{JMAX} = 7.5 \times 10^9 (E_R)_{JMAX+1/2}^{n+1/2} \qquad j = JMAX \ .$$

The expression for the absorption coefficient used in the CONRAD code can be obtained by integrating the frequency dependent absorption rate over frequency. From the definition of the radiation opacity, the frequency dependent absorption rate is

$$\omega_{R\nu} E_{R\nu} = cE_{R\nu} \sigma_{P\nu}^A (T_P) \ . \tag{4.31}$$

Using Eq. (4.20) to integrate Eq. (4.31) over frequency results in (including spontaneous emission)

$$\omega_R E_R = cE_R \sigma_P^A (T_R, T_P) \tag{4.32}$$

where

$$\rho \sigma_P^A (T_P, T_R) = \frac{15}{\pi^4} \int_0^\infty \frac{\kappa_\nu (T_P) U^3 (T_R) \ dU}{(e^{U(T_R)} - 1)} \ , \tag{4.33}$$

and

$$U(T_R) = \frac{h\nu}{T_R} \ . \tag{4.34}$$

where κ_ν is the absorption coefficient [16], and σ_P^A is the Planck absorption opacity. Equation (4.33) defines the nonequilibrium Planck opacity, which is the inverse of the frequency averaged distance that radiation with a temperature T_R will travel in a plasma at temperature T_P before being absorbed. The finite difference form of the absorption coefficient is

$$\omega_{R_{j-1/2}}^{n+1/2} = 3 \times 10^{10} \; \sigma_P^A(T_R, T_P)_{j-1/2}^{n+1/2} \quad . \tag{4.35}$$

The frequency dependent emission rate can be written as

$$\omega_{P_\nu} T_P = 4\pi V \eta_\nu(T_P) \tag{4.36}$$

where η_ν is the emissivity [16]. Averaging Eq. (4.42) over frequency yields

$$\omega_P T_P = 4\sigma T_P^4 \; \sigma_P^E(T_P) \quad , \tag{4.37}$$

where

$$\rho \sigma_P^E(T_P) = \frac{15}{\pi^4} \int_0^\infty \frac{\eta_\nu(T_P) U^3(T_P) \; dU}{B_\nu(T_P)(e^{U(T_P)} - 1)} \quad , \tag{4.38}$$

and

$$U(T_P) = \frac{h\nu}{T_P} \quad . \tag{4.39}$$

where $B_\nu(T_P)$ is the Planck function. Equation (4.37) defines the equilibrium Planck emission opacity σ_P^E. The finite difference form of the emission rate is

$$\omega_{P_{j-1/2}}^{n+1/2} = 4.12 \times 10^5 \; [T_P^3 \; \sigma_P^E(T_P)]_{j-1/2}^{n+1/2} \quad . \tag{4.40}$$

An expression for the internal energy deposition rate from target debris can be arrived at by equating the decrease in debris kinetic energy to the increase in the kinetic and internal energy of the gas:

$$- \frac{1}{V_d} u_d \frac{\partial u_d}{\partial t} = \frac{S}{V} + \frac{u}{V} \left(\frac{\partial u}{\partial t}\right)_{P=0} \quad , \qquad (4.41)$$

where u_d is the speed of the debris ions, and the quantity in parenthesis is the acceleration of the gas in the radial direction due to the debris alone, that is, excluding the pressure forces. From conservation of debris momentum it is clear that

$$\frac{1}{V} \left(\frac{\partial u}{\partial t}\right)_{P=0} = - \frac{1}{V_d} \frac{\partial u_{dr}}{\partial t} \quad . \qquad (4.42)$$

Note that $u_{dr} < u_d$ if the trajectory of the debris ions is not straight as they slow down in the plasma (such as when the ions scatter off the plasma nuclei). Combining Eqs. (4.41) and (4.42) and solving for the internal energy source term gives

$$S = - \frac{V}{V_d} u_d \frac{\partial u_d}{\partial t} + \frac{V}{V_d} u \frac{\partial u_{dr}}{\partial t} \quad . \qquad (4.43)$$

In finite difference form, Eq. (4.49) is

$$S_{j-1/2}^n = - \frac{\Delta m_{d_{j-1/2}}}{\Delta m_{o_{j-1/2}}} \frac{\Delta KE_{d_{j-1/2}}^n}{\Delta t^{n-1/2}} + \frac{u_d^{n+1/2}}{\Delta m_{o_{j-1/2}}} \frac{\Delta MOM_{j-1/2}^n}{\Delta t^{n+1/2}} \quad , \qquad (4.44)$$

where ΔKE_d is the change in debris kinetic energy during Δt^n. The change in

debris kinetic energy, the change in debris momentum, and the debris mass are calculated using the stopping power model described in Section 3.2.

4.2.2 Multifrequency Option

In the multifrequency option we have rewritten Eqs. (4.10-a) and (4.10-b) as

$$C_v \frac{\partial T_P}{\partial t} = \frac{\partial}{\partial m_o} (r^{\delta-1} K_P \frac{\partial T_P}{\partial r}) - P_P \dot{V} - (\frac{\partial E_P}{\partial V})_T \dot{V} - \dot{q}V + A - J + S \qquad (4.45\text{-}a)$$

$$V \frac{\partial E_R^g}{\partial t} = \frac{\partial}{\partial m_o} (r^{\delta-1} K_R^g \frac{\partial E_R^g}{\partial r}) - \frac{4}{3} E_R^g \dot{V} - c\sigma_{P,A}^g E_R^g + J^g \qquad g = 1,\ldots,G \qquad (4.45\text{-}b)$$

where: C_v is the specific heat at constant volume,

E_P is the plasma internal energy

K_P is the plasma thermal conductivity,

K_R^g is the radiation conductivity for frequency group g,

J^g is the rate of radiation emitted by the plasma into group g,

S is the rate of internal energy added to the plasma by the debris,

$$E_R^g = \int_{h\nu_g}^{h\nu_{g+1}} dh\nu \, E_R(r,h\nu,t) \qquad (4.46)$$

$$A^g = c\sigma_{P,A}^g E_R^g \qquad (4.47)$$

$$J^g = \frac{8\pi k T_P^4}{c^2 h^3} \sigma_{P,E}^g \int_{x_g}^{x_{g+1}} dx \frac{x^3}{e^x - 1} \quad ; \quad x = \frac{h\nu}{kT_P} \qquad (4.48)$$

$$K_R^g = \frac{cV}{3\sigma_R^g} \qquad (4.49)$$

$\sigma_{P,A}^g$ is the Planck absorption opacity for group g.

$\sigma_{P,E}^g$ is the Planck emission opacity for group g.

σ_R^g = Rosseland opacity for group g (cm^2/g)

$$A = \sum_{g=1}^{G} A^g \qquad (4.50)$$

$$J = \sum_{g=1}^{G} J^g \; . \qquad (4.51)$$

This set of G+1 equations is not solved simultaneously as in the 2-T model. Instead the multigroup equations are first solved individually and the terms A and J are computed. These terms are then explicitly included in the plasma temperature diffusion equation which is solved next. This different treatment of the multifrequency equations in no way affects the way that the 2-T method is solved in CONRAD. This leads to a very slight inefficiency in the number of subroutines but does not affect the execution time. The coding is kept very concise by doing this.

The multigroup equations are written in finite difference form as

$$\frac{E_R^{g,n+1} - E_R^{g,n}}{\Delta t^{n+1/2}} = \frac{1}{\Delta m_{o_{j-1/2}}} \left[\frac{r_j^{\delta-1}}{\left(\frac{\Delta r}{K_R^g}\right) + \left(\frac{\Delta E_R^g}{F_R^g}\right)_j} \left(E_{R_{j+1/2}}^{g,n+1} - E_{R_{j-1/2}}^{g,n+1}\right) \right.$$

$$\left. - \frac{r_{j-1}^{\delta-1}}{\left(\frac{\Delta r}{K_R^g}\right)_{j-1} + \left(\frac{\Delta E_R^g}{F_R^g}\right)_{j-1}} \left(E_{R_{j-1/2}}^{g,n+1} - E_{R_{j-3/2}}^{g,n+1}\right) \right] - E_{R_{j-1/2}}^{g,n+1} \frac{4}{3} \dot{V}_{n-1/2} \qquad (4.52)$$

$$- c\sigma_{P,A_{j-1/2}}^g E_R^{g,n+1} + J_R^{g,n+1}$$

28

for group g. This is reduced using the notation

$$\alpha_{j-1/2}(E_{R_{j-1/2}}^{g,n+1} - E_{R_{j-1/2}}^{g,n}) = a_j(E_{R_{j+1/2}}^{g,n+1} - E_{R_{j-1/2}}^{g,n+1}) - a_{j-1}(E_{R_{j-1/2}}^{g,n+1} - E_{R_{j-3/2}}^{g,n+1})$$

<div align="right">(4.53)</div>

$$- \gamma_{j-1/2}E_{R_{j-1/2}}^{g,n+1} - \omega_{j-1/2}E_{R_{j-1/2}}^{g,n+1} + \beta_{j-1/2}$$

where: $\alpha_{j-1/2} = V_{j-1/2} \, \Delta m_{0_{j-1/2}}/\Delta t^{n-1/2}$

$$a_j = r^{\delta-1}/((\Delta r/K_R^g)_j + \Delta E_{R_j}^g/F_{R_j}^g)$$

$$\gamma_{j-1/2} = (4 \, \dot{V}_{j-1/2}/3) \, \Delta m_{0_{j-1/2}}$$

$$\omega_{j-1/2} = C\sigma_{P,A_{j-1/2}}^g \, \Delta m_{0_{j-1/2}}$$

$$\beta_{j-1/2} = J_{j-1/2}^g \, \Delta m_{0_{j-1/2}} \quad .$$

The coefficients α, a, γ, ω, and β should be evaluated at $t^{n+1/2}$. However, values at that time are not yet known so they are evaluated at t^n. These terms are regrouped in the familiar form

$$-A_{j-1/2}E_{R_{j+1/2}}^{g,n+1} + B_{j-1/2}E_{R_{j-1/2}}^{g,n+1} - C_{j-1/2}E_{R_{j-3/2}}^{g,n+1} = D_{j-1/2} \qquad (4.54)$$

where: $A_{j-1/2} = a_j$

$B_{j-1/2} = \alpha_{j-1/2} + a_j + a_{j-1} + \gamma_{j-1/2} + \omega_{j-1/2}$

$C_{j-1/2} = a_{j-1}$

$D_{j-1/2} = \alpha_{j-1/2} E_{R_{j-1/2}}^{g,n} + \beta_{j-1/2}$.

We then express the solution as

$$E_{R_{j-1/2}}^{g,n+1} = EE_{j-1/2} * E_{R_{j+1/2}}^{g,n+1} + FF_{j-1/2} \qquad 1 \le j \le JMAX$$

(4.55)

$$E_{R_{JMAX+1/2}}^{n+1} = E_{R_{BC}} \qquad\qquad \text{Boundary Condition} \quad .$$

Then we can compute

$$EE_{j-1/2} = A_{j-1/2}/(B_{j-1/2} - C_{j-1/2} * EE_{j-3/2}) \qquad (4.56)$$

$$FF_{j-1/2} = (D_{j-1/2} + C_{j-1/2} * FF_{j-3/2})/(B_{j-1/2} - C_{j-1/2} * EE_{j-3/2}) \qquad (4.57)$$

for $2 < j \le JMAX$ and

$$EE_{1/2} = A_{1/2}/B_{1/2} \qquad (4.58)$$

$$FF_{1/2} = D_{1/2}/B_{1/2} \qquad (4.59)$$

for $j = 1$.

Once the radiation specific energies have been computed, then the absorption is computed as

$$A^g_{j-1/2} = c\sigma^g_{P,A_{j-1/2}} E^{g,n+1}_{R_{j-1/2}} \qquad (4.60)$$

$$A_{j-1/2} = \sum_{g=1}^{G} A^g_{j-1/2} \; . \qquad (4.61)$$

The source term in the plasma temperature equation is then computed as

$$\beta_{j-1/2} = \beta^{old}_{j-1/2} + (A - J)_{j-1/2} \Delta m_{o_{j-1/2}} \qquad (4.62)$$

where $\beta^{old}_{j-1/2}$ is the value computed in the 2-T description in part 4.2.1. The single plasma temperature equation is solved using the same standard implicit finite difference technique described for the 2-T and multifrequency diffusion equations.

4.3 Gas Equations of State and Opacity

The equation of state and opacities must be supplied in tabular form by the user of the CONRAD code. The quantities required are:

$Z(n_p, T_p)$	Charge State
$E_p(n_p, T_p)$	Specific Internal Energy
$C_v(n_p, T_p)$	Heat capacity
$(\partial E_p/\partial n_p)_T(-\rho/T^2)$	Scaled energy derivative wrt density
	(this equals $(\partial Z/\partial T)_V$ for an LTE plasma)

and either

31

$$\sigma_R(n_p, T_p, T_R) \qquad \text{2-T Rosseland Opacity}$$

$$\sigma_P^A(n_p, T_p, T_R) \qquad \text{2-T Planck Absorption Opacity}$$

$$\sigma_P^E(n_p, T_p, T_p) \qquad \text{2-T Planck Emission Opacity}$$

or

$$\sigma_R^g(n_p, T_p) \qquad \text{Multigroup Rosseland Opacity}$$

$$\sigma_{P,A}^g(n_p, T_p) \qquad \text{Multigroup Planck Absorption Opacity}$$

$$\sigma_{P,E}^g(n_p, T_p) \qquad \text{Multigroup Planck Emission Opacity}$$

These tables are generated for CONRAD by the IONMIX code [9]. Logarithmic interpolation is used to interpolate between points in the tables. For instance, the charge state is stored as log Z(log n_p, log T_p). In what follows, the indices associated with the dependent variables are

$$K - \log T_R \quad ,$$
$$L - \log T_p \quad ,$$
$$M - \log n_p \quad .$$

Points in the two-dimensional tables can be represented as a two-dimensional grid, as shown in Fig. 4.2. The indices with stars denote the location of a quantity located between points in the table, for instance log $Z(L^*, M^*)$. To compute the desired quantity we first interpolate along the M axis:

$$\log Z(L, M^*) = \log Z(L, M)$$

$$+ \frac{\log Z(L, M+1) - \log Z(L, M)}{\log n_p(M+1) - \log n_p(M)} \star (\log n_p - \log n_p(M)) \quad , \tag{4.63}$$

32
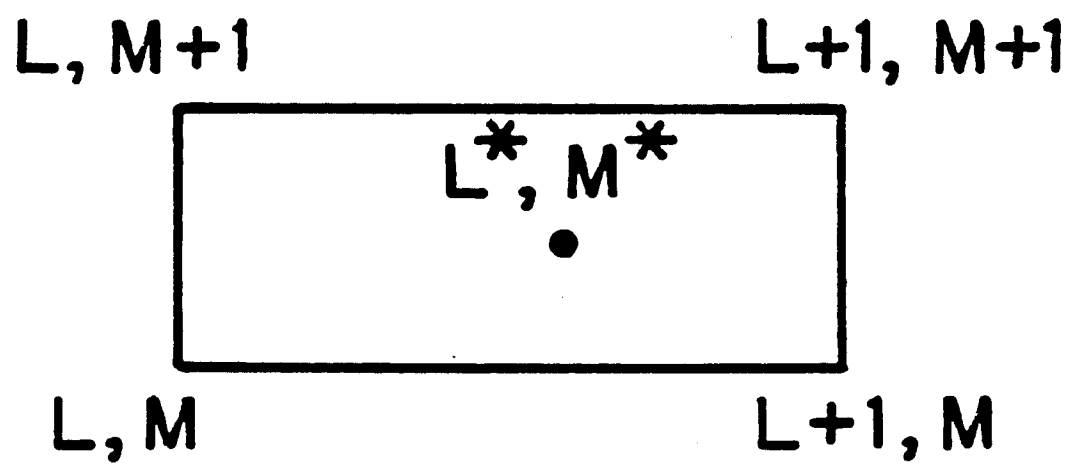
Figure 4.2. Interpolation grid in two-dimensional equation-of-state tables.

$$\log Z(L+1,M^*) = \log Z(L+1,M)$$

$$+ \frac{\log Z(L+1,M+1) - \log Z(L+1,M)}{\log n_p(M+1) - \log n_p(M)} * (\log n_p - \log n_p(M)) \ , \tag{4.64}$$

where n_p is the number density corresponding to $\log Z(L^*,M^*)$. Now interpolating along the L axis,

$$\log Z(L^*,M^*) = \log (L,M^*)$$

$$+ \frac{\log Z(L+1,M^*) - \log Z(L,M^*)}{\log T_p(L+1) - \log T_p(L)} * (\log T_p - \log T_p(L)) \ , \tag{4.65}$$

where T_p is the temperature corresponding to $\log Z(L^*,M^*)$.

The grids used to interpolate in the three-dimensional tables are shown in Fig. 4.3. First we interpolate for $\log \ell(M,K^*,L^*)$ and $\log \ell(M+1,K^*,L^*)$ in the manner prescribed above. Then interpolating in the third dimension,

$$\log \ell(M^*,K^*,L^*) = \log \ell(M,K^*,L^*)$$

$$+ \frac{\log \ell(M+1,K^*,L^*) - \log \ell(M,K^*,L^*)}{\log n_p(M+1) - \log n_p(M)} (\log n_p - \log n_p(M)) \ . \tag{4.66}$$

If the plasma temperature computed by solving the energy equations is less than the lowest temperature in the equation of state tables, then the code automatically computes Z and E_p by interpolating between the bounds of the table and the values for a perfect unionized gas. This procedure preserves the accuracy of the calculation at low temperatures. The number density, n_p, should never exceed the bounds of the tables, or inaccurate results will be obtained.

M PLANE

K,L+1   K+1,L+1

M,K*,L*
•

K,L   K+1,L

M+1 PLANE

K,L+1   K+1,L+1

M+1,K*,L*
•

K,L   K+1,L
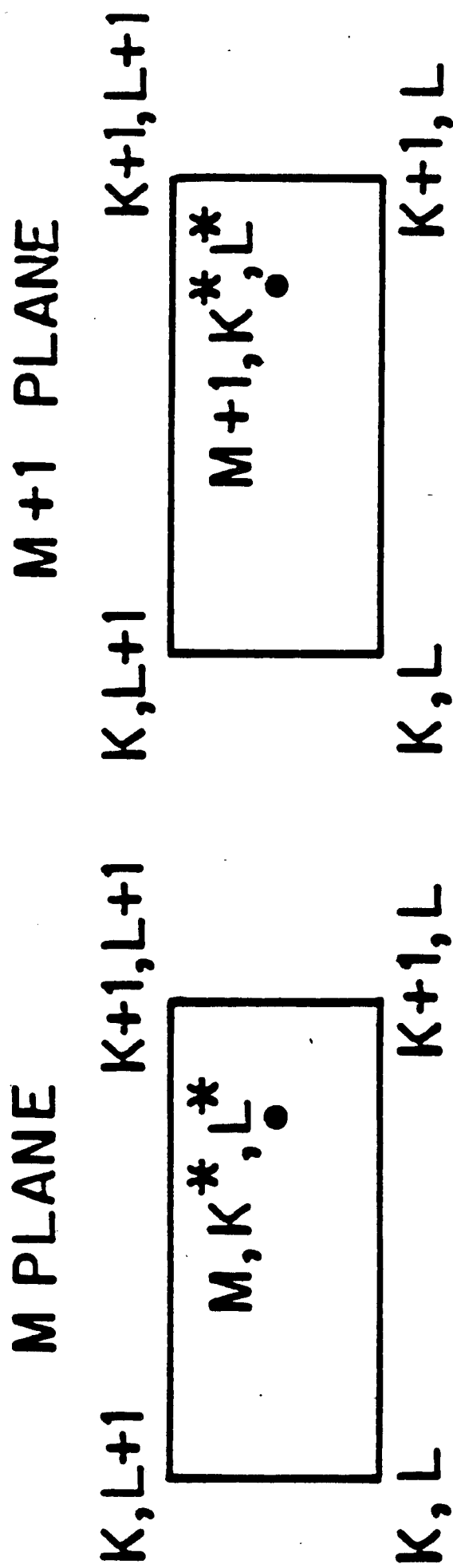
Figure 4.3.   Interpolation grid in three-dimensional equation-of-state tables.

The multigroup tables are treated like G two-dimensional tables where G is the number of groups.

5. WALL MATERIAL BEHAVIOR

CONRAD simulates the vaporization, hydrodynamic motion, and condensation of the first surface material. Under normal conditions, this material is in the form of a liquid or solid. We will refer to it as the "condensed region" or "condensate". Vaporization effectively occurs in two phases. During the first phase, hard X-rays from the target travel at the speed of light to the wall and, because of their long mean free paths, deposit their energy volumetrically in the condensed region. During the second phase, thermal radiation -- i.e., energy absorbed by the background gas and reemitted by the microfireball -- deposits its energy near the surface of the condensed region. In CONRAD, we model both of these phenomenon, using a "volumetric" vaporization model at very early times and a "surface" vaporization model at later times.

There are two separate vaporization/condensation models in CONRAD. The variable ISW(20) controls which model is used. In the original model (Model I), the number of Lagrangian vapor cells and the location of the vapor/condensate interface remain fixed throughout a calculation. The mass, momentum, and energy of the vaporized material is added to vapor cells within the cavity. Periodically, a rezoning procedure is used to redistribute mass throughout the Lagrangian mesh. This features of this model are described in Section 5.1.

In the second model (Model II), the Lagrangian mesh extends beyond the cavity (vapor region) into the condensed (wall) region. As material is

vaporized, the Lagrangian cells undergo hydrodynamic motion. Later, as each cell recondenses, hydrodynamic motion ceases. No mixing occurs between the background gas, which is assumed to be a non-condensable gas, and the vaporized wall material. This approach eliminates the need for rezoning, and allows for better numerical energy conservation. This model is described in in Section 5.2.

5.1. Vaporization/Condensation Model I

In Model I, there are three separate models to simulate the "volumetric" vaporization phase. The user can choose which model he wishes through the input variable ISW(25). Heat transfer into the material competes with the vaporization process if vaporization does not occur instantaneously as the x-rays currently do. This heat transfer is modeled in subroutine FILM with a standard finite difference method where node points are defined in the material. Condensation is calculated within a kinetic model, where the width of a condensing boundary layer is found from the mean free paths of the vapor atoms and all atoms within this layer that are moving towards the surface are assumed to condense. All of these things will be discussed in more detail in this section.

5.1.1 Vaporization

Three volumetric vaporization models are available in Model I. The differences between these models have to do with the handling of material that is heated above the sensible heat of the material at the boiling temperature but not exactly to the local heat of vaporization. These differences can be understood by consulting Fig. 5.1, where the energy density is schematically plotted against the distance from the surface of the material. Also depicted are the local energy densities required to vaporize material, E_1, and to have
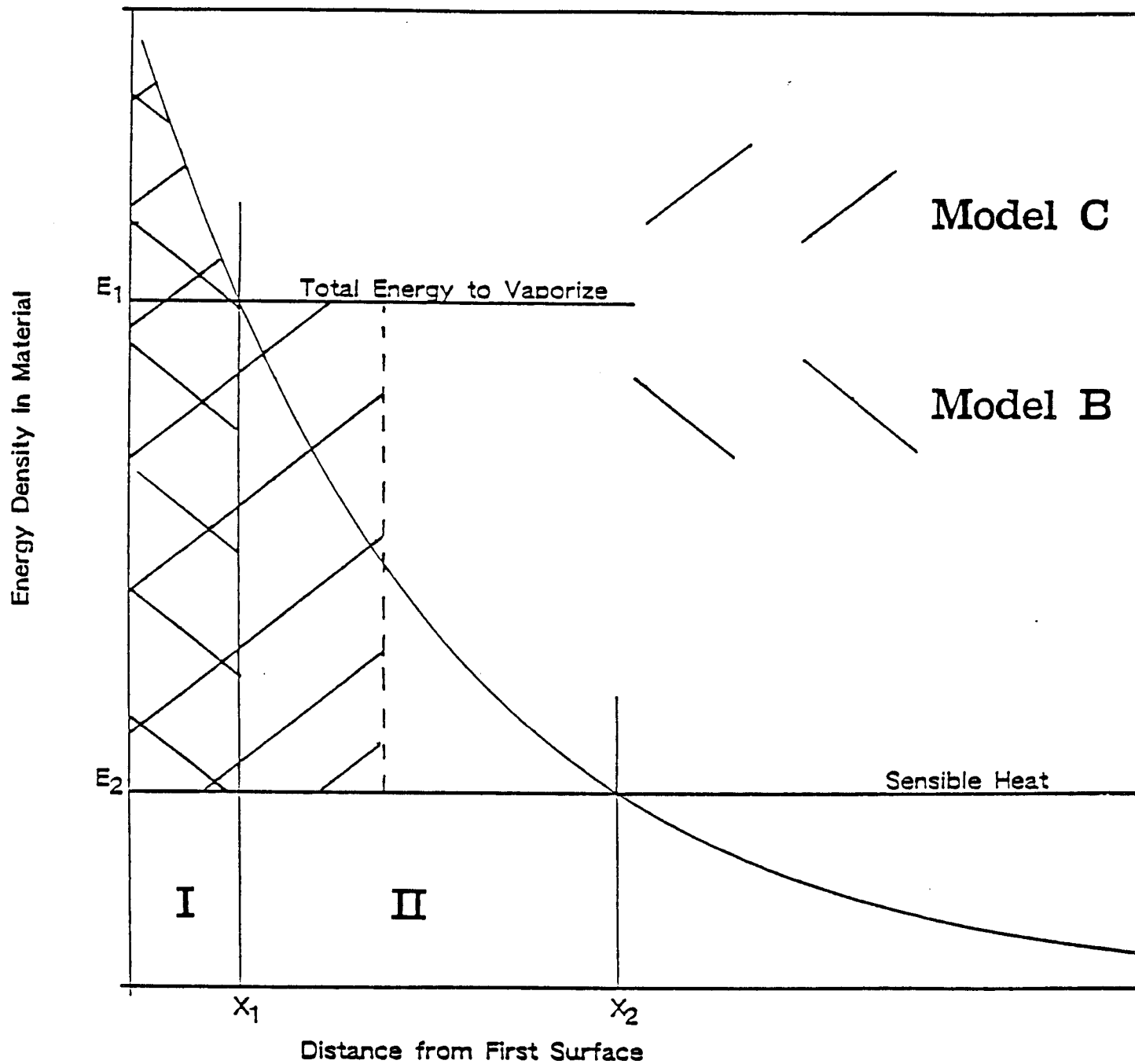
Figure 5.1. Model I vaporization models.

the material sitting at the boiling temperature T_{boil}, E_2. There are three regions on this plot: one where the energy density is greater than the local energy density required to vaporize E_1, referred to as region I; one where it is below the sensible heat, E_2; and one where there is not enough energy density to vaporize the material locally, but where the energy density is larger than E_2, referred to as region II. A major question is what happens in region II, because there is not enough energy density to vaporize any material locally, but there is more energy than is required for the material to be sitting at the boiling temperature. The three models handle this problem in different ways.

Model A

Model A, which is used if ISW(25) = 1, takes all of the energy above E_2 in regions I and II and repositions it so that there is no part that has more energy density than E_1 and no part that has energy density between E_1 and E_2. This model essentially assumes that the excess energy is moved about by some unspecified mechanism to vaporize the most amount of material. All of the vapor created in this model comes off of the surface at the boiling temperature.

Model B

Model B is used when ISW(25) = 2. This model assumes that only material in region I is vaporized and that the excess heat in region II is somehow transfered back into the cooler part of the material. The vapor comes off of the surface as a superheated vapor, that is, its temperature is greater than the boiling temperature. This model represents a lower bound on the vaporization and one could expect it to underestimate experimentally achieved values by a significant amount. It is essentially throwing away the excess energy in region II.

Model C

If ISW(25) = 0, which is the default value, one uses model C. In a way, model C is a hybrid between models A and B. Region I is treated as it is in model B, while region II is tested as it is in model A. The material in region I retains all of the energy deposited in it and is totally vaporized and comes off as a superheated vapor. The excess energy is repositioned in a way similar to that in model A. It is divided into two subregions: one adjacent to region I where the energy density is E_1, and another, next to the region with an energy density less than E_2, where the energy density is E_2. The vaporized material that comes off from region II is at the boiling temperature, but it mixes with the material from region I and the mixture is somewhat superheated. At the present time, this model is though to best represent the actual situation.

5.1.2. Heat Transfer

CONRAD models the heat transfer in the unvaporized material. Heat is deposited on the surface of the material by the absorption of radiation from the vapor, by condensation of vapor, and by thermal conduction from the vapor, which is almost never important. Target generated x-rays deposit their energy volumetrically in the material. The rate at which this energy is carried away from the front surface of the material determines the temperature at the surface and thus has a great influence on the condensation and vaporization. CONRAD solves the thermal conduction equation,

$$\frac{\partial}{\partial t} T(x) = \frac{\kappa}{\rho c_p} \frac{\partial^2}{\partial x^2} T(x) \tag{5.1}$$

to find the temperature profile in the material as a function of time, $T(x)$.

This equation is converted into a system of difference equations

$$-\theta\alpha_{i+1/2}T_{i+1} + \left(1 + \theta\alpha_{i+1/2} + \theta\alpha_{i-1/2}\right)T_i - \theta\alpha_{i-1/2}T_{i-1} = \text{explicit terms} \quad (5.2)$$

where $\quad \alpha = \dfrac{K\Delta t}{\rho C_p \Delta x^2} \quad$ and $\quad 0 \leq \theta \leq 1$

that are solved on a mesh of zones. There are NPT zones in the mesh, a number that is reduced as material is vaporized. Zone number 1 is the outermost zone. Zone i is DELX(i) m wide and has temperature TFLMA(i) in K. The properties of the material are the mass density in kg/m^3, RHOFLM(i), the heat capacity in MJ/kg/K, CP(i), and the thermal conductivity in MW/m-K, XK(i). This system of difference equations is tridiagonal and is solved in subroutine TRIDIG. The properties may be recalculated in subroutine FPROP if ISW(30) = 1.

5.1.3. Interface with Vapor Phase

CONRAD models the flow of momentum, energy and mass in subroutine WXCHNG. This subroutine controls the FILM subroutine where vaporization is calculated and it determines the condensation rate. It begins by determining the width of the boundary layer in the gas by finding the value of mass density times length required to stop an average vaporized atom, ρR_{stop}. This is expressed in g/cm^2 as

$$\rho R_{stop} = \frac{7.28 \times 10^{-8}\sqrt{8.617 \times 10^{-5}\ TSH\ AT\omega2B^{1.5}}}{Iz^{1.166667}} \quad (5.3)$$

where TSH is the surface temperature of the material in K, ATW2B is the atomic weight in amu and IZ is the atomic number of the vaporized material. It then

integrates the mass density out from the material-gas interface to find that zone that is ρR_{stop} from the interface. JXCHW is the innermost zone to be fully within the boundary layer, JLASTS is the next zone inward which is partially within the boundary layer and ZFRACT is the fraction of the JLASTS zone that is within the boundary layer. Mass transfer between the gas and the material all occurs in the boundary layer and is distributed within the boundary layer in an amount proportional to the local mass density.

The condensation rate is calculated by assuming that all atoms within the boundary layer have completely random directions of movement. Any atom that hits the material has a chance of sticking equal to FSTICK. This leads to a condensation rate of

$$\dot{\rho} = \frac{\overline{\rho} \cdot \overline{v} \cdot \text{FSTICK}}{4} \quad \text{g/cm}^2/\text{s} \tag{5.4}$$

where $\overline{\rho}$ is the average mass density in the boundary layer and $\overline{v}$ is the average speed of atoms in the boundary layer. This condensation rate puts a heat flux on the material of

$$q_{cond} = \dot{\rho}(\overline{\epsilon} + \Delta H_{vap}) \tag{5.5}$$

where $\overline{\epsilon}$ is the average internal energy density of the gas in the boundary layer and ΔH_{vap} is the average heat of vaporization in the boundary layer. This heat flux, along with that from thermal radiation and the volumetric heating due to x-rays is passed along to FILM for the heat transfer and vaporization calculations in the material.

42

Conservation of momentum and energy are invoked to recalculate the fluid velocity and temperature of gas within the boundary layer. The difference equation for the change in the velocity of a zone in the boundary layer is written as

$$\Delta u_j^{n+1/2} = 0.5 \left[\left(\left(u_{j-1/2}^{n+1/2} - \left(\left(\frac{v_1 \Delta m_v}{M_{BL}} \right) \right) \right) \frac{\Delta m_{o_{j-1/2}}^{I}}{\Delta m_{o_{j-1/2}}^{II}} \right) + \left(u_{j+1/2}^{n+1/2} - \left(\left(\frac{v_1 \Delta m_v}{M_{BL}} \right) \right) \right) \frac{\Delta m_{o_{j+1/2}}^{I}}{\Delta m_{o_{j+1/2}}^{II}} \right) \right.$$

$$\left. - 0.5 \left(u_{j-1/2}^{n+1/2} + u_{j+1/2}^{n+1/2} \right) \right. \tag{5.6}$$

where: v_1 = velocity of ions leaving material

Δm_v = total mass of material vaporized on current time step

M_{BL} = total mass of gas in boundary layer

$\Delta m_{o_{j-1/2}}^{I}$ = Lagrangian mass of zone before mass transfer of current time step

$\Delta m_{o_{j-1/2}}^{II}$ = Lagrangian mass of zone after mass transfer of current time step.

The change in the energy density of the gas in the boundary layer is written in a similar form as

$$\Delta E_{j-1/2}^{n+1/2} = 0.5 \left[\Delta m_{o_{j-1/2}}^{I} \Delta m_v \frac{v_1^2}{M_{BL}} + M_{BL} \left(u_{j-1/2}^{n+1/2} \right)^2 - \left(M_{BL} + \Delta m_v \right) \left(u_{j-1/2}^{II} \right)^2 \right] \tag{5.7}$$

where $u_{j-1/2}^{II} = 0.5 \left[u_{j-1}^{n+1/2} + \Delta u_{j-1}^{n+1/2} + u_{j+1}^{n+1/2} + \Delta u_{j+1}^{n+1/2} \right]$.

Both Eqs. (5.6) and (5.7) are for zones that are neither the innermost nor

outermost in the boundary layer; equations for momentum and energy transfer in those zones are slightly different. After the new internal energy density is calculated, the temperatures of the gas are recalculated.

5.1.4 Variable Temperature Properties

The thermal properties for the unvaporized material may be recalculated in subroutine FPROP if ISW(30) = 1. At the present time, the only thing that is recalculated is the boiling temperature as a function of the pressure in the vapor. Other things can easily be added to this subroutine.

Two methods of calculating the boiling temperature of the material can be used in Model I. One is based on the Clausius-Clapeyron equation [17], where one can relate the boiling temperature of the material at a given vapor density to the boiling temperature at a vapor pressure of one atmosphere:

$$T_{boiling} = 1/[\frac{1}{T_{boiling}(P=1atm)} - \frac{R}{\Delta H_v} \ln (P/1 \text{ atm})] \tag{5.8}$$

where ΔH_{vap} is the heat of vaporization, R is the gas law constant, and P is the local vapor pressure at the surface of the material. The only thing that is needed to use this formula that is not already present from other parts of the code is the boiling temperature at one atmosphere, something that is readily available for most materials. The second method is based on the work of Antoine [18], which leads to a law with a functional form similar to Eq. (5.8)

$$T_{boiling} = \frac{B}{[A - \ln (P/1 \text{ atm})]} - C \tag{5.9}$$

but now involves three empirical constants: A, B, and C. These constants are

tabulated for some materials [19], but not for others. When these constants are available, one should use Antoine's method because it is accurate over a broader range: Eq. (5.8) may yield suspicious results when the local vapor pressure is far from one atmosphere. CONRAD automatically chooses Eq. (5.8) if B is zero and Eq. (5.9) otherwise.

5.2. Vaporization/Condensation Model II

In Model II, the hard X-rays that are deposited "volumetrically" in the condensed region vaporize material during the first time cycle of a CONRAD simulation (or during the first few cycles if the time-dependent X-ray deposition option is used). A typical energy deposition profile is illustrated in Figure 5.2, where the energy density is plotted as a function of distance behind the vapor/condensate interface. The condensed layer is divided into 3 regions. In region A, the energy density is higher than the vaporization energy density. All material in this region becomes superheated vapor (T > T_{vap}, the vaporization temperature). In region C, the energy density remains lower than the "sensible" energy density. None of this material is vaporized during the volumetric vaporization phase, and the temperature remains below T_{vap}. In region B, the energy density lies between the vaporization and sensible energies, and the temperature throughout the region is equal to T_{vap}. To determine the amount of material from region B that gets vaporized, we redistribute the energy so that: (1) none of the condensed region has an energy density between the vaporization and sensible values, and (2) energy is conserved. The redistributed energy is represented by the dotted line in Figure 5.2. This model is similar to Model C described in Section 5.1.
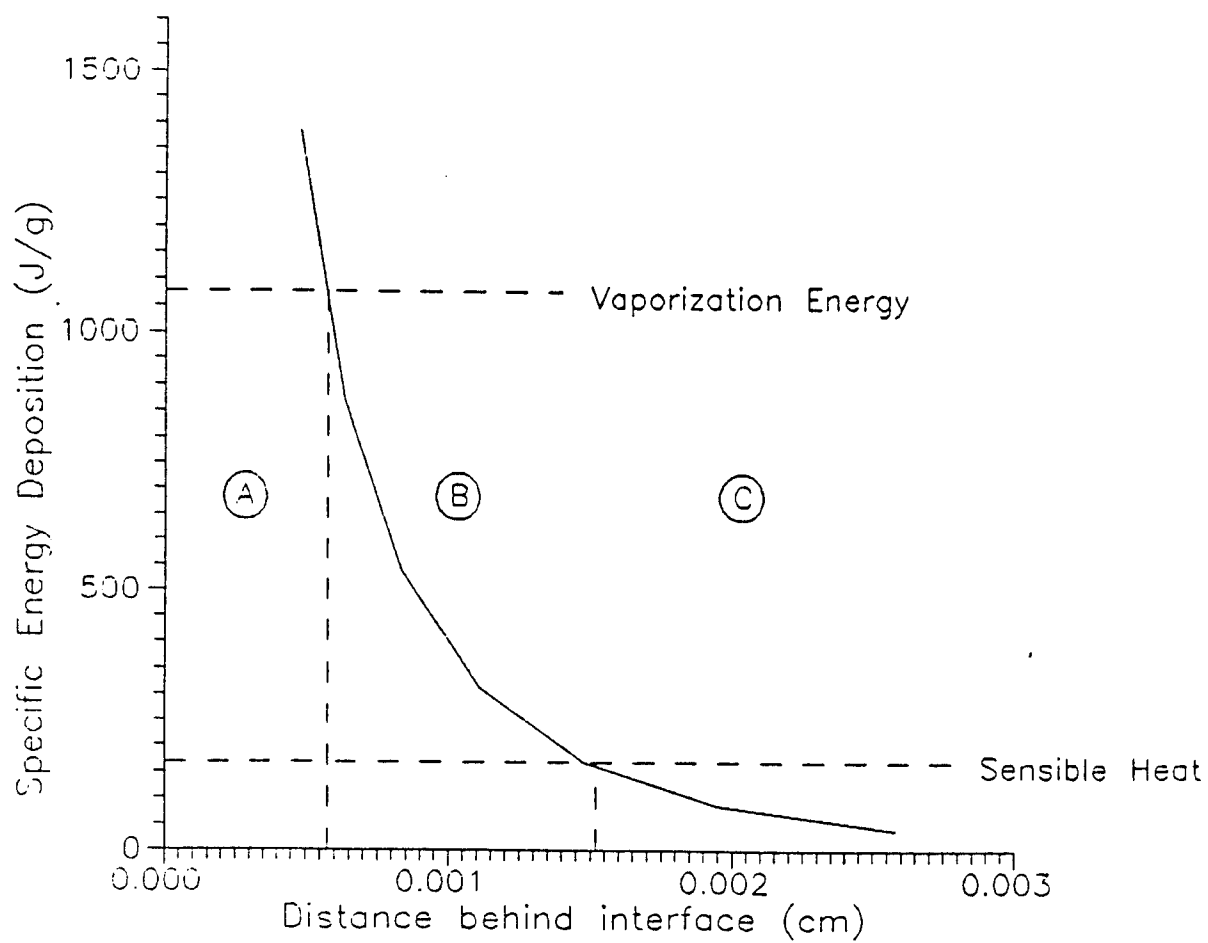
Figure 5.2. Model II vaporization models.

After material is vaporized, the pressure in the vapor region near the interface becomes very high because of the high density. This causes material to be rapidly accelerated away from the interface, and provides a "recoil" impulse to the wall. CONRAD monitors the pressure at the interface and computes the impulse on the wall directly.

The amount of material vaporized during the volumetric phase can be adjusted by setting ISW(25) = 2. This allows only material with energy densities greater than the vaporization energy density to be vaporized. That is, none of the material in region B is vaporized. This model is less reliable, however, because energy is not conserved.

In Model II, the primary distinction between the vapor and condensed phases is that vapor cells undergo hydrodynamic motion. The condensed region cells remain stationary due to chemical bonding. In addition, the conservation of momentum and energy equations are solved over all vapor cells. In the condensed region, a one-dimensional conduction equation is solved to determine the energy transport within the region.

After the volumetric deposition phase, radiant energy transported to the condensed region will be effectively deposited at the surface of the interface because of the shorter photon mean free paths. The vaporization and condensation rates are calculated using the kinetic theory model described by Labuntsov and Kryukov [20]. The mass vaporization rate is given by:

$$(dm/dt)_v = \frac{2}{3} P_{sat} A_{wall} \left(\frac{\mu}{RT_v}\right)^{1/2} \tag{5.10}$$

where A_{wall} is the surface area of the wall, T_v is the vapor temperature, R is the gas constant, μ is the mean atomic weight of the condensable material, and

P_{sat} is the saturation vapor pressure:

$$P_{sat} = \exp \left\{ \frac{\Delta H_v}{kT_{vap,o}} \left(1 - \frac{T_{vap,o}}{T_c}\right) \right\} \text{ bar} \qquad (5.11)$$

ΔH_v is the specific heat of vaporization, k is Boltzmann's constant, T_c is the condensate temperature at the interface, and $T_{vap,o}$ is the vaporization temperature at 1 bar. The mass condensation rate is:

$$(dm/dt)_c = \frac{2}{3} f_s f_{NC} P_{vap} A_{wall} \left(\frac{\mu}{RT_v}\right)^{1/2} \qquad (5.12)$$

where f_s is the sticking coefficient, F_{NC} is a correction factor for non-condensable gas effect, and P_{vap} is the vapor pressure given by the ideal gas law:

$$P_{vap} = \rho_v \frac{RT_v}{\mu} \qquad (5.13)$$

where ρ_v is the vapor density.

Lagrangian cells undergo hydrodynamic motion only after an entire cell is vaporized. Figure 5.3 illustrates the evolution of mesh points during a typical simulation. Vapor cells are to the left of the dashed line and the condensed region is to the right of it. The "+"s represent the cell boundaries and the vertical dashed line represents the vapor/condensate interface. A short time after the target explodes ($t_1 = t_0 + \varepsilon$), the target's hard X-rays are deposited in the condensed region, vaporizing a number of cells. Since the vaporized mass is not in general an integral number of cells, the
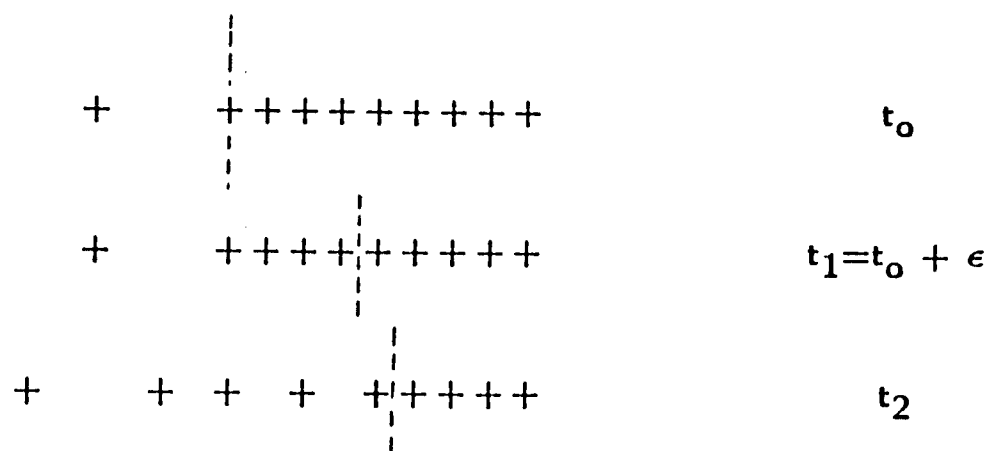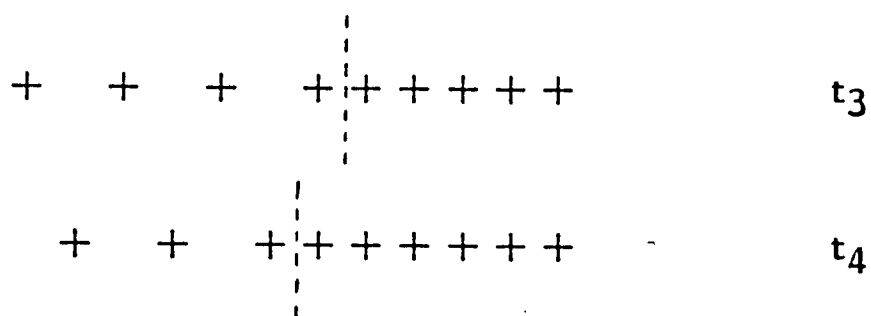
Figure 5.3. Evolution of mesh points during a vaporization/condensation
calculation

interface is located between cell boundaries. At later times (t_2), the vapor expands away from the wall while thermal radiation from the fireball vaporizes additional cells. No mass is ever exchanged between Lagrangian cells as mixing effects are neglected.

As the radiative flux from within the cavity subsides and the temperature at the surface of the condensed region drops, the condensation rate begins to exceed the vaporization rate. Again, the interface is tracked as condensation occurs. In Figure 5.3 shows vapor moving toward the interface as material recondenses back onto the surface (t_3 and t_4). If any portion of a Lagrangian cell has condensed, it no longer undergoes hydrodynamic motion.

To calculate energy transport withing the condensed region, CONRAD solves the one-dimensional conduction equation:

$$C_p \frac{dT}{dt} = \frac{\kappa}{\rho} \frac{d^2T}{dx^2} + S \qquad (5.14)$$

where C_p is the specific heat at constant pressure, κ is the thermal conductivity, ρ is the density in the condensed region, T is the temperature, and x the spatial coordinate. S is a source term which accounts for the energy deposition from the radiative heat flux and debris ions. In practice, only the first cell has a non-zero source term because the heat flux is assumed to be deposited at the surface. The conduction equation is also subject to the following boundary conditions. The temperature at the back of the condensed layer is constant (Dirichlet condition) as heat flows through the back of the condensed region. At the vapor/condensate interface, the conductive heat flux is assumed to be zero (Neumann condition).

6. THE ENERGY CONSERVATION CHECK

Energy conservation is monitored for the entire vapor/condensate system. At the end of each time step, a check is made to ensure that the difference equations are conserving energy. After integrating the energy equations over time and space, the conservation equations for the vapor (plasma), condensate, and radiation can be written as:

$$\text{Plasma} \qquad e_p + T_p = e_p^o + T_p^o + H_p + E_{RP} - F_p - G_R + J_{PT}$$

$$\text{Condensate} \qquad e_c = e_c^o + F_R + F_p - J_{PT} - Q_B + H_c$$

$$\text{Radiation} \qquad e_R = e_R^o - E_{RP} - F_R + G_R$$

$$\text{Total} \qquad e_{TOT} + T_p = e_{TOT}^o + T_P^o + H_p - Q_B$$

The superscript "o" signifies the initial values. The physical definitions of each term are:

e_x total internal energy of the plasma, condensate, or radiation.

T_p total kinetic energy of the plasma.

H_x total source of energy to the plasma or condensate.

E_{RP} total radiation energy exchanged between the plasma and radiation field.

F_x total energy conducted across the vapor/condensate interface from the plasma or radiation.

G_R work exchanged between the gas and radiation.

Q_B total energy conducted through the back of the condensed region.

J_{PT} total energy exchanged during phase transformation between the plasma and condensate.

Each of these terms at time step "n" are given in finite difference form as follows:

$$e_x^{n+1} = \sum_{j=1}^{JMAX} (e_x)_{j-1/2}^{n+1} \, \Delta m_{o_{j-1/2}} \tag{6.1}$$

$$T^{n+1} = \frac{1}{4} \, \Delta m_{o_{JMAX-1/2}} \, (u_{JMAX}^{n+1/2})^2 + \frac{1}{2} \sum_{j=1}^{JMAX} \Delta m_{o_j} (u_j^{n+1/2})^2 \tag{6.2}$$

$$H_x^{n+1} = H_x^n + \Delta t^{n+1/2} \sum_{j=1}^{JMAX} (H_x)_{j-1/2}^{n+1/2} \, \Delta m_{o_{j-1/2}} \tag{6.3}$$

$$E_{RP}^{n+1} = E_{RP}^n + \Delta t^{n+1/2} \sum_{j=1}^{JMAX} (E_{RP})_{j-1/2}^{n+1/2} \, \Delta m_{o_{j-1/2}} \tag{6.4}$$

$$G_R^{n+1} = G_R^n + \Delta t^{n+1/2} \sum_{j=1}^{JMAX} u_j^{n+1/2} \, (r^{\delta-1})_j^{n+1/2} \, (P_{R_{j+1/2}}^{n+1/2} - P_{R_{j-1/2}}^{n+1/2})$$

$$+ \Delta t^{n+1/2} \, u_{JMAX}^{n+1/2} \, (r^{\delta-1})_{JMAX}^{n+1/2} \, [P_{R_{JMAX+1}}^{n+1/2} - P_{R_{JMAX-1}}^{n+1/2}]/2 \tag{6.5}$$

$$F_P^{n+1} = F_P^n + \Delta t^{n+1/2} \, [\frac{r^{\delta-1}}{(\frac{\Delta r}{\kappa_P})}]_{JMAX}^{n+1/2} \, (T_{P_{JMAX+1/2}}^{n+1/2} - T_{P_{JMAX-1/2}}^{n+1/2}) \tag{6.6}$$

$$F_R^{n+1} = F_R^n + \Delta t^{n+1/2} \, [\frac{r^{\delta-1}}{(\frac{\Delta r}{\kappa_R}) + \frac{\Delta E_R}{F_R}}]_{JMAX}^{n+1/2} \, (E_{R_{JMAX+1/2}}^{n+1/2} - E_{R_{JMAX-1/2}}^{n+1/2}) \tag{6.7}$$

$$J_{PT}^{n+1} = J_{PT}^n + \Delta t^{n+1/2} \, [(\frac{dm}{dt})_v^n - (\frac{dm}{dt})_c^n] \cdot [e_v^{n+1} - e_c^{n+1}] \tag{6.8}$$

$$Q_B^{n+1} = Q_B^n + \Delta t^{n+1/2} \; (\frac{r^{\delta-1}}{\frac{\Delta r}{\kappa_p}})_{JMAXC}^{n+1/2} \; (T_{p_{JMAXC+1/2}}^{n+1} - T_{p_{JMAXC-1/2}}^{n+1}) \qquad (6.9)$$

The calculations usually conserve energy to within better than 10%.

7. INITIALIZATION

Before the first time step, CONRAD sets all variables in the common blocks to zero and then initializes. Default values are set in subroutine INIT1 and then the input parameters are read in as discussed in Section 10.4. If the run is a restart of another run, which is signaled by IRS = 1, CONRAD reads in all of the common blocks from the previous run by a call to subroutine UNREAD and reads in the changes needed for the present run. If the run is not a restart, CONRAD then initializes all of the variables whose values are dictated by the input parameters. These include the configuration of the Lagrangian mesh in the gas, the equation of state variables in the gas, initial temperature profiles in the gas due to x-ray deposition, and many other properties of the gas and material. This is done in subroutines INIT2, INIT3, INIT4 INITX, and INITF. A detailed list of initial values is printed out by subroutine INIT5.

CONRAD has the option of using one of several zoning procedures to initialize the Lagrangian mesh. The variable switch ISW(4) is used to select the desired option. If ISW(4) = 0, the user must input all of the zone widths, a sometimes tedious practice that is generally not recommended. If ISW(4) = 1, the initialization is done with the subroutine ZONER. For this option, one must input the variables NI, RI, NO, RO, and PMASS. Many of the

input parameters listing in Tables 1 and 2 are in the form of vectors, where each element is for a given zone. Because these are not generally the same for all zones and because the positions of the zones are not known at the time that the input is read in, one must provide CONRAD with the positions at which these zone parameters are taken. The vector RCENT is used for this purpose, where it represents the centers of the zones for the inputted zone parameters. ZONER does the zoning by dividing the gas into three regions: an inner and an outer region, each with constant mass zoning, and a region in between, where the ratio between the masses of neighboring zones is constant. The number of inner zones NI, the number of outer zones NO, the width of the whole gas region RADIUS, the width of the innermost zone RI, the position of the inside boundary of the outermost zone RO, and the target mass PMASS must be provided in the input file. It is possible that a combination of these parameters is not self-consistent and ZONER will print out an appropriate error message when this occurs. It is suggested that the user try several test runs with NMAX = 1 with various combinations of NI, NO, RI, RO, RADIUS and PMASS, and examine the masses in each zone to choose the most smoothly varying case. After the mesh is determined, the zone parameters are interpolated on the new mesh. Two of the input parameters are the number density in each zone, DN2B, and the atomic weight of the gas, ATW2B. This presents a problem for ZONER because the zone boundaries are dependent upon the mass density and the densities are interpolated on the mesh. An iterative technique is used to converge the densities and zone boundaries, but if the mass density profile is very sharply changing, ZONER will not converge. Therefore, the user should avoid discontinuous mass density profiles.

54

If $2 \leq ISW(4) < 10$, the Lagrangian mesh is initialized using the subroutine ZONER2. In this case, the mesh points of the vapor region are set up such that the mass change from cell to cell changes by a constant factor, β (= 1 + CON(36)):

$$\Delta m_{j+1} = \Delta m_j \cdot \beta \qquad (7.1)$$

Thus, when CON(36) = 0 (β = 1), the masses of all Lagrangian zones in the vapor region are equal. The total vapor mass is constrained by the vapor number density (DN2B) and the target chamber radius (RADIUS). The zoning option in the condensed region is also determined by the value of ISW(4). If ISW(4) = 3, the Lagrangian mesh in the condensed region is computed using Eq. (7.1) using the same value of β as the vapor region. If ISW(4) = 4, a new value of β is computed for the condensed region based on the total mass in the region, M_c = 4π RADIUS**2*DELXCT*RHOCND, and the number of zones, NCZONS.

The third automatic zoning option is used for condensation calculations. In this case, ISW(4) should be set to $\geq$ 10. Occasionally, it is useful to separate a problem into vaporization and condensation calculations because the time steps in the late stages of target explosion/vaporization problems are sometimes very small due to shocks moving throughout the target chamber. When this occurs, it is prudent to restart the problem without these large density and pressure gradients. For this option, the vapor masses of the non-condensable (VAPMAS(1)) and condensable (VAPMAS(2)) regions must be specified, as well as the indices of the zones bounding these regions (JMN, JMX). The mass progression factor for the non-condensable vapor region is again specified by CON(36). The factor for the condensable vapor region is found by

iteration. For the condensed region, the zoning is again initialized using either the mass progression factor of the adjacent vapor region (when ISW(4) = 13) or the total mass of the condensed region (when ISW(4) = 14).

Another part of the initialization process is the setting of equation of state tables for the gas. CONRAD allows either 1 or 2 sets of equation of state data to be used in the gas: the number is specified by NMAT, where 1 is the default. The data are read through unit 3 for gas type number 1 and through unit 13 for gas type number 2. For NMAT = 2, the data used for each zone is specified by the vector input parameter JMAT, which is either 1 or 2 and is defaulted to 1.

After the mesh has been determined and the equations of state and opacities have been read and if ISW(11) = 0, CONRAD simulates the deposition of x-rays in the gas and reinitializes the gas temperature profile. The x-ray deposition is calculated in subroutine GASDEP and is controlled by the input parameters in Table 10.3 There are two ways that the deposition can be done: with a blackbody x-ray spectrum or with an arbitrary histogram spectrum. If one wishes a blackbody spectrum, one must input the total energy in x-rays FLUX, the number of energy groups NXRG, and the blackbody temperature KEV. For an arbitrary spectrum, the energy group boundaries XEHIST and the amplitude of each group XAMP are required. The atomic number of each zone in the gas IZ is required in both cases. X-ray stopping data is read in through unit 11.

8. THE TIME STEP CONTROL

After each time step, the next time step is determined from a set of stability and accuracy constraints. The new time step is determined by

56

$$\Delta t^{n+3/2} = \text{Max}\left[\Delta t_{min}, \text{Min}\left(\Delta t_{max}, \frac{K_1}{R_1^{n+1}}, \frac{K_2 \Delta t^{n+1/2}}{R_2^{n+1}}, \ldots, \frac{K_7 \Delta t^{n+1/2}}{R_7^{n+1}}\right)\right] \qquad (8.1)$$

where: $\quad R_1^{n+1} = \text{Max}\left[(V_{j-1/2}^{n+1} \; P_{j-1/2}^{n+1})^{1/2}/\Delta r_{j-1/2}^{n+1/2}\right] \qquad (8.2)$

$$R_2^{n+1} = \text{Max}\left[(V_{j-1/2}^{n+1} - V_{j-1/2}^n)/V_{j-1/2}^{n+1/2}\right] \qquad (8.3)$$

$$R_3^{n+1} = \text{Max}\left[(E_{R_{j-1/2}}^{n+1} - E_{R_{j-1/2}}^n)/E_{R_{j-1/2}}^{n+1/2}\right] \qquad (8.4)$$

$$R_4^{n+1} = \text{Max}\left[(T_{P_{j-1/2}}^{n+1} - T_{P_{j-1/2}}^n)/T_{P_{j-1/2}}^{n+1/2}\right] \qquad (8.5)$$

$$R_5^{n+1} = \text{Max}\left[(T_{m_i}^{n+1} - T_{m_i}^n)/T_{m_i}^{n+1/2}\right] \qquad (8.6)$$

$$R_6^{n+1} = \text{Max}\left[(T_{boiling,i}^{n+1} - T_{boiling,i}^n)/T_{boiling,i}^{n+1/2}\right] \qquad (8.7)$$

$$R_7^{n+1} = \text{Max}\left[(\Delta m_{o_{j-1/2}}^{n+1} - \Delta m_{o_{j-1/2}}^n)/\Delta m_{o_{j-1/2}}^{n+1/2}\right] . \qquad (8.8)$$

The maximum values of R_1 through R_7 are found by sweeping over the zones. The input parameters K_1 through K_7 determine the severity of each constraint. The default value for K_1, K_2, K_4, K_5 and K_6 is 0.05. The default value of K_3 is set to 1.0×10^{35}, which in effect removes the radiation energy as a time step constraint. The radiation diffusion equation is solved using a fully implicit differencing scheme and is stable for large time steps. The time step can of course be constrained using the change in radiation energy density by simply inputting a different value for K_3. The default value of K_7 is 0.1.

9. DYNAMIC REZONING

When vaporization Model I is used (ISW(20) = 1) CONRAD allows mass to enter and leave the vapor phase through vaporization and condensation, the Lagrangian masses of zones near the outside edge of the vapor can change with time. To properly simulate the hydrodynamic motion of the vapor, one needs to have the Lagrangian masses of adjacent zones be roughly equal. Therefore, CONRAD needs a means of redefining the zone boundaries between time cycles. Dynamic rezoning also prevents the masses of some zones from going to zero because of condensation.

CONRAD dynamically rezones by calling the subroutine ZONER whenever ISW(20) = 1 the mass in a zone changes by a ratio more than RZCM, a parameter that can be changed from its default value of 0.01 through the namelist read during initialization. Because the rezoning is done through ZONER, the radius of the innermost zone and the outer radius of the next to the outermost zone must be calculated by REZONE. This occasionally causes problems with the running of the code because these two radii might not be compatible. The incompatibility between the two calculated radii can occur if a large amount of mass is added to a few of the outer zones. The radii are chosen so that the fraction of the mass of the vapor that is taken up by any zone remains constant.

Since the Lagrangian zones are constantly being redefined, care must be taken that physical properties such as density and temperature must be re-calculated on the new mesh. These properties are calculated through linear interpolation on the old mesh. This is done partly in ZONER, since this must be done for variables that can be set during initialization, and partially in REZONE. The user should be aware that there will be some smoothing of results that is caused by this interpolation.

10. CODE ORGANIZATION

10.1 Subroutines

The CONRAD code is for the most part written in FORTRAN 77. It is currently set up to run on the CRAY XMP at SDCC and can be run on other mainframes computer with only minor modifications. It is written in a top-down modular style, as shown in Fig. 10.1. Each subroutine performs a specific function. These functions are briefly described below:

ABCDEF - computes the A, B, C, D, E, and F matrices and vectors used to solve the energy transfer equations when using the 2-T option.

ABCPLS - computes A, B, C, D, E, and F coefficients used to solve the plasma temperature equation when using the multifrequency radiation option.

ABCRAD - computes A, B, C, D, E, and F coefficients used to solve the radiation energy equation for a specified frequency group when using the multifrequency radiation option.

AIPFUN - computes the average ionization potential of the background gas for use in the Bethe stopping power equation.

CLEAR - sets all common blocks to zero before the start of a calculation.

COND1D - solves the 1-dimensional conduction equation for the condensed region.

CONRAD - driver program

CROS - reads the photoionization cross sections for the x-ray atten uation model.

CROSI - searches through the x-ray cross section table and computes the cross section of the gas.

DEBUG - returns logical flag indicating if debug output for a particular subroutine is requested.

DEDX - computes the ion deposition stopping power.

DUMP - writes all common blocks on unit 2 at the end of a calculation.

DYNDEP - computes the x-ray deposition and the new absorption cross section of each zone.

Figure 10.1.

CONRAD FLOW DIAGRAM
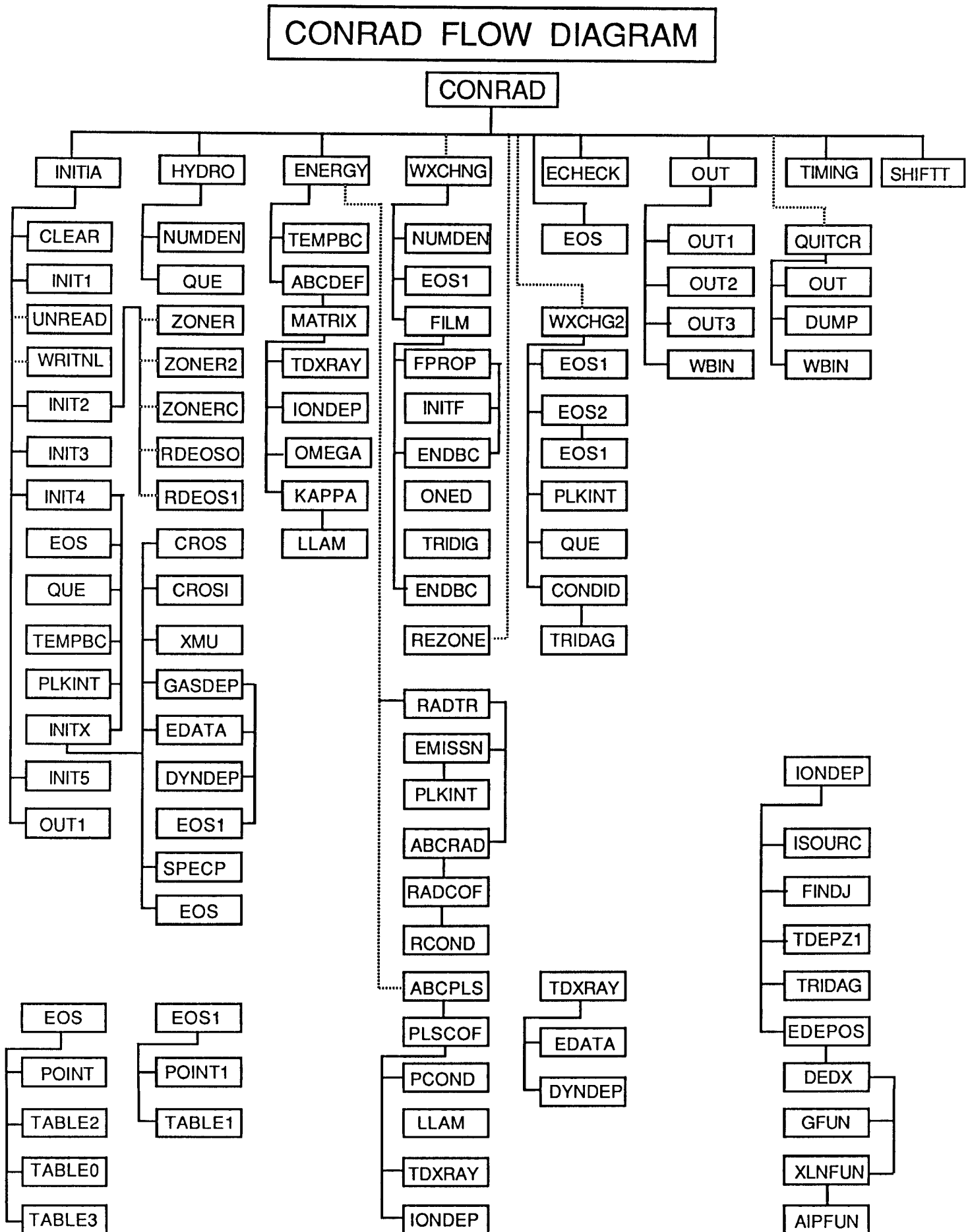
ECHECK –   computes the integrals used in the energy conservation check.

EDATA –   provides the electron shell structure of the gas for the x-ray deposition calculation.

EDEPOS –   computes the ion deposition stopping power.

EMISSN –   computes the frequency dependent radiation emission when using the multifrequency radiation option.

ENDBC –   computes boundary conditions for heat transfer in material.

ENERGY –   computes T_p, E_R, and then T_R.

EOS,EOS1, –   computes the equation of state quantities.
EOS2

FILM –   computes heat transfer and vaporization of material.

FINDJ –   finds the index of the zone an ion bunch is located within.

GASDEP –   computes the temperature of the gas after x-ray deposition.

GFUN –   computes the value of a mathematical function used in the stopping power calculation.

HYDRO –   solves the equation of motion for the fluid velocity, new zone radii, Δr's, zone volumes, and specific volumes.

INITF –   initializes variables in material.

INITIA –   reads namelist input and calls other initialization routines.

INITX –   initializes quantities for the x-ray deposition calculation.

INIT1 –   sets variable default values before reading input.

INIT2,3,4,5 – computes initial conditions and writes a summary of the initial conditions to unit 6.

IONDEP –   computes the ion energy deposition due to all debris ions.

ISOURC –   computes the number of debris ions emitted from the source during a given time interval.

KAPPA –   computes plasma and radiation thermal conductivity and the radiation flux limit.

LLAM –   computes log lambda for the thermal conductivity.

MATRIX   -   computes $\underline{a}$, $\underline{\alpha}$, $\underline{\gamma}$, and $\underline{\omega}$ matrices for use in the energy transfer calculation.

NUMDEN -   computes number densities from the specific volume.

OMEGA -   computes the radiation emission and absorption coefficients.

ONED -   solves 1-D heat transfer in outer material.

OUT,OUT1,2,3 -   writes output to unit 6 at the end of specified time cycles.

PCOND -   computes the plasma conductivity when using the multifrequency radiation option.

PLKINT -   returns the integral of the Planck function.

PLSCOF -   computes α, γ, a, and β coefficients used to solve the plasma temperature equation when using the multifrequency radiation option.

POINT,POINT1 -   finds pointers in the equation of state tables.

QUE -   computes the artificial viscosity.

QUITCR -   wraps up the calculation at the end.

RADCOF -   computes α, γ, ω, a, and β coefficients used to solve the radiation energy equation for a specified frequency group when using the multifrequency radiation option.

RADTR -   controls the multifrequency radiation calculation by calling EMISSN and ABCRAD and then computes the total radiation energy density and radiation temperature when using the multi-frequency radiation option.

RCOND -   computes the radiation conductivity for a specified frequency group when using the multifrequency radiation option.

RDEOSO,1 -   read in the equation of state and opacity data.

REZONE -   rezoning scheme used with the original vaporization model.

SHIFTT -   shifts values of variables at (n+1) to variables at (n) at the end of a time step.

SPECP -   computes the x-ray spectrum.

TABLE1,TABLE2 - interpolates in the equation of state tables using the
TABLE3,TABLEO - pointers.

TDEPZ1 -   computes the time-dependent debris ion ionization populations.

62

TDXRAY -   computes the time-dependent x-ray deposition.

TEMPBC -   computes the plasma temperature and radiation specific energy boundary conditions.

TIMING -   computes a new time step and determines whether the calculation is over.

TRIDAG -   tridiagonal matrix solver for the condensed region conduction equation and the rate equations for the time-dependent charge state calculations.

TRIDIG -   solves the tridiagonal matrix for heat transfer in material.

UNREAD -   reads in the common blocks from unit 4 at the beginning of a restarted calculation.

WBIN -   writes binary output to unit 8 for postprocessing.

WRITNL -   copies the namelist input file to the output file.

WXCHG2 -   new vaporization/condensation routine.

WXCHNG -   computes heat, momentum and mass transfer between vapor and material.

XLNFUN -   computes log Λ for the stopping power calculations.

XMU -   calculates the mass attenuation coefficients for the x-ray deposition calculations.

ZONER -   computes the Lagrangian zoning automatically.
ZONERZ, ZONERC

10.2 Input/Output Units

The CONRAD code uses ten different I/O units. These units are listed below along with their specific function.

Unit #	Function
2	CONRAD writes all common blocks to this unit at the end of a calculation to allow a restart.
3	CONRAD reads the equation of state tables of material #1 from this unit.
4	CONRAD reads the common blocks from this unit at the beginning of a restart calculation.
5	CONRAD reads the namelist input from this unit.
6	CONRAD writes line printer output to this unit.
8	CONRAD writes binary output to this unit for postprocessing into plots.
9	CONRAD writes the times corresponding to the stored heat fluxes on this unit.
10	CONRAD writes the radiation heat fluxes to the wall on this unit.
11	CONRAD reads x-ray cross section data on this unit.
12	CONRAD writes the pellet x-ray spectrum reaching the wall on this unit.
13	CONRAD reads the equation of state tables of material #2 from this unit.

When adding a variable to the common blocks, the block length (set in INITIA) must be changed so that DUMP and UNREAD will write and read the correct number of words for a restart. Notice that the lengths are measured in double words. This must be changed to single words if single precision is used. All of the variables should be changed to single precision if a 64 bit word length computer is used.

10.3 The Common Blocks

All of the real variables in the common blocks are in single precision, giving about 14 decimal places of accuracy on a CRAY computer.

For many of the variables, the second to the last letter indicates whether the variable is at a zone center or zone boundary, and the last letter denotes the time level. The suffixes are:

1 -- zone boundary

2 -- zone center

A -- t^{n+1}

B -- $t^{n+1/2}$

C -- t^n

D -- $t^{n-1/2}$

The letter R will appear in a variable name if the quantity is associated with the radiation field, and N if the quantity is associated with the plasma. Thus TR2B(J) is the radiation temperature in the center of zone j at time $t^{n+1/2}$, and U1D(J) is the fluid velocity on the zone j boundary at time $t^{n-1/2}$. The variables are grouped in common blocks so that a subroutine will find most of the variables that it needs in fewer than all of the blocks. The common blocks are listed below along with their meaning and units. A * superscript denotes mandatory input variables, and a ** superscript denotes a variable with a default value.

Common Blocks

COMMON/TIME/

1) TA t^{n+1} times (s)

2) TB $t^{n+1/2}$

3) TC t^n

4) TD $t^{n-1/2}$

5) DTB** $\Delta t^{n+1/2}$

6) DTC $\Delta t^n = (\Delta t^{n+1/2} + \Delta t^{n-1/2})/2$

7) DT $\Delta t^{n+3/2}$, the new time step

8) TMAX* Total time for the simulation

9) DTMIN** Min allowed time step

10) DTMAX** Max allowed time step

11) DTD $\Delta t^{n-1/2}$

12) DTIONT   Time step for updating debris ion deposition properties

13) TION   Ion deposition simulation time

COMMON/TEMPER/

1) TN2A $(T_p)^{n+1}_{j-1/2}$ Plasma temperatures (eV)

2) TN2B $(T_p)^{n+1/2}_{j-1/2}$

3) TN2C* $(T_p)^{n}_{j-1/2}$

4) TN1B $(T_p)^{n+1/2}_{j}$

5) TNSR2B $\sqrt{(T_p)^{n+1/2}_{j-1/2}}$ $(eV)^{1/2}$

6) TR2A $\quad (T_R)_{j-1/2}^{n+1}$ Radiation temperatures (eV)

7) TR2B $\quad (T_R)_{j-1/2}^{n+1/2}$

8) TR2C* $\quad (T_R)_{j-1/2}^{n}$

9) TR1B $\quad (T_R)_{j}^{n+1/2}$

10) TBC** $\quad$ temperature boundary condition (eV)

COMMON/CNTROL/

1) CON** $\quad$ real constants used in FIRE

2) ISW** $\quad$ control switches

3) IEDIT** $\quad$ intermediate output cycle frequencies

4) IO* $\quad$ primary output frequency vector

5) INDEX $\quad$ a vector used for output indexing

6) T1

7) T2 $\qquad$ temporary vectors to be used for any purpose within a

8) T3 $\qquad$ subroutine

9) T4

10) T5

11) T6

12) T7

13) T8

14) T9

15) T10

16) TGRØW** $\quad$ max percentage that Δt can increase in one cycle

67

17) TEDIT[**]   time at which output freq. switches from IO(1) to IO(11) (s)

18) GEOFAC   a geometry factor; 1, 2π, 4π

19) R3N   worst case for $\Delta T_p/T_p$

20) TSCC[**]   Courant condition time step control

21) TSCV[**] $\Delta V/V$ time step control

22) R1   worst case for Courant condition

23) R2   worst case for $\Delta V/V$

24) IDELTA[**]   1 = cartesian   2 = cylindrical   3 = spherical

25) IDELM1   0 = cartesian   1 = cylindrical   2 = spherical

26) NCYCLE   time cycle index

27) NMAX[*]   max number of time steps

28) JMAX[*]   max number of spatial zones

29) JMAXM1   JMAX-1

30) JMAXP1   JMAX+1   used for indexing

31) JMAXP2   JMAX+2

32) JMAXVØ   maximum spatial index for vapor phase at t=0

33) JMAXV   maximum spatial index for vapor phase

34) JMINC   minimum spatial index for condensed phase

35) JMAXT   maximum spatial index for condensed phase

36) NCZONS   initial number of zones in condensed phase

37) ILUNIT   output units for flux quantities

38) JCOUR   zone # of Courant condition worst case

39) JSPVOL   zone # of $\Delta V/V$ worst case

40) JNTEMP   zone # of $\Delta T_p/T_p$ worst case

41) IZONE   zone # of worst case of Courant, $\Delta V/V$, $\Delta T_p/T_p$

42) ITYPE   1 = Courant   2 = $\Delta V/V$ 3 = $\Delta E_R/E_R$ 4 = $\Delta T_p/T_p$ worst restriction

43) IITYPE 0 = physical -1 = min Δt 1 = max Δt

44) IIZONE   zone # of worst case if the Δt is Δt_{max} or Δt_{min}

45) ICOND   principal time step constraint

46) ICOND2   secondary time step constraint if primary is Δt_{min} or Δt_{max}

47) IUNIT cm^2, radian-cm, steradian for $\delta = 1, 2, 3$

48) TSCTN** $\Delta T_p/T_p$ time step control

49) IOBIN**   output frequency of binary output

50) RADIUS**   the radius of the first wall (41-47 are for automatic zoning option)

51) PMASS**   the mass of the pellet

52) RI**   the radius of the first zone, #1

53) RO**   the inner radius of the last zone, #JMAX

54) RO2   not used

55) NI**   the number of zones in the inner constant mass region

56) NO**   the number of zones in the outer constant mass region

57) RATIO   mass ratio between successive zones in transition region

58) R3R   worst case for $\Delta E_R/E_R$

59) TSCTR* $\Delta E_R/E_R$ time step control

60) JRTEMP   zone # of $\Delta E_R/E_R$ worst case

61) NFG**   the number of frequency groups

62) NMAT   number of gas types

63) TSCTB   boiling temperature time step control

64) TSCTF   material temperature time step control

65) TSCLM   Lagrangian mass time step control

COMMON/HYDROD/

1) U1D $u_j^{n-1/2}$ fluid velocity (cm/s)

2) U1B** $u_j^{n+1/2}$

3) DR2B $\Delta r_{j-1/2}^{n+1/2}$ zone widths (cm)

4) DR2A $\Delta r_{j-1/2}^{n+1}$

5) R1C r_j^n radius (cm)

6) R1B $r_j^{n+1/2}$

7) R1A r_j^{n+1}

8) RS1C $(r_j^n)^{\delta-1}$

9) RS1B $(r_j^{n+1/2})^{\delta-1}$

10) RS1A $(r_j^{n+1})^{\delta-1}$

11) PR2C $(P_R)_{j-1/2}^n$ radiation pressure (J/cm^3)

12) PR2B $(P_R)_{j-1/2}^{n+1/2}$

13) PR2A $(P_R)_{j-1/2}^{n+1}$

14) PN2C $(P_P)_{j-1/2}^n$ gas pressure (J/cm^3)

15) PN2B $(P_P)_{j-1/2}^{n+1/2}$

16) PN2A $(P_P)_{j-1/2}^{n+1}$

17) P2C $P^n_{j-1/2}$ total pressure (J/cm^3)

18) P2A $P^{n+1}_{j-1/2}$

19) V2C $V^n_{j-1/2}$ specific volume (cm^3/g)

20) V2B $V^{n+1/2}_{j-1/2}$

21) V2A $V^{n+1}_{j-1/2}$

22) VO   initial specific volume

23) COMPR   VO/V compression

24) VDOT2B $\dot{V}^{n+1/2}_{j-1/2}$ time derivative of sp. volume ($cm^3/g\text{-}s$)

25) DMASS2 $\Delta m_{o_{j-1/2}}$ Lagrangian mass $\delta=1$ g/cm^2

                                         $\delta=2$ g/cm-radian

                                         $\delta=3$ g/steradian

26) DMASS1 $\Delta m_{o_j} = (\Delta m_{o_{j-1/2}} + \Delta m_{o_{j+1/2}})/2$

27) Q2B $q^{n+1/2}_{j-1/2}$ artificial viscosity (J/cm^3)

28) VOL2B $V^{n+1/2}_{j-1/2}$ zone volume (cm^3)

29) VOL2A $V^{n+1/2}_{j-1/2}$

30) DMOM1C   Momentum lost by debris ions during Δt^n

31) DMASSØ   Initial values of DMASS2

32) VMAX   max compression

33) TAVMAX   time of max compression (s)

34) TOTMSØ   initial mass (gm)

COMMON/ESCOM/

1) ER2C $E_{R_{j-1/2}}^{n}$ radiation energy density (J/cm^3)

2) ENT2B $(C_v)_{j-1/2}^{n+1/2}$ plasma specific heat (J/eV-g)

3) ER2B $E_{R_{j-1/2}}^{n+1/2}$ radiation energy density (J/cm^3)

4) PNT2B $(P_p)_{T_{j-1/2}}^{n+1/2}$ temperature derivative of gas pressure (J/cm^3-eV)

5) ER2A $(E_R)_{j-1/2}^{n+1}$ radiation energy density (J/cm^3)

6) EN2A $(E_p)_{j-1/2}^{n+1}$ plasma specific internal energy (J/g)

7) DE2A $(n_e)_{j-1/2}^{n+1}$ electron number density (1/cm^3)

8) DN2A $(n_p)_{j-1/2}^{n+1}$ ion number density

9) DE2B** $(n_e)_{j-1/2}^{n+1/2}$ electron number density

10) DN2B* $(n_p)_{j-1/2}^{n+1/2}$ ion number density

11) ATW2B* $A_{j-1/2}^{n+1/2}$ average ion atomic weight (amu)

12) ZT2B $\partial Z/\partial T_{j-1/2}^{n+1/2}$ temperature derivative of average charge (esu/eV)

13) Z2B** $Z^{n+1/2}_{j-1/2}$ average charge (esu)

14) ZSQ2B $(Z^{n+1/2}_{j-1/2})^2$ average squared charge $(esu)^2$

15) EPSLON   a parameter that indicates how far out of equilibrium the radiation energy density is

16) JMAT   material type index

17) JMN   minimum spatial index for vapor and condensed phases

18) JMX   maximum spatial index for vapor and condensed phases

19) VBC**   specific volume boundary condition (cm^3/g)

20) AD

21) AT   coefficients defining the grid for the equations of state

22) BD

23) BT

24) EBC   radiation energy density boundary condition

25) RAD   1/AD

26) RAT   1/AT

27) RBT   1/BT

28) RBD   1/BD

COMMON/ESCOM1/

1) HEADR1   character description of EOS table #1

2) HEADR2   character description of EOS table #2

3) ZTAB   plasma charge state table

4) ENTAB   plasma specific internal energy table

5) CVTAB   heat capacity table

6)	DZDTAD		charge state temperature derivative table
7)	RRTAB		multigroup Rosseland opacity table
8)	RPTAB		multigroup Planck opacity table
9)	RPETAB		multigroup Planck emission opacity table
10)	RMFTAB		Planck opacity table
11)	ROSTAB		Rosseland opacity table

COMMON/COEFF/

1)	ROSS2B	$(\sigma_R)_{j-1/2}^{n+1/2}$	Rosseland opacity (cm^2/g)
2)	KANM1B	$(K_P^-)_j^{n+1/2}$	plasma thermal conductivity (J/cm-eV-s)
3)	KANP1B	$(K_P^+)_j^{n+1/2}$	
4)	KARM1B	$(K_R^-)_j^{n+1/2}$	radiation thermal conductivity (cm^2/s)
5)	KARP1B	$(K_R^+)_j^{n+1/2}$	
6)	OMP2B	$(\omega_P)_{j-1/2}^{n+1/2}$	plasma emission coefficient (J/eV-g-s)
7)	OMR2B	$(\omega_R)_{j-1/2}^{n+1/2}$	plasma absorption coefficient (cm^3/s-g)
8)	RMFP2B	$(\sigma_P)_{j-1/2}^{n+1/2}$	Planck opacity (cm^2/g)
9)	RMFT2B	$(\sigma_P)_{j-1/2}^{n+1/2}$	Planck opacity for $T_P = T_R$ (cm^2/g)
10)	SION2B	$\Delta KE_{d\,j-1/2}^{n}$	change in debris kinetic energy during Δt^n (J/gm/sec)
11)	SHOK2B		shock heating (J/gm/s)

12) LAMN2B $\quad (\ell n\Lambda_{ei})_{j-1/2}^{n+1/2}$ Spitzer log Λ

13) FLIM1B $\quad$ radiation flux limit $(J/cm^2 \cdot s)$

14) RFLU1B $\quad$ diffusion flux $(J/cm^2 \cdot s)$

15) TDXRED $\quad S_{j-1/2}^{n}$ time-dependent x-ray source term (J/g)

COMMON/COEFF1/

1) BET12B $\quad (\beta_1)_{j-1/2}^{n+1/2}$

Beta Vector

2) BET22B $\quad (\beta_2)_{j-1/2}^{n+1/2}$

3) AL112B $\quad (\alpha_{11})_{j-1/2}^{n+1/2}$

Diagonal Elements of Alpha Matrix

4) AL222B $\quad (\alpha_{22})_{j-1/2}^{n+1/2}$

5) OM112B $\quad (\omega_{11})_{j-1/2}^{n+1/2}$

Diagonal Elements of Omega Matrix

6) OM222B $\quad (\omega_{22})_{j-1/2}^{n+1/2}$

7) GM112B $\quad (\gamma_{11})_{j-1/2}^{n+1/2}$

Diagonal Elements of Gamma Matrix

8) GM222B $\quad (\gamma_{22})_{j-1/2}^{n+1/2}$

9) AA111B $\quad (a_{11})_{j}^{n+1/2}$

Diagonal Elements of "a" Matrix

10) AA221B $\quad (a_{22})_{j}^{n+1/2}$

11) OM122B $\quad (\omega_{12})_{j-1/2}^{n+1/2}$

Off Diagonal Elements of Omega Matrix

12) OM212B $\quad (\omega_{21})_{j-1/2}^{n+1/2}$

COMMON/COEFF2/

1) E11 (E_{11})

2) E12 (E_{12})

                         All Elements of the "E" Matrix

3) E21 (E_{21})

4) E22 (E_{22})

5) F1 (F_1)

                         Both Components of the "F" Vector

6) F2 (F_2)

7) B11 (B_{11})

8) B12 (B_{12})

                         All Elements of the "B" Matrix

9) B21 (B_{21})

10) B22 (B_{22})

11) D1 (D_1)

                         Both Elements of the "D" Vector

12) D2 (D_2)

COMMON/ECKCOM/

1) T1A $(T)_j^{n+1}$ kinetic energy of fluid (J/x)

2) GGGE2A $(G_e)_{j-1/2}^{n+1}$ radiation-gas work (J/x)

3) HHHR2B $(H_R)_{j-1/2}^{n+1/2}$ radiation source (J/x)

4) HHHN2B $\quad (H_p)_{j-1/2}^{n+1/2}$ $\quad$ gas source (J/x)

5) EEEC2A $\quad (E_c)_{j-1/2}^{n+1}$ $\quad$ radiation-gas energy exchange (J/x)

6) FSAVE $\quad$ heat fluxes at first wall (J/cm^2-s)

7) PSAVE $\quad$ pressures at first wall (J/cm^3)

8) TSAVE $\quad$ times of heat fluxes and pressures (s)

9) EEEERO $\quad E_{R_o}$ $\quad$ total initial radiation internal energy (J/x)

10) EEEENO $\quad E_{p_o}$ $\quad$ total initial gas internal energy (J/x)

11) EEEEER $\quad (E_R)^{n+1}$ $\quad$ total radiation internal energy (J/x)

12) EEEEEN $\quad (E_p)^{n+1}$ $\quad$ total gas internal energy (J/x)

13) TTTTT $\quad (T)^{n+1}$ $\quad$ total fluid kinetic energy (J/x)

14) HHHHHR $\quad (H_R)^{n+1}$ $\quad$ total radiation source (J/x)

15) HHHHHN $\quad (H_p)^{n+1}$ $\quad$ total gas source (J/x)

16) EEEEEC $\quad (E_c)^{n+1}$ $\quad$ total radiation-gas energy exchanged (J/x)

17) GGGGGE $\quad (G_e)^{n+1}$ $\quad$ total radiation-gas work (J/x)

18) WWWWWR $\quad (W_R)^{n+1}$ $\quad$ total work done on radiation (J/x)

19) WWWWWN $\quad (W_p)^{n+1}$ $\quad$ total work done on gas (J/x)

20) FFFFFR $\quad (F_R)^{n+1}$ $\quad$ total radiation heat lost across outer boundary (J/x)

21) FFFFFN $(F_p)^{n+1}$ total gas heat lost across outer boundary (J/x)

22) WWWWR $(W_R)^{n+1}$ total work done on radiation on last cycle (J/x)

23) WWWWN $(W_p)^{n+1}$ total work done on gas on last cycle (J/x)

24) FFFFR $(f_R)^{n+1}$ total radiation lost at outer bd. on last cycle (J/x)

25) FFFFN $(f_p)^{n+1}$ total gas energy lost at outer bd. on last cycle (J/x)

26) HHHHR $(h_R)^{n+1}$ total radiation source on last cycle (J/x)

27) HHHHN $(h_p)^{n+1}$ total gas source on last cycle (J/x)

28) EEEEC $(e_c)^{n+1}$ total radiation-gas heat exchange on last cycle (J/x)

29) GGGGE $(g_e)^{n+1}$ total work to maintain one fluid on last cycle (J/x)

30) ENLHS   left side of gas energy balance equation (J/x)

31) ETLHS   left side of total energy balance equation (J/x)

32) ERRHS   right side of radiation energy balance equation (J/x)

33) ENRHS   right side of gas energy balance equation (J/x)

34) ETRHS   right side of total energy balance equation (J/x)

35) TTTTNO   initial kinetic energy (J/x)

36) PMAX   maximum pressure at the wall (J/cm^3)

37) TPMAX   time of maximum pressure (s)

38) FMAX   maximum radiation heat flux at the wall (J/cm^2-s)

39) TFMAX   time of maximum heat flux (s)

40) NPMAX   time step of max. pressure

41) NSAVE   index into FSAVE, PSAVE, and TSAVE

42) NFMAX   time step of max. heat flux

43) XXXXXN   energy exchanged between vapor and condensed phases
               (old vaporization model)

44) HFINTGL   Time-integrated heat flux at the wall (J/cm**2)

45) TIMPLS   Time-integrated pressure at the wall (J/sec/cm**3)

where $\delta=1$ $x = cm^2$

   $\delta=2$ $x = cm-radian$

   $\delta=3$ $x = steradian$

COMMON/IONCOM/

1) ATN2B*   Atomic number of the background plasma

2) DIMASS   Debris ion mass deposited in each Lagrangian cell during
             one time step (g)

3) XIKE2B   Debris ion energy deposited in the plasma (J)

4) TOTION   Total debris energy deposited in each Lagrangian cell (J)

5) XIONIN*   Ion flux array (ions/sec)

6) EIONIN*   Ion energy array (keV/particle)

7) TIONIN*   Ion time array (sec)

8) AWION*   Atomic weight of the debris ions (amu)

9) ANION*   Atomic number of the debris ions

10) Q1INIT*   Initial charge state of the debris ions

11) CDEPCN   Constants used in stopping power calculation

12) TIONDP   Ion deposition update times (sec)

13) ATNION   Debris ion atomic number

14) ATWION   Debris ion atomic weight (amu)

15) WALION   Debris ion energy deposited in the wall (J)

16) TIONEN   Estimated ending time of ion energy deposition (sec)

17) SRCION   Total ion energy emitted by the source (J)

18) NIX*   Number of debris ion species

19) NIE*   Number of debris ion energy bins

20) NIT*   Number of debris ion time bins

21) PLSION   Time-integrated ion energy deposited in the entire
               background plasma (J)

22) PLSIKE   Time-integrated ion energy deposited in the background
               plasma by stopped ions (J)

23) Z1EFF   Effective charge state of debris ions

24) ITION   Ion deposition update cycle number

25) WALIEB   Ion energy deposition rate at the wall (J/sec)

26) TIDEPR   Ion deposition time step ratio

COMMON/XRAY/

1) EXRAY   the energy of the x-rays in each group (keV)

2) FXRAY   the energy in each x-ray group (J/keV)

3) UXRAY   x-ray attenuation coefficients computed from tables (cm^2/g)

4) IZ[**]   the atomic number of the plasma in each zone

5) TDXAMP   time-dependent x-ray amplitudes

6) ATTENC   attenuation coefficients

7) COEF   coefficients computed from x-ray cross section tables

8) ELIM   a vector used in computing the x-ray cross sections

9) XRTIM   times at which x-ray amplitudes are specified

10) XAMP[**]   the amplitude of an input x-ray spectrum (J/keV)

11) XEHIST[**]   the energy of the x-rays in each group of the input spectrum (keV)

12) CRLOC
13) CRA
14) CRB
15) CRHD   data for x-ray stopping cross sections
16) CRZOA
17) CONFAC

18) IATTEN

19) EDGE   the minimum x-ray energy required for absorption by electrons in each shell (keV)

20) SHELEL   the number of electrons in each shell

21) KEDGE   the number of shells the plasma atoms have

22) ONEZOA   a coefficient used in computing the x-ray scattering cross section

23) NXRG   number of x-ray groups

24) KEV[**]   the blackbody temperature of a blackbody x-ray spectrum (keV)

25) FLUX[**]   the total energy in x-rays input by the user (J)

81

26) SUMFLU   the energy in the x-ray spectra computed by FIRE (J)

27) NXRT   the number of times at which the input intensity is given

28) NUM   a number generated by the code in searching through the x-ray cross section tables

29) TXRED   the x-ray energy absorbed by the plasma (Joules)

30) ETXR

31) EETXR

32) STDXR

33) SSTDXR

34) EXRW

35) EEXRW

36) NIZJ

COMMON/MFRAD/

1) ERFD2A   frequency dependent radiation specific energy at t^{n+1} (J/g)

2) ERFD2C   frequency dependent radiation specific energy at t^{n} (J/g)

3) SRFE2B   frequency dependent radiation emission term at $t^{n+1/2}$ (J/g/s)

4) SR2B   frequency dependent Rosseland opacity (cm^{-1})

5) SP2B   frequency dependent Planck ABSORPTION opacity (cm^{-1})

6) SPE2b   frequency dependent Planck emission opacity (cm^{-1})

7) SER2B   frequency integrated radiation absorption (J/g/s)

8) SRE2B   frequency integrated radiation emission term (J/g/s)

9) HNU1   boundaries of frequency groups (keV)

10) HNU2   centers of frequency groups (keV)

11) RFDOUT   frequency dependent radiation energy flux at first wall on a given time cycle (J)

12) RFDINT   time integrated frequency dependent radiation energy flux at
            first wall up through a given time cycle (J)

COMMON/REZCM/

1) TMASS$\emptyset$ initial total mass of gas

2) NCREZ   number of cycles since last rezone

3) NDUM1   dummy variable

4) RZCM   fractional change in Lagrangian mass allowed before a rezone

5) DMOLD   Lagrangian masses at end of last rezone (cm)

6) DINTR1   interpolation variable

7) DINTR2   interpolation variable

8) RCENT   positions of zone centers (cm)

9) INDZN1   interpolation variable

10) INDZN2   interpolation variable

COMMON/XCHCOM/

1) TAVER   average temperature in boundary layer (ev)

2) TOTMS   total mass in boundary layer (g)

3) BDFLUX   radiant flux on wall (w/cm^2)

4) AWFILM   atomic weight of material (amu)

5) RSTPFM   width of boundary layer (cm)

6) V1   average speed of ions leaving material (cm/s)

7) DLTMSV   mass vaporized on current time step (g)

8) DLTMSC   mass condensed on current time step (g)

9) DLTENG   change in gas energy due to mass transfer

10) DUFLM1   temporary variable

11) DUFLM2   temporary variable

12) INFILM   temporary variable

13) DXWE2B   change in energy density in gas zones due to mass transfer (J/steradian)

14) DXWU1B   change in velocity of gas zones due to mass transfer (cm/s)

15) VAVER   average particle speed in gas in boundary layer (cm/s)

16) DAVER   average mass density in gas in boundary layer (g/cm^3)

17) TSH   temperature of surface of material (K)

18) CMFILM   time-integrated mass condensed (g)

19) SURFAR   surface area (cm^2)

20) RFILM   distances between material surface and temperature nodes in material (m)

21) R   constant used in heat transfer in material

22) CFLM1   constant used in heat transfer in material

23) CFLM2   constant used in heat transfer in material

24) RHOFLM   mass density at material nodes (kg/m^3)

25) TBPC   boiling temperature at material nodes at time n-1 (K)

26) XK   thermal conductivity at material nodes (MW/m-K)

27) DELX   distance between material nodes (m)

28) RHOHFG   phase change energy at material nodes (MJ/m^3)

29) CP   specific heat at material nodes (MJ/kg-K)

30) THETA   implicitness parameter

31) NX   number of material nodes

32) L1BC   type of boundary condition on back of material indicator

33) BC1   boundary condition on back of material

34) TFLMA   temperature at material nodes at time n (K)

35) TFLMB   temperature at material nodes at time n-1/2 (K)

36) TFLMC   temperature at material nodes at time n-1 (K)

37) TBPA   boiling temperature at material nodes at time n (K)

38) TBPB   boiling temperature at material nodes at time n-1/2 (K)

39) TNP1   temperature at material nodes at time n+1 (K)

40) MAT   material type at material nodes

41) EPS   surface emissivity

42) SIGSB   Stefan-Boltzmann constant = 5.729×10^{-16} (W/m^2-K^4)

43) CONST2   constant used in heat transfer in material

44) CONA1   constant used in heat transfer in material

45) DXOLD   distances between material nodes on previous time step (m)

46) QRAD   radiant energy loss from material (MW/m^2)

47) CONV   convergence criterion in model A vaporization

48) RHOCP   rhofilm * cp * xarea   (MJ/m^3-K)

49) RHOCPX   temporary variable

50) QINT   surface flux of volumetric heat source (MW/m^2)

51) FXMU   linear attenuation coefficient for each energy group in material (m^2/kg)

52) QVOL   volumetric heat source at material nodes (MW/m^3)

53) NVOL   number of energy groups for volumetric x-ray deposition in material

54) ENAVER   average energy density of gas in boundary layer (J/g)

55) TOTMSN   total mass (gm)

56) AMSDN   average mass density in gas (gm/cm^3)

57) XAREA   heat transfer enhancement factor to account for increased surface area

58) UNFLM   energy density at material node (MJ/m^3)

59) UNFVAP   energy going into vaporization (MJ/m^2)

60) QCOND   condensation energy on surface of material in current time step (J)

61) TBPO   boiling temperature of material at 1 atmosphere vapor pressure (K)

62) VCONA   Antoine's constant A

63) VCONB   Antoine's constant B

64) VCONC   Antoine's constant C

65) TBPO1   inverse of TBPO (1/K)

66) UNFLM1   energy density required to vaporize material (MJ/m^3)

67) FSTICK   sticking coefficient

COMMON/XCHCM2/

1) DELXC   cell sizes in the condensed region (cm)

2) TCN2A   temperature in the condensed region (eV)

3) TCN2B   temperature in the condensed region (eV)

4) TCN2C*   temperature in the condensed region (eV)

5) XKCOND*   thermal conductivity in the condensed region (J/cm/s/eV)

6) RHOCND*   mass density of the condensed region (g/cm^3)

7) QHEATV*   specific heat of varporization of the condensed region (J/g)

8) CPHEAT*   specific heat of the condensed region (J/g/eV)

9) TVAPØ   vaporization temperature at 1 bar (eV)

10) TWALLB*   temperature at the back of the condensed region (eV)

11) DELXCT   total width of the condensed region (cm)

12) UNSENS   specific internal energy at the vaporization temperature (J/g)

13) UNVAP   specific internal energy required to vaporize (J/g) (UNSENS + QHEATV)

14) TVAP   vaporization temperature (eV)

15) DMVCDT   net vaporization rate (g/sec)

16) IZFILM*   atomic number of the condensed region

17) TMASVP   total mass vaporized (g)

18) FRACMV   mass fraction of the interface zone in the vapor phase

19) FRACMC   mass fraction of the interface zone in the condensed phase

20) UNFINP   time-integrated radiation and debris ion energy added to the condensed region (J)

21) DUFINP   radiation and ebris ion energy added to the condensed region (J)

22) HVSTOR   time-integrated energy stored in the heat of vaporization (J)

23) DHVSTO   energy stored in the heat of vaporization (J)

24) WVSTOR   time-integrated work energy due to phase change (J)

25) DWVSTO   work energy due to phase change (J)

26) HVSTO∅   energy stored in the heat of vaporization due to prompt x-rays (J)

27) UNFLM∅   initial internal energy of the condensed region (J)

28) UNFLMT   total internal energy of the condensed region (J)

29) UNBACK   time-integrated energy conducted through the back of the condensed region (J)

30) DUNBAK   energy conducted through the back of the condensed region (J)

31) UVAPMT   time-integrated energy added to the vapor phase due to phase change (J)

32) DUVPMT   energy added to the vapor phase due to phase change (J)

33) UCNDMT   time-integrated energy added to the condensed region due to phase change (J)

34) DUCNMT   energy added to the condensed region due to phase change (J)

35) VAPMAS   vapor mass of the non-condensable and condensable gases (g)

COMMON/DBUGCM/

1) NOBUG*   logical flag; true if no debug output requested

2) NAMEDB   subroutine names for which debug output is requested

3) NCYCLD*   beginning cycle number for debug output

4) ICYCLD*   cycle increment for debug output

5) TBEGDB*   simulation time at which debug output begins (sec)

6) TENDDB*   simulation time at which debug output ends (sec)

COMMON/TDION/

1) NQTDEP*   maximum number of ionization states tracked in a
               time-dependent debris ion calculation

2) IQMIN   minimum charge state for debris ions in rate equation solution

3) IQMAX   maximum charge state for debris ions in rate equation solution

4) Q1MIN*   minimum allowable charge state for debris ions

5) POTEN   ionization potentials for debris ions (eV)

6) FRACIZ   fractional ionization abundances of the debris ions

7) BGPOTN   ionization potentials for the background plasma (eV)

8) RATCON   constants used in rate equations for debris ions

9) NPRING   principle quantum number of the outermost bound electron
               of an ion

10) Z1AVER   average charge state for each debris ion group

COMMON/LENGTH/

 1) LTIME   number of words in common block /TIME/

 2) LTEMPE   number of words in common block /TEMPER/

 3) LCNTRL   number of words in common block /CNTROL/

 4) LHYDRO   number of words in common block /HYDROD/

 5) LESCM   number of words in common block /ESCOM/

 6) LESCM1   number of words in common block /ESCOM1/

 7) LCOEFF   number of words in common block /COEFF/

 8) LCOEF1   number of words in common block /COEFF1/

 9) LCOEF2   number of words in common block /COEFF2/

10) LECCOM   number of words in common block /ECKCOM/

11) LIONCM   number of words in common block /IONCOM/

12) LXRAY   number of words in common block /XRAY/

13) LMFRAD   number of words in common block /MFRAD/

14) LRZCOM   number of words in common block /REZCM/

15) LXCHNG   number of words in common block /XCHCOM/

16) LXCHG2   number of words in common block /XCHCM2/

17) LDEBUG   number of words in common block /DBUGCM/

17) LTDION   number of words in common block /TDION/

10.4 The Input Variables

The CONRAD code reads namelist input from I/O unit 5. The variables that must appear in the namelist called INPUT are given in Table 1. Real variables are denoted by RV, and integer variables by IV. The variables with default values are given in Table 2, and they need not appear in the namelist unless another value is desired. Table 3 contains the variables used for an x-ray deposition calculation. Table 4 contains the variables used if the automatic zoning option is specified. Tables 5a and 5b contains input variables for vaporization/condensation model. Table 6 contains the variables used to run a debris ion deposition calculation. Table 7 contains definitions of the integer switches used to control the code. Table 8 lists the real constants used by the code that can be changed by input. Table 9 gives the intermediate output vector that allows all internally computed quantities to be output for debugging.

Table 1. Input Variables

Variable	Type	Default Value	Description
JMAX	(IV)	---	Number of spatial zones $3 \leq$ JMAX ≤ 259
NMAX	(IV)	---	Maximum number of time steps
TMAX	(RV)	---	Maximum problem time (s)
IO	(IV)	---	Output frequencies IO(1) -- hydrodynamics IO(2) -- energy IO(3) -- mfp's and # densities IO(4) -- short edit IO(5) -- multifrequency radiation IO(11) -- same as IO(1)-(5) except after IO(12) time TEDIT (see TEDIT description) IO(13) IO(14) IO(15)
DR2B	(RV)	---	Δr of each zone (cm) (DR2B is only input if automatic zoning is not used)
DN2B	(RV)	---	Plasma number density (cm^{-3})
TN2C	(RV)	---	Plasma temperature (eV)
TR2C	(RV)	---	Radiation temperature (eV)
ATW2B	(RV)	---	Atomic weight (amu)
RCENT	(RV)	---	Positions of input vectors (cm)
RZCM	(RV)	0.01	Mass change before rezone

Table 2. Optional Input Variables

Variable	Type	Default Value	Description
IDELTA	(IV)	3	Geometry = 1 planar = 2 cylindrical = 3 spherical
TA	(RV)	0	Simulation time (s)
DTB	(RV)	10^{-12}	Initial time step (s)
DTMIN	(RV)	10^{-1}*DTB	Minimum time step (s)
DTMAX	(RV)	10^{-2}*TMAX	Maximum time step (s)
TSCC	(RV)	5×10^{-2}	Time Step Controls - Courant
TSCV	(RV)	5×10^{-2}	- $\Delta V/V$
TSCTR	(RV)	1×10^{35}	- $\Delta E_R/E_R$
TSCTN	(RV)	5×10^{-2}	- $\Delta T_p/T_p$
TSCTF	(RV)	5×10^{-2}	Film temperature
TSCTB	(RV)	5×10^{-2}	Boiling temperature
TSCLM	(RV)	0.1	Lagrangian mass
TEDIT	(IV)	-1	If TEDIT $\neq$ 0 then before time TEDIT IO(1)-(4) are used and after IEDIT IO(11)-(14) are used as output frequencies
IOBIN	(IV)	-1	Binary output frequency written to unit 8 for postprocessing
TGROW	(RV)	1.5	Time step is allowed to increase no more than TGROW*DTB on each successive cycle
TBC	(RV)	2.5×10^{-2}	Temperature boundary condition (eV)
Z2B	(RV)	0	Initial background plasma charge state.
VBC	(RV)	0.1	Specific volume boundary condition (cm^3/g)
R1B	(RV)	0	Zone boundary positions (cm)
U1B	(RV)	0	Initial velocity (cm/s)

Variable	Type	Default Value	Description
IRS	(IV)	0	Restart calculation flag = 0 Normal calculation = 1 Restarted calculation
ISW	(IV)	---	See Table 7 for definitions of these switches
CON	(IV)	---	See Table 8 for the definitions of these numerical coefficients
IEDIT	(IV)	-1	See Table 8 for the definitions of these intermediate output frequencies
ROSS2B	(RV)	---	Rosseland opacity; must be input if ISW(12)=1 or ISW(15)=1, and NFG-0
RMFP2B	(RV)	---	Planck opacity; must be input if ISW(12)=1 or ISW(14)=1, and NFG=0
RMFT2B	(RV)	---	Planck opacity for $T_R = T_p$; must be input if ISW(12)=1 or ISW(14)=1, and NFG=0
NFG	(IV)	0	Number of frequency groups for a multi-frequency radiation calculation. If NFG=0 then the 2-T option is used. $0 \le NFG \le 20$.
SP2B	(RV)	---	Planck group absorption opacity (cm^2/g); must be input if ISW(12)=1 and NFG$\neq$0
SPE2B	(RV)	---	Planck group emission opacity (cm^2/g); must be input if ISW(12)=1 and NFG$\neq$0
SR2B	(RV)	---	Rosseland group opacity (cm^2/g); must be input if ISW(12)=1 and NFG$\neq$0.
NMAT	(IV)	1	Number of materials
JMAT	(IV)	1	Material index for each zone
NAMEDB	(IV)	---	Subroutine name for debug output
NCYCLD	(IV)	---	Cycle increment for debug output
TBEGDB	(RV)	0	Simulation time to begin debug output(s)
TENDDB	(RV)	10^{10}	Simulation time to end debug output(s)

Table 3. Input Variables for X-Ray Deposition

Variable	Type	Default Value	Description
FLUX	(RV)	---	The total energy of a blackbody x-ray spectrum in Joules
NXRG	(IV)	25	The number of energy groups in the x-ray spectrum ≤ 20 for arbitrary histogram ≤ 100 for a blackbody spectrum
IZ	(IV)	---	The atomic number of each zone in the gas
KEV	(RV)	---	The blackbody temperature of a blackbody x-ray spectrum
XEHIST	(RV)	---	The bounds of energy groups in an arbitrary histogram in keV, JK+1 boundaries, lowest to highest, equal group widths are required
XAMP	(RV)	---	The amplitude of the groups of an arbitrary histogram in J/keV, JK amplitudes
CONFAC	(RV)	1	Density multiplier in x-ray deposition calculation.
NXRT	(IV)	---	Number of mesh times in time-dependent x-ray history
XRTIM	(RV)	---	Mesh times in time-dependent x-ray history(s)
TDXAMP(K,I)	(RV)	---	Time dependent x-ray amplitudes (J/Kev-S). In this 2-dimensional matrix, the first index, K, is the frequency group and the second index I is the time.

Table 4. Input Variables for Automatic Zoning

Variable	Type	Default Value	Description
NI	(IV)	---	Number of zones in the inner, constant mass region
RI	(RV)	---	The radius of the first zone (cm)
NO	(IV)	---	Number of zones in the outer, constant mass region
RO	(RV)	---	The radius of the inner boundary of the outermost zone (cm)
RADIUS	(RV)	---	The radius of the first wall (cm)
PMASS	(RV)	---	The pellet mass (g)

Table 5a. Input Variables for Vaporization/Condensation, Model I

Variable	Type	Default Value	Description
NX	(IV)	---	The initial number of material nodes
THETA	(RV)	---	The degree of implicitness in the heat transfer calculation in the material $0 \leq THETA \leq 1$ $= 0$ for explicit $= 1$ for fully implicit
MAT	(IV)	---	The material type for each node
EPS	(RV)	1.0	The surface emissivity of material
TBPO	(RV)	0.	The boiling temperature of the material at 1 atmosphere of vapor pressure (K)
TBPC	(RV)	---	The initial boiling temperature of the material at each node (K)
RHOFLM	(RV)	---	The mass density at each material node (kg/m^3)
CP	(RV)	---	The specific heat at each material node (MJ/kg-K)
DELX	(RV)	---	The initial spacing between material nodes (m)
RHOHFG	(RV)	---	The phase change energy (liquid or solid to vapor) at each material node (MJ/m^3)
L1BC	(IV)	---	The type of boundary condition on the back surface of material $= 1$ for Dirichlet $= 2$ for Neuman $= 3$ for Radiation
BC1	(RV)	---	The boundary value at the back of the material (K)
TFLMC	(RV)	---	The initial temperatures at the material nodes (K)
CONV	(RV)	0.005	The convergence criterion for model A type vaporization

96

Variable	Type	Default Value	Description
XK	(RV)	---	The thermal conductivity at the material nodes (MW/m-K)
AWFILM	(RV)	---	The atomic weight of the material (amu)
XAREA	(RV)	1.0	The heat transfer enhancement factor due to a larger surface area from a granular surface
VCONA	(RV)	0.0	Antoine's constant A
VCONB	(RV)	0.0	Antoine's constant B
VCONC	(RV)	0.0	Antoine's constant C
FSTICK	(RV)	1.0	The sticking coefficient
CMFILM	(RV)	0	Time-integrated mass condensed (g)
NTMSH	(IV)	0	# of mesh points for thermal properties input grid
CPMSH	(RV)	---	Mesh specific heats (MJ/Kg-K)
XKMSH	(RV)	---	Mesh thermal conductivities (Mw/m-K)
TMSH	(RV)	---	Mesh temperatures (K)
JVDEP	(IV)	---	# of gas zones over which vaporized mass is spread. Only used if ISW(27)≠0.

Table 5b. Input Variables for Vaporization/Condensation, Model II

Variable	Type	Default Value	Description
NCZONS	(IV)	0	Number of Lagrangian cells in the condensed region
RHOCND	(RV)	---	Mass density of the condensed region (g/cm^3)
XKCOND	(RV)	---	Thermal conductivity of the condensed region $(J/cm/s/eV)$
QHEATV	(RV)	---	Specific heat of vaporization of the condensed region (J/g)
CPHEAT	(RV)	---	Specific heat of the condensed region $(J/g/eV)$
IZFILM	(RV)	---	Atomic number of the condensed region
TVAPØ	(RV)	---	Vaporization temperature at 1 bar (eV)
TWALLB	(RV)	---	Temperature at the back of the condensed region (eV)
DELXC	(RV)	---	Zone widths for the condensed region (cm)
TCN2C	(RV)	---	Temperatures in the condensed region (eV)
DELXCT	(RV)	---	Total width of the condensed region (cm)
VAPMAS	(RV)	---	Vapor mass of the non-condensable and condensable gases (g)
JMN	(IV)	---	Minimum zone indices for the vapor and condensed regions
JMX	(IV)	---	Maximum zone indices for the vapor and condensed regions

Table 6. Input Variables for Debris Ion Deposition

Variable	Type	Default Value	Description
NIX	(IV)	---	Number of debris ion species
NIE	(IV)	---	Number of debris ion energy bins
NIT	(IV)	---	Number of debris ion time bins
XIONIN	(RV)	---	Ion flux array (ions/sec)
EIONIN	(RV)	---	Ion energy array (keV/particle)
TIONIN	(RV)	---	Ion time array (sec)
ANION	(RV)	---	Atomic number of the debris ions
AWION	(RV)	---	Atomic weight of the debris ions (amu)
ATN2B	(RV)	---	Atomic number of the background plasma
Q1MIN	(RV)	---	Minimum allowable charge state for the debris ions
TIONDP	(RV)	---	Ion deposition update times (sec)
TIDEPR	(RV)	0.	Ion deposition time step ratio

Table 7. Control Switches

ISW		Description
1	= 0*	$T_R \sim E_R^{1/4}$
	= 1	$T_R \sim$ dilute Planckian
2	= 10*	number of constant time steps used at the beginning of a calculation
3	not used	
4	= 0*	user specifies zoning with DR2B
	= 1	automatic zoning (see Table XII-4)
5	= 20*	frequency of tabulation of overpressure and heat flux at the first wall
6	= 0*	hydrodynamic motion is computed
	= 1	no hydro motion -- allows a pure temperature diffusion problem
7	not used	
8	= 0*	no pellet debris deposition
	= 1	pellet debris expands into the gas
9	not used	
10	= 1*	frequency of time step calculation
11	= 0*	initial x-ray deposition is computed
	= 1	calculation begins from input temperatures
	= 2	time-dependent x-rays only
	= 3	both time-dependent and initial x-ray deposition
12	= 0*	equation of state tables are used
	= 1	ideal gas equation of state is used. RMFP2B, RMFT2B, ROSS2B, and CON(5) must be input via &INPUT
13	= 20/NFG	number of subgroups to divide frequency groups into when doing the integration
14	= 0*	Planck opacity is computed from tables
	= 1	Planck opacity is computed as a constant
15	= 0*	Rosseland opacity is computed from tables
	= 1	Rosseland opacity is inputted as a constant
16	= 0*	normal program termination
	= 1	stops in QUITCR; allows for FLOWTRACE option

100

ISW	Description	
17	≤ 0*	no dynamic rezoning
	> 0	mass # of cycles between rezonings
18	not used	
19	not used	
20	= 0*	no condensation or vaporization
	= 1	condensation on surface done
21	= 0*	momentum exhcange calculated between film and gas
	= 1	no momentum exchange
22	= 0*	energy exchange calculated between films and gas
	= 1	no energy exchange
23	not used	
24	= 0*	
	= 1	
25	= 0*	use model C for vaporization
	= 1	use model A for vaporization
	= 2	use model B for vaporization
26	= 0*	
27	= 0*	equation of state tables in MIXERG format
	= 1	equation of state tables in IONMIX format
	= 2	equation of state tables in SESAME format
28	= 0*	use bi-linear interpolation with SESAME data
	= 1	use bi-quadratic interpolation with SESAME data
	= 2	use bi-rational-function interpolation with SESAME data
30	= 0*	use input values for properties of film
	= 1	calculate properties of film
31	= 0*	use Q1INIT (= constant) for ion deposition calculations
	= 1	compute time-dependence of debris ion charge states
32	= 0*	no debris ion mass added to vapor cells
	= 1	add debris ion mass to vapor cells as ions stop.

*Denotes the default value.

Table 8. Real Constants Used in CONRAD

CON	Default	Description
1	1.2175×10^2	gas thermal conductivity
2	1×10^{10}	radiation thermal conductivity
3	0.1	the percentage by which the radiation can be out of equilibrium before the nonequilibrium mean free path is used in the absorption term
4	1×10^{-30}	small term to avoid zero divide in flux limited radiation conduction term AA221B
5	0	if non-zero then it is used as a constant value of $\log \Lambda$. Normally $\log \Lambda$ is computed.
6	1.37×10^{-5}	$4\sigma/c$ $(J/cm^3 \cdot eV^4)$
7	4.12×10^5	radiation emission term
8	3×10^{10}	radiation absorption term
9	1.602×10^{-19}	gas pressure
10	3×10^{10}	radiation flux limit
11		not used
12	1.602×10^{-19}	gas pressure derivative
13		not used
14	2.403×10^{-19}	gas specific heat
15	2.403×10^{-19}	gas specific internal energy
16	1.37×10^{-5}	radiation specific internal energy $(J/cm^3 \cdot eV^4)$
17	0.0	up-stream average parameter
18	1.0	ion shock heating term
19		not used
20		not used
21	1.414	artificial viscosity coefficient
22	3×10^{10}	multifrequency radiation absorption term

CON	Default	Description
23	6.334918×10^4	multifrequency radiation emission term
24	10^{10}	multifrequency radiation conductivity term
25	3×10^{10}	multifrequency radiation flux limit
26	1×10^{-20}	minimum allowable multifrequency radiation specific energy
27		not used
28		not used
29		not used
30	1.381×10^{-29}	Boltzmann constant for use in subroutine FILM (MJ/K)
31	1.	vaporization rate multiplier
32	1.	condensation rate multiplier
33	0.	vaporization/condensation flux correction term
34	31.2	constant for reducing condensation rate due to the presence of a non-condensable gas
35	1.	Charge exchange cross section multiplier for debris ion energy deposition
36	0.	mass progression factor for automatic zoning ($\emptyset. \rightarrow$ zones of constant mass)
37		not used
38		not used
39		not used
40		not used
41		not used
42		not used
43	1.	x-ray flux multiplier
44	1.	debris ion flux multiplier

CON	Default	Description
45	2.	ion thermal velocity term
46	1.	relative debris ion velocity term
47		not used
48		not used
49		not used

Table 9. Description of the Intermediate Output Switches in IEDIT

IEDIT	Subroutine	Variables
1	ABCDEF	A11, A22, B11, B12, B21, B22, C11, C22, D1, D2, E11, E12, E21, E22, F1, F2
2	MATRIX	AL112B, AL222B
3	MATRIX	OM112B, OM122B, OM212B, OM222B
4	MATRIX	GM112B, GM222B
5	MATRIX	AA111B, AA221B
6	MATRIX	BET12B, BET22B
10	OMEGA	OMR2B, OMP2B
11	KAPPA	KARM1B, KARP1B, KANM1B, KANP1B, LAMN2B, FLIM1B
12	POINT	KEOS, LEOS, MEOS
13	TABLE2,3,0	aa, aader
14	HYDRO	U1B, R1A, R1B, DR2A, DR2B, RS1A, RS1B, V2A, V2B, VDOT2B
15	QUE	Q2B
16	TEMPBC	T1(1) → T1(9), TR2A (JMAXP1), TN2A (JMAXP1)
17	RADTR	ER2A, ERFD2A
19	NUMDEN	DN2B, DE2B, DN2A, DE2A
20	EMISSN	SRE2B, SRFD2B
21	ABCRAD	A22, B22, C22, D2, E22, F2
22	RADCOF	AL222B
23	RADCOF	GM222B
24	RADCOF	AA221B
25	RADCOF	BET22B
26	RCOND	KARM1B, KARP1B, FLIM1B
27	PLSCOF	AL112B

IEDIT	Subroutine	Variables
28	PLSCOF	GM112B
29	PLSCOF	AA111B
30	PLSCOF	BET12B
31	PCOND	KANM1B, KANP1B, LAMN2B
32	ABCPLS	A11, B11, C11, D1, E11, F1
33	RADCOF	OM222B
41	EOS1	DN2A1, TN2A1, EN2A1, Z2B1
50	IONDEP	SION2B, DMOM1C, WALION, Z1AVER, RION, XION
51	ECHECK	SUMION, TOTION
91	WXCHNG	
92	REZONE	
93	FILM	

10.5 Input Data

In addition to the NAMELIST input described in Section 11, CONRAD requires equation of state data and x-ray deposition data to be read in through units 3 and 11, respectively. Therefore, before one executes CONRAD, one must create files 3 and 11 and fill them with data that is in the proper form.

The x-ray deposition data is the same for all CONRAD runs. The source tape for CONRAD includes this file and one must only copy it into file 11 before executing CONRAD.

The equation of state data is dependent on the gas species and the range of densities and temperatures one is considering. One way of creating this data is to use the computer code IONMIX [13]. The data file created by IONMIX for the examples quoted in this paper is included on the CONRAD source tape. The files created by IONMIX are not in the proper form for use in CONRAD.

11. Sample Calculations

Two sample calculations are present here. One illustrates the use of CONRAD in calculating vaporization by target x-rays. The second shows a condensation calculation. For both calculations, the input file and sample output are shown. For calculations not involving vaporization or condensation, the reader is encouraged to consult the MF-FIRE documentation [3].

References

[1] G.A. Moses and R.R. Peterson, "FIRE - A Computer Code to Simulate Cavity Gas Response to Inertial Confinement Target Explosions," University of Wisconsin Fusion Technology Institute Report UWFDM-336 (January 1980).

[2] T.J. McCarville, R.R. Peterson, and G.A. Moses, "Improvements in the FIRE Code for Simulating the Response of a Cavity Gas to Inertial Confinement Fusion Target Explosions," Computer Physics Communications 28, 367 (1983).

[3] G.A. Moses, R.R. Peterson and T.J. McCarville, "MFFIRE - A Multifrequency Radiative Heat Transfer Hydrodynamics Code," Computer Physics Communications 36, 249 (1985).

[4] T.J. Bartel, R.R. Peterson and G.A. Moses, "Numerical Simulations of a Stratified Gas ICF Cavity," University of Wisconsin Fusion Technology Institute Report UWFDM-679 (April, 1986).

[5] T.J. McCarville, G.A. Moses, and G.L. Kulcinski, "A Model for Depositing Inertial Confinement Fusion X-Rays and Pellet Debris Into a Cavity Gas," University of Wisconsin Fusion Technology Institute Report UWFDM-406, April 1981.

[6] K.G. Adams and F. Biggs, "Efficient Computer Access to Sandia Photon Cross Sections II," SC-RR-71-0507, Sandia Laboratory, Albuquerque, NM, December 1971.

[7] T.A. Melhorn, "A Finite Material Temperature Model for Ion Energy Deposition in Ion-Driven ICF Targets," SAND80-0038, Sandia National Laboratories, Albuquerque, NM, May 1980.

[8] J. Lindhard and M. Scharff, "Energy Dissipation by Ions in the keV Range," Phys. Rev. 124, 128 (1961).

[9] J.J. MacFarlane, "IONMIX - A Code for Computing the Equation of State and Radiative Properties of LTE and Non-LTE Plasmas," University of Wisconsin Fusion Technology Institute Report UWFDM-750, December 1987, submitted to Computer Physics Communications.

[10] H. Knudson, H.K. Haugen, and P. Hvelplund, "Single-Electron-Capture Cross Sections for Medium and High Velocity, Highly Charged Ions Colliding with Atoms," Phys. Rev. A23, 597 (1981).

[11] E. Hyman, M. Mulbrandon, and J.L. Giuliani, "Charge Exchange Cross Section Update," ETHANL Proceedings #7, SRI International, Menlo Park, CA, July 1987.

[12] R. Kidder and W. Barnes, "WAZER - A One-Dimensional, Two-Temperature Hydrodynamic Code," UCRL-50583, Lawrence Radiation Laboratory, Livermore, California.

[13] R.D. Richtmyer and K.W. Morton, Difference Methods for Initial Value Problems, Interscience Publishers, New York, (1967) 200.

[14] L. Spitzer, Physics of Fully Ionized Gases, Second Edition, Interscience Publishers, New York, (1962) 144.

[15] Y.B. Zel'dovich and Y.P. Raizer, Physics of Shock Waves and Other High Temperature Hydrodynamic Phenomena, W.D. Hayes and P.F. Probstein, eds., Academic Press, New York, (1966) Vol. 1, Chapt. 2.

[16] D. Mihalas, Stellar Atmospheres, Freeman, New York (1978).

[17] H.A. Bent, The Second Law, Oxford University Press, New York, (1965).

[18] C. Antoine, C.R. Acad. Sci, Paris 107, 681, 1143 (1888).

[19] Boublik, Vapor Pressure Tables.

[20] D.A. Labuntsov and A.P. Kryukov, "Analysis of Intensive Evaporation and Condensation," Int. J. Heat Mass Transfer 22, 989 (1979).

Acknowledgment

Input for Example Vaporization Problem

```
c .... time step variables
      nmax = 1000
      tmax= 1.e-3
      tsctr=0.08
      tsctn = 0.04
      tscc = 0.08
      tscv = 0.04
      dtmax=1.e-6
      dtb=1.0e-15
c .... background gas properties
      iz=5(2)
      atn2b=5(2.)
      atw2b=5(4.00)
      tbc=5.e-2
      tn2c=5(0.40e0)
      tr2c=5(0.40e0)
      dn2b=5(3.55e12)
c .... target chamber properties and zoning
      idelto=3
      jmax=5
      isw(4) = 4
      delxct = 0.2
      con(36) = 0.20
      radius = 500.
      pmass=0.0e0
c .... target x-ray spectrum
      isw(11)= 0
      con(43) = 1.30
      nxrg=22
      xehist=1.0000e-5,.056234,.13335,.31623,.74989,1.,
      1.2,1.5,1.7783,2.,2.5,3.2,4.217,5.,6.,7.,8.,9.,
      10.,23.714,56.234,133.,300.
      xamp=193632.,1505280.,5926400.,1.48096e+07,2.00768e+07,
      2.00768e+07,2.00768e+07,2.00768e+07,1.01568e+07,
      1.01568e+07,1.01568e+07,1.01568e+07,1693120.,1693120.,
      1693120.,1693120.,1693120.,1693120.,16051.2,1870.72,
      2755.2,411.2
c .... new vaporization model variables
      nmat = 2
      isw(20)= 2
      nczons = 70
      rhocnd = 9.55
      cpheat = 1510.
      qheatv = 911.
      xkcond = 3030.
      tvap0 = 0.177
      twallb = 0.0666
      awfilm = 172.
      izfilm = 69
      tcn2c(6) = 70(0.0666)
c .... target debris ion properties
      isw(8)=1
      q1min = 1. 1. 1. 1.
      q1init = 1. 1. 1. 1.
      anion=1. 2. 3. 82.
      awion=2.5 4. 7. 207.
      tionin=0. 1.e-9 101.e-9 102.e-9
      xionin(1,1,1)=0. 5.36e27 5.36e27 0.
      xionin(1,1,2)=0. 1.15e27 1.15e27 0.
    . xionin(1,1,3)=0. 1.78e28 1.78e28 0.
```

```
      xionin(1,1,4)=0.  7.54e27 7.54e27 0.
      eionin(1,1)=2.38
      eionin(1,2)=3.8
      eionin(1,3)=6.64
      eionin(1,4)=198.
      nix=4
      nie=1
      nit=10
      nfg=20
c ... thermal radiation parameters
      isw(27) = 1
c ... input/output control variables
      io=2(1000) -1 -1 -1
      iobin=1000
      isw(5)=500
   $
```

Output for Sample Vaporization Problem

```
*************************************************
*                                               *
*   conrad - a code to compute the radiative transfer,  *
*   condensation & hydromotion of vapor         *
*                                               *
*   written by r. peterson, g. moses & j. macfarlane   *
*                                               *
*   this code is under development              *
*                                               *
*   date of this version - 07/16/88             *
*                                               *
*************************************************
```

spherical geometry - energy quantities are absolute

```
no. of zones.................... 5
outer boundary(cm).............. 5.0000e+02
starting time(s)................ 0.
starting cycle.................. 1
no. of time cycles.............. 1000
max. problem time(s)............ 1.0000e-03
time step for first  10 cycles(s) 1.0000e-15
min. time step(s)............... 1.0000e-16
max. time step(s)............... 1.0000e-06
time step growth limit.......... 1.5000e+00
time step control parameters....
   courant...................... 8.0000e-02
   percent v change............. 4.0000e-02
   percent tn change............ 4.0000e-02
   percent er change............ 8.0000e-02
   percent t change in film..... 5.0000e-02
   percent tbp change in film... 5.0000e-02

temperature bc.(ev)............. 5.0000e-02
```

primary output frequencies

```
hydrodynamics...... 1000
energy............. 1000
number densities.. -1
short edit........ -1
multi-freq rad.... -1

binary output...... 1000
```

intermediate variable frequencies - iedit

```
 1) -1   2) -1   3) -1   4) -1   5) -1   6) -1   7) -1   8) -1   9) -1  10) -1
11) -1  12) -1  13) -1  14) -1  15) -1  16) -1  17) -1  18) -1  19) -1  20) -1
21) -1  22) -1  23) -1  24) -1  25) -1  26) -1  27) -1  28) -1  29) -1  30) -1
31) -1  32) -1  33) -1  34) -1  35) -1  36) -1  37) -1  38) -1  39) -1  40) -1
41) -1  42) -1  43) -1  44) -1  45) -1  46) -1  47) -1  48) -1  49) -1  50) -1
51) -1  52) -1  53) -1  54) -1  55) -1  56) -1  57) -1  58) -1  59) -1  60) -1
61) -1  62) -1  63) -1  64) -1  65) -1  66) -1  67) -1  68) -1  69) -1  70) -1
71) -1  72) -1  73) -1  74) -1  75) -1  76) -1  77) -1  78) -1  79) -1  80) -1
81) -1  82) -1  83) -1  84) -1  85) -1  86) -1  87) -1  88) -1  89) -1  90) -1
91) -1  92) -1  93) -1  94) -1  95) -1  96) -1  97) -1  98) -1  99) -1 100) -1
```

#	radius (cm)	zone width (cm)	mass dens (g/cm3)	mass (g)	e density (1/cm3)	ion density (1/cm3)	r temp (ev)	ion temp (ev)	atomic wt (amu)	charge (esu)
0	0.									
1	2.5610e+02	2.5610e+02	2.3578e-11	1.6596e-03	1.9867e+10	3.5500e+12	4.0000e-01	1.7280e+00	4.0000e+00	5.5963e-03
2	3.3309e+02	7.6982e+01	2.3578e-11	1.9908e-03	2.5361e+07	3.5500e+12	4.0000e-01	1.1830e+00	4.0000e+00	7.1440e-06
3	3.9396e+02	6.0871e+01	2.3578e-11	2.3889e-03	1.9807e+04	3.5500e+12	4.0000e-01	9.1414e-01	4.0000e+00	5.5795e-09
4	4.4842e+02	5.4464e+01	2.3578e-11	2.8667e-03	3.2328e+02	3.5500e+12	4.0000e-01	7.8818e-01	4.0000e+00	9.1065e-11
5	5.0000e+02	5.1580e+01	2.3578e-11	3.4401e-03	1.3356e+01	3.5500e+12	4.0000e-01	7.0637e-01	4.0000e+00	3.7624e-12
				1.2346e-02						

#	r press (j/cm3)	ion press (j/cm3)	r int ene (j/)	ion int ene (j/)	velocity (cm/s)
0					0.
1	1.1693e-07	9.8821e-07	2.4682e+01	2.1180e+02	0.
2	1.1693e-07	6.7276e-07	2.9618e+01	8.5252e+01	0.
3	1.1693e-07	5.1988e-07	3.5542e+01	7.9032e+01	0.
4	1.1693e-07	4.4824e-07	4.2651e+01	8.1757e+01	0.
5	1.1693e-07	4.0172e-07	5.1181e+01	8.7915e+01	0.
			1.8367e+02	5.4575e+02	0.

Initial properties of the condensed region

zone index	radius (cm)	zone width (cm)	mass (grams)	integrated mass (g)	temperature (ev)
6	5.0000000e+02	1.523e-10	4.570e-03	4.570e-03	6.660e-02
7	5.0000000e+02	2.024e-10	6.072e-03	1.064e-02	6.660e-02
8	5.0000000e+02	2.689e-10	8.066e-03	1.871e-02	6.660e-02
9	5.0000000e+02	3.572e-10	1.072e-02	2.942e-02	6.660e-02
10	5.0000000e+02	4.745e-10	1.424e-02	4.366e-02	6.660e-02
11	5.0000000e+02	6.304e-10	1.891e-02	6.257e-02	6.660e-02
12	5.0000000e+02	8.374e-10	2.512e-02	8.770e-02	6.660e-02
13	5.0000000e+02	1.112e-09	3.338e-02	1.211e-01	6.660e-02
14	5.0000000e+02	1.478e-09	4.434e-02	1.654e-01	6.660e-02
15	5.0000000e+02	1.963e-09	5.891e-02	2.243e-01	6.660e-02
16	5.0000000e+02	2.608e-09	7.826e-02	3.026e-01	6.660e-02
17	5.0000000e+02	3.465e-09	1.040e-01	4.065e-01	6.660e-02
18	5.0000000e+02	4.603e-09	1.381e-01	5.447e-01	6.660e-02
19	5.0000000e+02	6.116e-09	1.835e-01	7.281e-01	6.660e-02
20	5.0000000e+02	8.124e-09	2.437e-01	9.719e-01	6.660e-02
21	5.0000000e+02	1.079e-08	3.238e-01	1.296e+00	6.660e-02
22	5.0000000e+02	1.434e-08	4.302e-01	1.726e+00	6.660e-02
23	5.0000000e+02	1.905e-08	5.715e-01	2.297e+00	6.660e-02
24	5.0000000e+02	2.531e-08	7.592e-01	3.057e+00	6.660e-02
25	5.0000000e+02	3.362e-08	1.009e+00	4.065e+00	6.660e-02
26	5.0000000e+02	4.466e-08	1.340e+00	5.405e+00	6.660e-02
27	5.0000000e+02	5.933e-08	1.780e+00	7.185e+00	6.660e-02
28	5.0000000e+02	7.882e-08	2.365e+00	9.550e+00	6.660e-02
29	5.0000000e+02	1.047e-07	3.142e+00	1.269e+01	6.660e-02
30	5.0000000e+02	1.391e-07	4.174e+00	1.686e+01	6.660e-02
31	5.0000000e+02	1.848e-07	5.544e+00	2.241e+01	6.660e-02
32	5.0000000e+02	2.455e-07	7.366e+00	2.978e+01	6.660e-02
33	5.0000000e+02	3.261e-07	9.785e+00	3.956e+01	6.660e-02
34	5.0000000e+02	4.333e-07	1.300e+01	5.256e+01	6.660e-02
35	5.0000000e+02	5.756e-07	1.727e+01	6.983e+01	6.660e-02
36	5.0000000e+02	7.647e-07	2.294e+01	9.277e+01	6.660e-02
37	5.0000000e+02	1.016e-06	3.048e+01	1.232e+02	6.660e-02

38	5.0000001e+02	1.350e-06	4.049e+01	1.637e+02	6.660e-02
39	5.0000001e+02	1.793e-06	5.379e+01	2.175e+02	6.660e-02
40	5.0000001e+02	2.382e-06	7.146e+01	2.890e+02	6.660e-02
41	5.0000001e+02	3.164e-06	9.493e+01	3.839e+02	6.660e-02
42	5.0000002e+02	4.204e-06	1.261e+02	5.100e+02	6.660e-02
43	5.0000002e+02	5.584e-06	1.675e+02	6.776e+02	6.660e-02
44	5.0000003e+02	7.419e-06	2.226e+02	9.002e+02	6.660e-02
45	5.0000004e+02	9.856e-06	2.957e+02	1.196e+03	6.660e-02
46	5.0000005e+02	1.309e-05	3.928e+02	1.589e+03	6.660e-02
47	5.0000007e+02	1.739e-05	5.219e+02	2.111e+03	6.660e-02
48	5.0000009e+02	2.311e-05	6.933e+02	2.804e+03	6.660e-02
49	5.0000012e+02	3.070e-05	9.210e+02	3.725e+03	6.660e-02
50	5.0000016e+02	4.078e-05	1.224e+03	4.948e+03	6.660e-02
51	5.0000022e+02	5.418e-05	1.625e+03	6.574e+03	6.660e-02
52	5.0000029e+02	7.197e-05	2.159e+03	8.733e+03	6.660e-02
53	5.0000039e+02	9.562e-05	2.869e+03	1.160e+04	6.660e-02
54	5.0000051e+02	1.270e-04	3.811e+03	1.541e+04	6.660e-02
55	5.0000068e+02	1.687e-04	5.063e+03	2.048e+04	6.660e-02
56	5.0000091e+02	2.242e-04	6.726e+03	2.720e+04	6.660e-02
57	5.0000120e+02	2.978e-04	8.935e+03	3.614e+04	6.660e-02
58	5.0000160e+02	3.956e-04	1.187e+04	4.801e+04	6.660e-02
59	5.0000213e+02	5.256e-04	1.577e+04	6.378e+04	6.660e-02
60	5.0000282e+02	6.983e-04	2.095e+04	8.473e+04	6.660e-02
61	5.0000375e+02	9.276e-04	2.783e+04	1.126e+05	6.660e-02
62	5.0000498e+02	1.232e-03	3.697e+04	1.495e+05	6.660e-02
63	5.0000662e+02	1.637e-03	4.912e+04	1.986e+05	6.660e-02
64	5.0000880e+02	2.175e-03	6.525e+04	2.639e+05	6.660e-02
65	5.0001169e+02	2.889e-03	8.669e+04	3.506e+05	6.660e-02
66	5.0001552e+02	3.838e-03	1.152e+05	4.658e+05	6.660e-02
67	5.0002062e+02	5.099e-03	1.530e+05	6.187e+05	6.660e-02
68	5.0002740e+02	6.774e-03	2.032e+05	8.220e+05	6.660e-02
69	5.0003639e+02	8.999e-03	2.700e+05	1.092e+06	6.660e-02
70	5.0004835e+02	1.195e-02	3.587e+05	1.451e+06	6.660e-02
71	5.0006423e+02	1.588e-02	4.765e+05	1.927e+06	6.660e-02
72	5.0008552e+02	2.110e-02	6.331e+05	2.560e+06	6.660e-02
73	5.0011335e+02	2.802e-02	8.411e+05	3.401e+06	6.660e-02
74	5.0015057e+02	3.722e-02	1.117e+06	4.519e+06	6.660e-02
75	5.0020001e+02	4.944e-02	1.484e+06	6.003e+06	6.660e-02

Total mass of condensed region (grams) = 6.003e+06

coefficients used in conrad - con

ion thermal cond.........(1)	1.2175e+02		2-t r thermal cond......(2)	1.0000e+10
rad. eq. cond...........(3)	1.0000e-01		flux limit epsilon term.(4)	1.0000e-30
const log lambda........(5)	0.		4*sigma/c...............(6)	1.3713e-05
2-t plasma emiss. coef..(7)	4.1138e+05		2-t plasma absorp. coef.(8)	3.0000e+10
ion press(i.gas)........(9)	1.6020e-19		r flux limit............(10)	3.0000e+10
(11)	0.		ion press deriv(i.gas)..(12)	1.6020e-19
(13)	0.		ion sp heat(i.gas)......(14)	2.4030e-19
ion int energy(i.gas)...(15)	2.4030e-19		rad sp. energy coef.....(16)	1.3713e-05
up-stream ave parameter.(17)	0.		ion shock heating.......(18)	1.0000e+00
(19)	0.		(20)	0.
artificial viscosity....(21)	1.4140e+00		multi-freq rad absorption(22)	3.0000e+10
multi-freq rad emission.(23)	6.3349e+04		multi-freq rad conduct..(24)	1.0000e+10
multi-freq rad flux lim.(25)	3.0000e+10		min init m-f rad energy.(26)	1.0000e-20
(27)	0.		(28)	0.
(29)	0.		Boltzman const (MJ/K)...(30)	1.3810e-29
vap. rate multiplier....(31)	1.0000e+00		condensation rate mult..(32)	1.0000e+00

1

```
vap/cond flux term......(33) 0.           non-condensable gas term.(34) 3.1200e+01
chrg exch x-section mult.(35) 1.0000e+00  mass factor auto zoning..(36) 2.0000e-01
                        (37) 0.                                    (38) 0.
                        (39) 0.                                    (40) 0.
x-ray flux multiplier....(41) 1.3000e+00  debris ion flux mult.....(42) 1.0000e+00
ion thermal vel term.....(43) 2.0000e+00                           (44) 0.
rel debris ion vel term..(45) 1.0000e+00                           (46) 0.
                        (47) 0.                                    (48) 0.
                        (49) 0.                                    (50) 0.

            calculation options used in conrad - isw

radiation temperature op.( 1) 0    no. of const time steps..( 2) 10
                        ( 3) 0     automatic zoning.........( 4) 4
freq of wall output......( 5) 500  hydrodynamic motion......( 6) 0
                        ( 7) 0     ion deposition source....( 8) 1
                        ( 9) 0     freq. of dtb calculation.(10) 1
automatic xray deposition(11) 0    eqn of state option......(12) 0
no. freq. gr. sub-divns..(13) 0    arbitrary radiation opc..(14) 0
arbitrary rosseland opc..(15) 0    allow flowtrace..........(16) 0
dynamic rezoning.........(17) 0                             (18) 0
                        (19) 0     mass trans calc..........(20) 2
momentum exch w film.....(21) 0    energy exch with film....(22) 0
                        (23) 0     adjust temp in rezoning..(24) 0
ablation model choice....(25) 0    kinetic vapor model......(26) 0
eos and opacity data.....(27) 1    eos interpolation........(28) 0
                        (29) 0     variable film properties.(30) 0
t-dep debris ion calc....(31) 0    add db ion mass to vap...(32) 0
                        (33) 0                             (34) 0
                        (35) 0                             (36) 0
                        (37) 0                             (38) 0
                        (39) 0                             (40) 0
                        (41) 0                             (42) 0
                        (43) 0                             (44) 0
                        (45) 0                             (46) 0
                        (47) 0                             (48) 0
                        (49) 0                             (50) 0

            equation of state table indices

density slope........   1.0000e+00
density base.........   1.4000e+01
temperature slope....   2.5000e-01
temperature base.....  -3.9794e-01
min density(1/cm3)...    1.0000e+14
max density(1/cm3)...    1.0000e+23
min temperature(ev)..   4.0000e-01
max temperature(ev)..   2.2494e+04
```

header records from equation of state files:

material # 1   IONMIX calculation performed on date 03/29/88   at time   21:01:09
atomic #s of gases: 2
relative fractions: 1.00e+00

material # 2   - IONMIX calculation performed on date 02/01/88   at time   18:09:35

0

0

115

```
      atomic #s of gases:        3       82
      relative fractions:   1.70e-01  8.30e-01

  material #s for zones:
      1 1 1 1 1 2 2 2 2 2 2 2 2 2 2 2 2 2 2 2 2 2 2 2 2 2 2 2 2 2
      2 2 2 2 2 2 2 2 2 2 2 2 2 2 2 2 2 2 2 2 2 2 2 2 2 2 2 2 2
  0

      there is an initial xray fluence

      the blackbody temperature was 0.           kev for the x-rays
      the x-ray spectra contained 8.2423e+07 joules
      the x-ray energy deposited in the gas = 3.6892e+02 joules


  ************** xray flux to wall **************

  energy    energy       exiting       attenuation
  group                  energy        coefficient
            (kev)        (j/kev)         (/cm)

    1      2.8122e-02    2.5094e+05     2.6297e+05
    2      9.4792e-02    1.9551e+06     7.6048e+04
    3      2.2479e-01    7.7037e+06     7.3637e+03
    4      5.3306e-01    1.9252e+07     5.6090e+02
    5      8.7495e-01    2.6100e+07     8.9288e+01
    6      1.1000e+00    2.6100e+07     4.2580e+01
    7      1.3500e+00    2.6100e+07     2.2350e+01
    8      1.6392e+00    2.6100e+07     1.1809e+01
    9      1.8892e+00    1.3204e+07     7.3712e+00
   10      2.2500e+00    1.3204e+07     4.2377e+00
   11      2.8500e+00    1.3204e+07     1.9863e+00
   12      3.7085e+00    1.3204e+07     9.1860e-01
   13      4.6085e+00    2.2011e+06     5.1557e-01
   14      5.5000e+00    2.2011e+06     3.6923e-01
   15      6.5000e+00    2.2011e+06     2.8829e-01
   16      7.5000e+00    2.2011e+06     2.4756e-01
   17      8.5000e+00    2.2011e+06     2.2481e-01
   18      9.5000e+00    2.2011e+06     2.1104e-01
   19      1.6857e+01    2.0867e+04     1.9348e-01
   20      3.9974e+01    2.4319e+03     1.7348e-01
   21      9.4617e+01    3.5818e+03     1.4977e-01
   22      2.1650e+02    5.3456e+02     1.1945e-01
  0
         ion source term

  number of ion species................      4
  number of energy groups...............      1
  number of time levels.................     10
  number of locations in storage vectors.     40
  0
  0
  ion # = 1  atomic # = 1.0  atomic wt = 2.50
  initial charge state for stopping power calc =  1.0

  energy                          times(sec)
  spectrum   0.      1.0000e-09 1.0100e-07 1.0200e-07 0.      0.      0.      0.      0.      0.

  2.3800e+00 0.      5.3600e+27 5.3600e+27 0.      0.      0.      0.      0.      0.
```

```
0
ion # = 2  atomic # = 2.0  atomic wt =  4.00
initial charge state for stopping power calc =   1.0

energy                              times(sec)
spectrum   0.   0.          1.0000e-09 1.0100e-07 1.0200e-07 0.     0.     0.     0.

3.8000e+00 0.               1.1500e+27 1.1500e+27 0.            0.     0.     0.     0.
0
ion # = 3  atomic # = 3.0  atomic wt =  7.00
initial charge state for stopping power calc =   1.0

energy                              times(sec)
spectrum   0.   0.          1.0000e-09 1.0100e-07 1.0200e-07 0.     0.     0.     0.

6.6400e+00 0.               1.7800e+28 1.7800e+28 0.            0.     0.     0.     0.
0
ion # = 4  atomic # = 82.0  atomic wt =207.00
initial charge state for stopping power calc =   1.0

energy                              times(sec)
spectrum   0.   0.          1.0000e-09 1.0100e-07 1.0200e-07 0.     0.     0.     0.

1.9800e+02 0.               7.5400e+27 7.5400e+27 0.            0.     0.     0.     0.
0
    radiation group structure
```

#	lower bd (ev)	upper bd (ev)	ave (ev)
1	1.0000e-01	3.1600e-01	2.0800e-01
2	3.1600e-01	1.0000e+00	6.5800e-01
3	1.0000e+00	1.5800e+00	1.2900e+00
4	1.5800e+00	2.5100e+00	2.0450e+00
5	2.5100e+00	3.9700e+00	3.2400e+00
6	3.9700e+00	6.2900e+00	5.1300e+00
7	6.2900e+00	1.0000e+01	8.1450e+00
8	1.0000e+01	1.5800e+01	1.2900e+01
9	1.5800e+01	2.5100e+01	2.0450e+01
10	2.5100e+01	3.9700e+01	3.2400e+01
11	3.9700e+01	6.2900e+01	5.1300e+01
12	6.2900e+01	1.0000e+02	8.1450e+01
13	1.0000e+02	1.7800e+02	1.3900e+02
14	1.7800e+02	3.1600e+02	2.4700e+02
15	3.1600e+02	5.6200e+02	4.3900e+02
16	5.6200e+02	1.0000e+03	7.8100e+02
17	1.0000e+03	3.1600e+03	2.0800e+03
18	3.1600e+03	1.0000e+04	6.5800e+03
19	1.0000e+04	1.0000e+05	5.5000e+04
20	1.0000e+05	1.0000e+06	5.5000e+05

#	rad temp (ev)	rad energy (j/g)	rad press (j/cm3)
1	4.0000e-01	3.5079e-07	1.1693e-07
2	4.0000e-01	3.5079e-07	1.1693e-07
3	4.0000e-01	3.5079e-07	1.1693e-07
4	4.0000e-01	3.5079e-07	1.1693e-07
5	4.0000e-01	3.5079e-07	1.1693e-07

0

Spatial energy depostion in the condensed region:

Total target x-ray energy reaching the wall (J)   = 8.242e+07
Target x-ray energy absorbed by the wall (J)   = 8.240e+07
X-ray energy going through back of the wall (J)   = 2.559e+04

position wrt wall inner bd (cm)	x-ray energy depos. (J/cm3/s)	x-ray energy depos. (J)	x-ray energy depos. (J/g)
-1.3616e-12	1.0038e+21	4.8042e+02	1.0511e+05
1.5051e-10	1.0020e+21	6.3704e+02	1.0492e+05
3.5142e-10	9.9952e+20	8.4423e+02	1.0466e+05
6.1963e-10	9.9631e+20	1.1179e+03	1.0433e+05
9.7524e-10	9.9212e+20	1.4789e+03	1.0389e+05
1.4487e-09	9.8668e+20	1.9539e+03	1.0332e+05
2.0784e-09	9.7968e+20	2.5774e+03	1.0258e+05
2.9147e-09	9.7075e+20	3.3928e+03	1.0165e+05
4.0263e-09	9.5952e+20	4.4551e+03	1.0047e+05
5.5035e-09	9.4565e+20	5.8330e+03	9.9021e+04
7.4652e-09	9.2891e+20	7.6119e+03	9.7269e+04
1.0072e-08	9.0935e+20	9.8993e+03	9.5220e+04
1.3536e-08	8.8741e+20	1.2834e+04	9.2923e+04
1.8139e-08	8.6411e+20	1.6602e+04	9.0482e+04
2.4254e-08	8.4106e+20	2.1467e+04	8.8069e+04
3.2377e-08	8.2028e+20	2.7814e+04	8.5893e+04
4.3169e-08	8.0363e+20	3.6200e+04	8.4150e+04
5.7506e-08	7.9205e+20	4.7398e+04	8.2938e+04
7.6553e-08	7.8508e+20	6.2413e+04	8.2207e+04
1.0186e-07	7.8107e+20	8.2492e+04	8.1788e+04
1.3547e-07	7.7818e+20	1.0918e+05	8.1484e+04
1.8013e-07	7.7509e+20	1.4447e+05	8.1161e+04
2.3946e-07	7.7116e+20	1.9095e+05	8.0750e+04
3.1828e-07	7.6601e+20	2.5199e+05	8.0211e+04
4.2299e-07	7.5927e+20	3.3181e+05	7.9505e+04
5.6210e-07	7.5048e+20	4.3570e+05	7.8584e+04
7.4690e-07	7.3908e+20	5.7004e+05	7.7391e+04
9.9240e-07	7.2443e+20	7.4226e+05	7.5856e+04
1.3185e-06	7.0576e+20	9.6068e+05	7.3902e+04
1.7518e-06	6.8230e+20	1.2338e+06	7.1445e+04
2.3274e-06	6.5328e+20	1.5694e+06	6.8407e+04
3.0921e-06	6.1810e+20	1.9726e+06	6.4723e+04
4.1080e-06	5.7648e+20	2.4442e+06	6.0365e+04
5.4576e-06	5.2863e+20	2.9775e+06	5.5354e+04
7.2504e-06	4.7537e+20	3.5570e+06	4.9777e+04
9.6322e-06	4.1812e+20	4.1564e+06	4.3782e+04
1.2796e-05	3.5875e+20	4.7377e+06	3.7566e+04
1.7000e-05	2.9941e+20	5.2529e+06	3.1352e+04
2.2584e-05	2.4234e+20	5.6480e+06	2.5376e+04
3.0003e-05	1.8964e+20	5.8717e+06	1.9858e+04
3.9859e-05	1.4301e+20	5.8826e+06	1.4975e+04
5.2952e-05	1.0349e+20	5.6551e+06	1.0837e+04
7.0346e-05	7.1527e+19	5.1924e+06	7.4897e+03
9.3453e-05	4.7134e+19	4.5456e+06	4.9355e+03
1.2415e-04	2.9738e+19	3.8101e+06	3.1140e+03
1.6493e-04	1.8157e+19	3.0905e+06	1.9013e+03
2.1911e-04	1.0901e+19	2.4648e+06	1.1414e+03
2.9108e-04	6.5527e+18	1.9683e+06	6.8615e+02
3.8670e-04	3.9943e+18	1.5940e+06	4.1826e+02
5.1372e-04	2.4637e+18	1.3061e+06	2.5798e+02
6.8247e-04	1.5020e+18	1.0578e+06	1.5728e+02

Auxiliary data block (unlabeled columns):

9.0665e-04	8.1100e+05	8.6680e+17	9.0764e+01
1.2045e-03	5.6089e+05	4.5125e+17	4.7251e+01
1.6001e-03	3.3662e+05	2.0385e+17	2.1346e+01
2.1257e-03	1.7167e+05	7.8257e+16	8.1944e+00
2.8240e-03	7.6963e+04	2.6409e+16	2.7654e+00
3.7516e-03	3.7483e+04	9.6817e+15	1.0138e+00
4.9840e-03	2.7981e+04	5.4404e+15	5.6967e-01
6.6211e-03	2.9410e+04	4.3043e+15	4.5071e-01
8.7959e-03	3.3063e+04	3.6424e+15	3.8140e-01
1.1685e-02	3.6094e+04	2.9931e+15	3.1341e-01
1.5523e-02	3.7419e+04	2.3358e+15	2.4458e-01
2.0623e-02	3.6424e+04	1.7114e+15	1.7921e-01
2.7396e-02	3.2950e+04	1.1654e+15	1.2203e-01
3.6395e-02	2.7490e+04	7.3187e+14	7.6635e-02
4.8349e-02	2.1200e+04	4.2485e+14	4.4487e-02
6.4229e-02	1.5596e+04	2.3526e+14	2.4634e-02
8.5324e-02	1.1869e+04	1.3477e+14	1.4112e-02
1.1335e-01	1.0144e+04	8.6703e+13	9.0789e-03
1.5057e-01	9.4563e+03	6.0837e+13	6.3704e-03

```
cycle     time(s)       delta t(s)        criterion(cour) in zone ( 6) otherwise (cour) in zone ( 6)
1000      2.3348e-06    3.4351e-08
```

#	radius (cm)	zone width (cm)	mass dens (g/cm3)	compression (v0/v)	velocity (cm/s)	r temp (ev)	ion temp (ev)	r press (j/cm3)	ion press (j/cm3)	art visc (j/cm3)
0	0.				0.					
1	2.5733e+02	2.5733e+02	2.3243e-11	9.8579e-01	1.0352e+06	5.1724e-01	4.0614e+01	3.2717e-07	6.8309e-05	0.
2	3.3310e+02	7.5773e+01	2.3859e-11	1.0119e+00	2.7105e+04	5.1724e-01	2.2054e+00	3.2717e-07	1.5735e-06	4.8467e-06
3	3.9379e+02	6.0684e+01	2.3661e-11	1.0035e+00	-2.2602e+05	5.1724e-01	1.1598e+00	3.2717e-07	6.6194e-07	3.0309e-07
4	4.4474e+02	5.0959e+01	2.5436e-11	1.0788e+00	-2.5410e+06	5.1724e-01	1.7576e+00	3.2717e-07	1.0862e-06	2.7230e-05
5	4.8463e+02	3.9888e+01	3.1763e-11	1.3471e+00	-6.1553e+06	5.1724e-01	7.1546e+00	3.2717e-07	1.4456e-05	8.2807e-05
6	4.8473e+02	9.4714e-02	1.6347e-08	1.7117e-09	-6.1235e+06	5.1724e-01	2.7755e+00	3.2717e-07	7.7606e-05	0.
7	4.8545e+02	7.2431e-01	2.8349e-08	2.9685e-10	-6.2305e+06	5.1724e-01	2.4362e+00	3.2717e-07	1.1212e-05	6.4689e-06
8	4.8639e+02	9.3579e-01	2.9051e-09	3.0419e-10	-5.8451e+06	5.1724e-01	1.6755e+00	3.2717e-07	6.4731e-06	0.
9	4.8716e+02	7.7677e-01	4.6331e-09	4.8514e-10	-5.5172e+06	5.1724e-01	1.1051e+00	3.2717e-07	5.8260e-06	0.
10	4.8784e+02	6.8079e-01	7.0017e-09	7.3316e-10	-5.2261e+06	5.1724e-01	1.0027e+00	3.2717e-07	7.9167e-06	0.
11	4.8846e+02	6.1508e-01	1.0268e-08	1.0752e-09	-4.9621e+06	5.1724e-01	9.8733e-01	3.2717e-07	1.1416e-05	0.
12	4.8903e+02	5.6575e-01	1.4795e-08	1.5492e-09	-4.7185e+06	5.1724e-01	9.7517e-01	3.2717e-07	1.6228e-05	0.
13	4.8955e+02	5.2491e-01	2.1136e-08	2.2132e-09	-4.4925e+06	5.1724e-01	9.4712e-01	3.2717e-07	2.2457e-05	0.
14	4.9004e+02	4.8955e-01	3.0045e-08	3.1461e-09	-4.2823e+06	5.1724e-01	8.8648e-01	3.2717e-07	2.9698e-05	0.
15	4.9050e+02	4.5859e-01	4.2526e-08	4.4530e-09	-4.0859e+06	5.1724e-01	8.1701e-01	3.2717e-07	3.8447e-05	0.
16	4.9093e+02	4.3110e-01	5.9989e-08	6.2815e-09	-3.9017e+06	5.1724e-01	7.5871e-01	3.2717e-07	5.0017e-05	0.
17	4.9134e+02	4.0596e-01	8.4486e-08	8.8467e-09	-3.7281e+06	5.1724e-01	7.1125e-01	3.2717e-07	6.5619e-05	0.
18	4.9172e+02	3.8240e-01	1.1896e-07	1.2457e-08	-3.5648e+06	5.1724e-01	6.8225e-01	3.2717e-07	8.0537e-05	0.
19	4.9208e+02	3.6051e-01	1.6738e-07	1.7527e-08	-3.4112e+06	5.1724e-01	6.6361e-01	3.2717e-07	1.0401e-04	0.
20	4.9242e+02	3.4088e-01	2.3484e-07	2.4590e-08	-3.2659e+06	5.1724e-01	6.4816e-01	3.2717e-07	1.3614e-04	0.
21	4.9274e+02	3.2364e-01	3.2815e-07	3.4362e-08	-3.1277e+06	5.1724e-01	6.3994e-01	3.2717e-07	1.8322e-04	0.
22	4.9305e+02	3.0847e-01	4.5679e-07	4.7832e-08	-2.9958e+06	5.1724e-01	6.3427e-01	3.2717e-07	2.4810e-04	0.
23	4.9335e+02	2.9514e-01	6.3347e-07	6.6332e-08	-2.8697e+06	5.1724e-01	6.2856e-01	3.2717e-07	3.3469e-04	0.
24	4.9363e+02	2.8333e-01	8.7559e-07	9.1685e-08	-2.7485e+06	5.1724e-01	6.2269e-01	3.2717e-07	4.4987e-04	0.
25	4.9390e+02	2.7339e-01	1.2042e-06	1.2609e-07	-2.6314e+06	5.1724e-01	6.1665e-01	3.2717e-07	6.0142e-04	0.
26	4.9417e+02	2.6536e-01	1.6463e-06	1.7239e-07	-2.5178e+06	5.1724e-01	6.1049e-01	3.2717e-07	7.9918e-04	0.
27	4.9443e+02	2.5971e-01	2.2323e-06	2.3375e-07	-2.4062e+06	5.1724e-01	6.0477e-01	3.2717e-07	1.0557e-03	0.
28	4.9468e+02	2.5626e-01	3.0024e-06	3.1439e-07	-2.2959e+06	5.1724e-01	6.0185e-01	3.2717e-07	1.3972e-03	0.
29	4.9494e+02	2.5484e-01	4.0067e-06	4.1955e-07	-2.1859e+06	5.1724e-01	6.0072e-01	3.2717e-07	1.8551e-03	0.
30	4.9520e+02	2.5601e-01	5.2930e-06	5.5424e-07	-2.0747e+06	5.1724e-01	5.9942e-01	3.2717e-07	2.3864e-03	0.
31	4.9546e+02	2.6358e-01	6.8226e-06	7.1441e-07	-1.9592e+06	5.1724e-01	5.9805e-01	3.2716e-07	3.0311e-03	0.
32	4.9574e+02	2.7753e-01	8.5988e-06	9.0040e-07	-1.8386e+06	5.1724e-01	5.9697e-01	3.2716e-07	3.7732e-03	0.
33	4.9602e+02	2.7992e-01	1.1313e-05	1.1846e-06	-1.7240e+06	5.1723e-01	5.9659e-01	3.2715e-07	4.9103e-03	0.

```
 34  4.9627e+02  2.5430e-01  1.6526e-05  1.7304e-06 -1.6068e+06  5.1725e-01  5.9184e-01  3.2713e-07  6.9588e-03  0.
 35  4.9651e+02  2.4104e-01  2.3138e-05  2.4229e-06 -1.5011e+06  5.1720e-01  5.9011e-01  3.2707e-07  9.5812e-03  0.
 36  4.9676e+02  2.5252e-01  2.9313e-05  3.0694e-06 -1.3951e+06  5.1679e-01  5.8463e-01  3.2604e-07  1.1808e-02  0.
 37  4.9703e+02  2.6572e-01  3.6967e-05  3.8709e-06 -1.2823e+06  5.1446e-01  5.7705e-01  3.2019e-07  1.4311e-02  0.
 38  4.9730e+02  2.6995e-01  4.8289e-05  5.0564e-06 -1.1670e+06  5.1230e-01  5.7246e-01  3.1485e-07  1.8160e-02  0.
 39  4.9757e+02  2.6942e-01  6.4208e-05  6.7234e-06 -1.0520e+06  5.1045e-01  5.6900e-01  3.1032e-07  2.3570e-02  0.
 40  4.9783e+02  2.6522e-01  8.6558e-05  9.0636e-06 -9.3882e+05  5.0864e-01  5.6576e-01  3.0595e-07  3.1077e-02  0.
 41  4.9809e+02  2.5723e-01  1.1844e-04  1.2402e-05 -8.2936e+05  5.0664e-01  5.6232e-01  3.0117e-07  4.1616e-02  0.
 42  4.9834e+02  2.4500e-01  1.6503e-04  1.7281e-05 -7.2535e+05  5.0407e-01  5.5820e-01  2.9509e-07  5.6708e-02  0.
 43  4.9857e+02  2.2958e-01  2.3374e-04  2.4475e-05 -6.2778e+05  4.9982e-01  5.5229e-01  2.8528e-07  7.8289e-02  0.
 44  4.9878e+02  2.1221e-01  3.3564e-04  3.5145e-05 -5.3809e+05  4.9080e-01  5.4213e-01  2.6523e-07  1.0849e-01  0.
 45  4.9897e+02  1.8698e-01  5.0566e-04  5.2948e-05 -4.6002e+05  4.7325e-01  5.2364e-01  2.2929e-07  1.5483e-01  0.
 46  4.9913e+02  1.6494e-01  7.6097e-04  7.9683e-05 -3.8259e+05  4.3496e-01  4.8319e-01  1.6361e-07  2.1068e-01  0.
 47  4.9930e+02  1.7333e-01  9.6134e-04  1.0066e-04 -2.9692e+05  3.1918e-01  3.4604e-01  4.7440e-08  1.8827e-01  0.
 48  4.9947e+02  1.6119e-01  1.3725e-03  1.4371e-04 -2.2964e+05  2.6144e-01  1.8677e-01  2.1354e-08  1.4449e-01  0.
 49  4.9958e+02  1.1202e-01  2.6220e-03  2.7456e-04 -1.8235e+05  2.5479e-01  1.0232e-01  1.9262e-08  1.5090e-01  0.
 50  4.9966e+02  8.6369e-02  4.5161e-03  4.7289e-04 -1.4558e+05  2.4749e-01  5.2329e-02  1.7149e-08  1.3264e-01  0.
 51  4.9972e+02  5.9145e-02  8.7587e-03  9.1714e-04 -1.1981e+05  2.3842e-01  2.9652e-02  1.4770e-08  1.4573e-01  0.
 52  4.9977e+02  4.4726e-02  1.5384e-02  1.6108e-03 -1.0127e+05  2.2661e-01  1.5959e-02  1.2054e-08  1.3775e-01  0.
 53  4.9980e+02  3.7205e-02  2.4564e-02  2.5722e-03 -8.4830e+04  2.1145e-01  1.0992e-02  9.1373e-09  1.5149e-01  0.
 54  4.9984e+02  3.9896e-02  3.0427e-02  3.1861e-03 -6.7768e+04  1.9452e-01  9.2705e-03  6.5445e-09  1.5824e-01  0.
 55  4.9989e+02  4.1995e-02  3.8395e-02  4.0204e-03 -4.9541e+04  1.7675e-01  7.7009e-03  4.4614e-09  1.6587e-01  0.
 56  4.9993e+02  4.6508e-02  4.6050e-02  4.8220e-03 -2.9443e+04  1.5938e-01  6.8233e-03  2.9492e-09  1.7627e-01  0.
 57  5.0000e+02  6.7876e-02  4.1908e-02  4.3883e-03  0.          1.3335e-01  7.8279e-03  1.4455e-09  1.8403e-01  0.
                                                                 0.          6.4178e-02
0
  #  r energy    ion energy  kin energy  r source    ion source  ion->r ex   flux lim    heat flux
     (j/    )    (j/    )    (j/    )    (j/    )    (j/    )    (j/    )    (j/cm2-s)   (j/cm2-s)
  0                          0.
  1  7.0056e+01  1.0494e+04  9.7775e+01  0.          9.8273e+01  7.8846e-03  7.5000e-11  0.
  2  8.1898e+01  5.6667e+02  8.0444e-02  0.          0.          6.6575e-03  7.5000e-11  0.
  3  9.9097e+01  1.0029e+02  6.7122e+00  0.          0.         -9.8784e-07  7.5000e-11  0.
  4  1.1062e+02  3.8703e+02  1.0180e+03  0.          0.         -7.3230e-05  7.5000e-11  0.
  5  1.0630e+02  7.2941e+03  7.5876e+03  0.          0.          5.0550e-01  7.5000e-11  0.
  6  2.7443e-01  9.8173e+01  9.9763e+03  0.          0.          5.3559e-01  7.5000e-11  0.
  7  2.1022e+00  1.0839e+02  1.3720e+04  0.          0.          6.7222e-01  7.5000e-11  0.
  8  2.7253e+00  8.0126e+01  1.6042e+04  0.          0.          5.1326e-01  7.5000e-11  0.
  9  2.2701e+00  6.3058e+01  1.8988e+04  0.          0.          5.5885e-01  7.5000e-11  0.
 10  1.9956e+00  7.9526e+01  2.2633e+04  0.          0.          4.4411e-01  7.5000e-11  0.
 11  1.8078e+00  1.0478e+02  2.7107e+04  0.          0.          5.3617e-01  7.5000e-11  0.
 12  1.6668e+00  1.3828e+02  3.2563e+04  0.          0.          6.5517e-01  7.5000e-11  0.
 13  1.5499e+00  1.8086e+02  3.9214e+04  0.          0.          7.0208e-01  7.5000e-11  0.
 14  1.4485e+00  2.3193e+02  4.7335e+04  0.          0.          5.7440e-01  7.5000e-11  0.
 15  1.3596e+00  2.9494e+02  5.7248e+04  0.          0.          6.3545e-01  7.5000e-11  0.
 16  1.2804e+00  3.7650e+02  6.9347e+04  0.          0.          6.7050e-01  7.5000e-11  0.
 17  1.2078e+00  4.8280e+02  8.4114e+04  0.          0.          6.4632e-01  7.5000e-11  0.
 18  1.1395e+00  5.4699e+02  1.0217e+05  0.          0.          9.1242e-02  7.5000e-11  0.
 19  1.0759e+00  6.5352e+02  1.2428e+05  0.          0.         -1.8262e-02  7.5000e-11  0.
 20  1.0188e+00  7.9330e+02  1.5135e+05  0.          0.          7.1579e-02  7.5000e-11  0.
 21  9.6853e-01  1.0016e+03  1.8440e+05  0.          0.          4.7289e-01  7.5000e-11  0.
 22  9.2433e-01  1.2802e+03  2.2475e+05  0.          0.          7.0840e-01  7.5000e-11  0.
 23  8.8547e-01  1.6352e+03  2.7396e+05  0.          0.          1.0430e+00  7.5000e-11  0.
 24  8.5105e-01  2.0860e+03  3.3386e+05  0.          0.          1.5042e+00  7.5000e-11  0.
 25  8.2210e-01  2.6573e+03  4.0655e+05  0.          0.          2.1263e+00  7.5000e-11  0.
 26  7.9883e-01  3.3813e+03  4.9445e+05  0.          0.          2.9854e+00  7.5000e-11  0.
 27  7.8264e-01  4.3133e+03  5.9996e+05  0.          0.          4.5253e+00  7.5000e-11  0.
 28  7.7305e-01  5.5827e+03  7.2561e+05  0.          0.          8.4047e+00  7.5000e-11  0.
 29  7.6957e-01  7.2024e+03  8.7383e+05  0.          0.          1.2346e+01  7.5000e-11  0.
 30  7.7391e-01  9.2901e+03  1.0458e+06  0.          0.          1.7733e+01  7.5000e-11  0.
 31  7.9762e-01  1.1999e+04  1.2389e+06  0.          0.          2.4824e+01  7.5000e-11  0.
```

32	8.4073e-01	1.5555e+04	0.	0.	3.5191e+01	7.5000e-11	0.
33	8.4892e-01	2.0189e+04	0.	0.	5.4871e+01	7.5000e-11	0.
34	7.7198e-01	2.5283e+04	0.	0.	5.9857e+01	7.5000e-11	0.
35	7.3233e-01	3.2383e+04	0.	0.	8.6048e+01	7.5000e-11	0.
36	7.6554e-01	4.0717e+04	0.	0.	6.1298e+01	7.5000e-11	0.
37	7.9197e-01	4.9727e+04	0.	0.	2.1549e+01	7.5000e-11	0.
38	7.9199e-01	6.1633e+04	0.	0.	1.2199e+01	7.5000e-11	0.
39	7.7992e-01	7.6802e+04	0.	0.	1.1564e+01	7.5000e-11	0.
40	7.5775e-01	9.5712e+04	0.	0.	1.2973e+01	7.5000e-11	0.
41	7.2419e-01	1.1898e+05	0.	0.	1.4469e+01	7.5000e-11	0.
42	6.7652e-01	1.4704e+05	0.	0.	1.2549e+01	7.5000e-11	0.
43	6.1347e-01	1.7965e+05	0.	0.	-2.2523e+00	7.5000e-11	0.
44	5.2766e-01	2.1434e+05	0.	0.	-3.4254e+01	7.5000e-11	0.
45	4.0224e-01	2.4367e+05	0.	0.	-7.5235e+01	7.5000e-11	0.
46	2.5338e-01	2.4588e+05	0.	0.	-1.6036e+02	7.5000e-11	0.
47	7.7257e-02	1.7032e+05	0.	0.	-1.3830e+02	7.5000e-11	0.
48	3.2360e-02	1.2212e+05	0.	0.	-2.6993e+01	7.5000e-11	0.
49	2.0298e-02	8.8881e+04	0.	0.	-3.8703e+00	7.5000e-11	0.
50	1.3938e-02	5.6722e+04	0.	0.	-4.5094e+00	7.5000e-11	0.
51	8.2232e-03	4.2699e+04	0.	0.	-4.5019e+00	7.5000e-11	0.
52	5.0759e-03	3.0531e+04	0.	0.	-4.9135e+00	7.5000e-11	0.
53	3.2012e-03	2.7935e+04	0.	0.	-4.8354e+00	7.5000e-11	0.
54	2.4591e-03	3.0536e+04	0.	0.	-4.0375e+00	7.5000e-11	0.
55	1.7648e-03	3.3698e+04	0.	0.	-3.1309e+00	7.5000e-11	0.
56	1.2922e-03	3.9665e+04	0.	0.	-2.3446e+00	7.5000e-11	0.
57	9.2457e-04	6.0453e+04	0.	0.	-1.1959e+00	7.5000e-11	0.

Energy conservation check — units are (J/   )

Initial Energies	Current Energies	Total Energy Exchanged	E. Exchanged last time step
ion int E = 5.4575e+02	ion int E = 2.3446e+06	ion -> rad = 1.6647e+05	ion -> rad =-3.1840e+00
rad int E = 1.8367e+02	rad int E = 5.1049e+02	rad -> wall = 1.7308e+05	rad -> wall = 3.3735e+00
ion kin E = 0.	ion kin E = 6.6725e+07	sorc -> ions = 1.5129e+05	sorc -> ions = 9.8273e+01
wall int E=-4.8652e+09	wall int E=-4.8529e+09	outr wal loss= 2.4139e+04	outr wal loss=-2.1269e+01
		tot rad->wall= 8.2595e+07	tot rad->wall= 3.3735e+00
		wall E->vap E= 6.8524e+07	wall E->vap E=-2.0899e+00
		ph trans work=-1.7655e+06	ph trans work= 1.9305e-01
		ph trans heat= 3.8122e+07	ph trans heat=-3.4794e+01

Totals

Initial Energies	Current Energies	Initial minus Losses
radiation = 1.8367e+02	radiation = 5.1049e+02	radiation =-6.5587e+03
ion (int+KE) = 5.4575e+02	ion (int+KE) = 6.9069e+07	ion (int+KE) = 6.8510e+07
total cavity = 7.2943e+02	total cavity = 6.9070e+07	total cavity = 6.8503e+07
wall region =-4.8652e+09	wall region =-4.8529e+09	wall region =-4.8529e+09
wall + cavity=-4.8652e+09	wall + cavity=-4.7838e+09	w.+c.-ph.tr.w=-4.7844e+09

ion source parameters — units are (j/   )

total ion source upto present time ..	2.6349e+07
total ion energy deposited in gas ...	1.5129e+05
total ion kinetic energy in gas	2.8718e+03
total ion energy deposited in wall ..	0.

energy in in-flight ions .... 2.6197e+07

Properties of wall material

heat capacity (J/g/eV)	= 1.510e+03	
mass density (j/cm**3)	= 9.550e+00	
heat of vaporization(J/g)	= 9.110e+02	
thermal conductivity(J/cm/s/eV)	= 3.030e+03	

vaporization temperature at 1 bar (eV)	= 1.770e-01
current vaporization temperature (eV)	= 1.097e-01
temperature at back of wall (eV)	= 6.666e-02
sensible internal energy (J/g)	= -7.453e+02
vaporization internal energy (J/g)	= 1.657e+02

current interface zone index (j-1)	= 58
fraction of interface zone vaporized	= 0.48099
fraction of interface zone condensed	= 0.51901

total mass vaporized (grams)	= 4.185e+04
current net vaporization rate (g/s)	= -1.112e+06

zone index	radius (cm)	zone width (cm)	temperature (eV)	internal energy (J/g)
58	5.0000160e+02	3.956e-04	6.712e-02	-8.097e+02
59	5.0000213e+02	5.256e-04	6.663e-02	-8.104e+02
60	5.0000282e+02	6.983e-04	6.558e-02	-8.120e+02
61	5.0000375e+02	9.276e-04	6.460e-02	-8.135e+02
62	5.0000498e+02	1.232e-03	6.424e-02	-8.140e+02
63	5.0000662e+02	1.637e-03	6.418e-02	-8.141e+02
64	5.0000880e+02	2.175e-03	6.418e-02	-8.141e+02
65	5.0001169e+02	2.889e-03	6.418e-02	-8.141e+02
66	5.0001552e+02	3.838e-03	6.418e-02	-8.141e+02
67	5.0002062e+02	5.099e-03	6.418e-02	-8.141e+02
68	5.0002740e+02	6.774e-03	6.418e-02	-8.141e+02
69	5.0003639e+02	8.999e-03	6.418e-02	-8.141e+02
70	5.0004835e+02	1.195e-02	6.418e-02	-8.141e+02
71	5.0006423e+02	1.588e-02	6.418e-02	-8.141e+02
72	5.0008532e+02	2.110e-02	6.418e-02	-8.141e+02
73	5.0011335e+02	2.802e-02	6.418e-02	-8.141e+02
74	5.0015057e+02	3.722e-02	6.418e-02	-8.141e+02
75	5.0020001e+02	4.944e-02	6.660e-02	-8.141e+02

behind condensed region

max over-pressure= 9.0646e+03 (j/cm3)   time= 1.0772e-08 (s)   cycle= 709

max heat flux= 4.1203e+08 (j/cm2*s)   time= 4.3099e-13 (s)   cycle= 203

instantaneous and integrated values at first wall

time(s)	pres(mpa)	e flx(w/cm2)	impulse(mpo-s)	t heat(j/cm2)	surf t(k)
6.8035e-10	3.4383e+02	2.3376e+06	2.3392e-07	1.5612e-02	0.
2.3348e-06	1.8403e-01	3.1260e+01	9.3214e-05	5.5094e-02	0.
0.					0.

time(s) (sec)	vaporized mass (g)	mass vaporization rate (g/s)
6.8035e-10	4.1850e+04	-3.1764e+06
2.3348e-06	4.1847e+04	-1.1119e+06
0.	0.	0.

122

Input for Sample Condensation Problem

```
c .... cavity and zoning parameters
      idelta=3
      jmax = 55
      jmn(1) = 2,  7
      jmx(1) = 6, 56
      isw( 4) = 13
      con(36) = 0.3285
      radius = 500.
c .... time step parameters
      nmax = 1000
      tmax = 1.e-1
      dtmax= 1.e-4
      dtb  = 1.0e-7
      tsctr= 0.20
      tsctn= 0.04
      tscc = 5.00
      tscv = 0.04
c .... background gas properties
      atw2b = 5(4.0), 70(172.)
      atn2b = 5(2.), 70(69.)
      vapmas = 1.24e-2, 30.0e3
      tn2c = 5(0.90), 70(0.66)
      tr2c = 5(0.40), 70(0.40)
      dn2b = 5(2.00e17), 70(2.00e17)
      tbc = 5.e-2
c .... new vaporization model variables
      isw(20) = 2
      con(31) = 1.
      con(32) = 1.
      nczons = 20
      rhocnd = 9.55
      cpheat = 1510.
      qheatv = 911.
      xkcond = 3030.
      tvap0 = 0.177
      twallb = 0.0666
      awfilm = 172.
      izfilm = 69
      tcn2c(6) = 70(0.0666)
      nmat = 2
c .... other parameters
      isw( 8) = 0
      isw(11) = 1
      nfg=20
c .... input/output variables
      isw(27) = 1
      io = 2(100) -1 -1 -1
      iobin = 1000
      isw( 5) = 500
      $
```

Output for Sample Condensation Problem

```
**********************************************************
*                                                        *
*   conrad - a code to compute the radiative transfer,   *
*   condensation & hydromotion of vapor                  *
*                                                        *
*   written by r. peterson, g. moses & j. macfarlane     *
*                                                        *
*   this code is under development                       *
*                                                        *
*   date of this version - 07/16/88                      *
*                                                        *
**********************************************************

spherical geometry - energy quantities are absolute

no. of zones........................            55
outer boundary(cm)..................    5.0000e+02
starting time(s)....................    0.
starting cycle......................
no. of time cycles..................          1000
max. problem time(s)................             1
time step for first 10 cycles(s)....    1.0000e-01
min. time step(s)...................    1.0000e-07
max. time step(s)...................    1.0000e-08
time step growth limit..............    1.0000e-04
time step control parameters........    1.5000e+00
   courant..........................    5.0000e+00
   percent v change.................    4.0000e-02
   percent tn change................    4.0000e-02
   percent er change................    2.0000e-01
   percent t change in film.........    5.0000e-02
   percent tbp change in film.......    5.0000e-02

temperature bc.(ev).................    5.0000e-02

primary output frequencies

hydrodynamics......  1000
energy.............  1000
number densities..     -1
short edit........     -1
multi-freq rad....     -1

binary output......  1000

intermediate variable frequencies - iedit
```

(1) -1	(2) -1	(3) -1	(4) -1	(5) -1	(6) -1	(7) -1	(8) -1	(9) -1	(10) -1
(11) -1	(12) -1	(13) -1	(14) -1	(15) -1	(16) -1	(17) -1	(18) -1	(19) -1	(20) -1
(21) -1	(22) -1	(23) -1	(24) -1	(25) -1	(26) -1	(27) -1	(28) -1	(29) -1	(30) -1
(31) -1	(32) -1	(33) -1	(34) -1	(35) -1	(36) -1	(37) -1	(38) -1	(39) -1	(40) -1
(41) -1	(42) -1	(43) -1	(44) -1	(45) -1	(46) -1	(47) -1	(48) -1	(49) -1	(50) -1
(51) -1	(52) -1	(53) -1	(54) -1	(55) -1	(56) -1	(57) -1	(58) -1	(59) -1	(60) -1
(61) -1	(62) -1	(63) -1	(64) -1	(65) -1	(66) -1	(67) -1	(68) -1	(69) -1	(70) -1
(71) -1	(72) -1	(73) -1	(74) -1	(75) -1	(76) -1	(77) -1	(78) -1	(79) -1	(80) -1
(81) -1	(82) -1	(83) -1	(84) -1	(85) -1	(86) -1	(87) -1	(88) -1	(89) -1	(90) -1
(91) -1	(92) -1	(93) -1	(94) -1	(95) -1	(96) -1	(97) -1	(98) -1	(99) -1	(100) -1

#	radius (cm)	zone width (cm)	mass dens (g/cm3)	mass (g/)	e density (1/cm3)	ion density (1/cm3)	r temp (ev)	ion temp (ev)	atomic wt (amu)	charge (esu)
0	0.									
1	6.1558e+00	6.1558e+00	1.3283e-06	1.2979e-03	7.2384e+08	2.0000e+17	4.0000e-01	9.0000e-01	4.0000e+00	3.6192e-09
2	8.1591e+00	8.0033e+00	1.3283e-06	1.7243e-03	7.2384e+08	2.0000e+17	4.0000e-01	9.0000e-01	4.0000e+00	3.6192e-09
3	9.8471e+00	1.6881e+00	1.3283e-06	2.2987e-03	7.2384e+08	2.0000e+17	4.0000e-01	9.0000e-01	4.0000e+00	3.6192e-09
4	1.1452e+01	1.6045e+00	1.3283e-06	3.0432e-03	7.2384e+08	2.0000e+17	4.0000e-01	9.0000e-01	4.0000e+00	3.6192e-09
5	1.3062e+01	1.6099e+00	1.3283e-06	4.0429e-03	7.2384e+08	2.0000e+17	4.0000e-01	9.0000e-01	4.0000e+00	3.6192e-09
6	1.3105e+01	4.3870e-02	5.7119e-05	5.3901e-03	7.5122e+16	2.0000e+17	4.0000e-01	6.6000e-01	1.7200e+02	3.7561e-01
7	1.3164e+01	5.8101e-02	5.7119e-05	7.1945e-03	7.5122e+16	2.0000e+17	4.0000e-01	6.6000e-01	1.7200e+02	3.7561e-01
8	1.3240e+01	7.6759e-02	5.7119e-05	9.6027e-03	7.5122e+16	2.0000e+17	4.0000e-01	6.6000e-01	1.7200e+02	3.7561e-01
9	1.3341e+01	1.0109e-01	5.7119e-05	1.2817e-02	7.5122e+16	2.0000e+17	4.0000e-01	6.6000e-01	1.7200e+02	3.7561e-01
10	1.3474e+01	1.3258e-01	5.7119e-05	1.7107e-02	7.5122e+16	2.0000e+17	4.0000e-01	6.6000e-01	1.7200e+02	3.7561e-01
11	1.3647e+01	1.7299e-01	5.7119e-05	2.2833e-02	7.5122e+16	2.0000e+17	4.0000e-01	6.6000e-01	1.7200e+02	3.7561e-01
12	1.3871e+01	2.2427e-01	5.7119e-05	3.0475e-02	7.5122e+16	2.0000e+17	4.0000e-01	6.6000e-01	1.7200e+02	3.7561e-01
13	1.4160e+01	2.8847e-01	5.7119e-05	4.0675e-02	7.5122e+16	2.0000e+17	4.0000e-01	6.6000e-01	1.7200e+02	3.7561e-01
14	1.4527e+01	3.6760e-01	5.7119e-05	5.4288e-02	7.5122e+16	2.0000e+17	4.0000e-01	6.6000e-01	1.7200e+02	3.7561e-01
15	1.4991e+01	4.6338e-01	5.7119e-05	7.2456e-02	7.5122e+16	2.0000e+17	4.0000e-01	6.6000e-01	1.7200e+02	3.7561e-01
16	1.5568e+01	5.7703e-01	5.7119e-05	9.6703e-02	7.5122e+16	2.0000e+17	4.0000e-01	6.6000e-01	1.7200e+02	3.7561e-01
17	1.6277e+01	7.0914e-01	5.7119e-05	1.2906e-01	7.5122e+16	2.0000e+17	4.0000e-01	6.6000e-01	1.7200e+02	3.7561e-01
18	1.7136e+01	8.5961e-01	5.7119e-05	1.7225e-01	7.5122e+16	2.0000e+17	4.0000e-01	6.6000e-01	1.7200e+02	3.7561e-01
19	1.8164e+01	1.0278e+00	5.7119e-05	2.2989e-01	7.5122e+16	2.0000e+17	4.0000e-01	6.6000e-01	1.7200e+02	3.7561e-01
20	1.9377e+01	1.2128e+00	5.7119e-05	3.0681e-01	7.5122e+16	2.0000e+17	4.0000e-01	6.6000e-01	1.7200e+02	3.7561e-01
21	2.0791e+01	1.4137e+00	5.7119e-05	4.0948e-01	7.5122e+16	2.0000e+17	4.0000e-01	6.6000e-01	1.7200e+02	3.7561e-01
22	2.2421e+01	1.6302e+00	5.7119e-05	5.4649e-01	7.5122e+16	2.0000e+17	4.0000e-01	6.6000e-01	1.7200e+02	3.7561e-01
23	2.4283e+01	1.8624e+00	5.7119e-05	7.2935e-01	7.5122e+16	2.0000e+17	4.0000e-01	6.6000e-01	1.7200e+02	3.7561e-01
24	2.6394e+01	2.1109e+00	5.7119e-05	9.7340e-01	7.5122e+16	2.0000e+17	4.0000e-01	6.6000e-01	1.7200e+02	3.7561e-01
25	2.8772e+01	2.3774e+00	5.7119e-05	1.2991e+00	7.5122e+16	2.0000e+17	4.0000e-01	6.6000e-01	1.7200e+02	3.7561e-01
26	3.1435e+01	2.6638e+00	5.7119e-05	1.7338e+00	7.5122e+16	2.0000e+17	4.0000e-01	6.6000e-01	1.7200e+02	3.7561e-01
27	3.4408e+01	2.9725e+00	5.7119e-05	2.3140e+00	7.5122e+16	2.0000e+17	4.0000e-01	6.6000e-01	1.7200e+02	3.7561e-01
28	3.7714e+01	3.3064e+00	5.7119e-05	3.0884e+00	7.5122e+16	2.0000e+17	4.0000e-01	6.6000e-01	1.7200e+02	3.7561e-01
29	4.1383e+01	3.6688e+00	5.7119e-05	4.1219e+00	7.5122e+16	2.0000e+17	4.0000e-01	6.6000e-01	1.7200e+02	3.7561e-01
30	4.5446e+01	4.0633e+00	5.7119e-05	5.5012e+00	7.5122e+16	2.0000e+17	4.0000e-01	6.6000e-01	1.7200e+02	3.7561e-01
31	4.9946e+01	4.4937e+00	5.7119e-05	7.3423e+00	7.5122e+16	2.0000e+17	4.0000e-01	6.6000e-01	1.7200e+02	3.7561e-01
32	5.4904e+01	4.9643e+00	5.7119e-05	9.7995e+00	7.5122e+16	2.0000e+17	4.0000e-01	6.6000e-01	1.7200e+02	3.7561e-01
33	6.0384e+01	5.4796e+00	5.7119e-05	1.3079e+01	7.5122e+16	2.0000e+17	4.0000e-01	6.6000e-01	1.7200e+02	3.7561e-01
34	6.6429e+01	6.0446e+00	5.7119e-05	1.7456e+01	7.5122e+16	2.0000e+17	4.0000e-01	6.6000e-01	1.7200e+02	3.7561e-01
35	7.3093e+01	6.6647e+00	5.7119e-05	2.3299e+01	7.5122e+16	2.0000e+17	4.0000e-01	6.6000e-01	1.7200e+02	3.7561e-01
36	8.0439e+01	7.3459e+00	5.7119e-05	3.1096e+01	7.5122e+16	2.0000e+17	4.0000e-01	6.6000e-01	1.7200e+02	3.7561e-01
37	8.8534e+01	8.0945e+00	5.7119e-05	4.1504e+01	7.5122e+16	2.0000e+17	4.0000e-01	6.6000e-01	1.7200e+02	3.7561e-01
38	9.7451e+01	8.9176e+00	5.7119e-05	5.5395e+01	7.5122e+16	2.0000e+17	4.0000e-01	6.6000e-01	1.7200e+02	3.7561e-01
39	1.0727e+02	9.8230e+00	5.7119e-05	7.3935e+01	7.5122e+16	2.0000e+17	4.0000e-01	6.6000e-01	1.7200e+02	3.7561e-01
40	1.1809e+02	1.0819e+01	5.7119e-05	9.8681e+01	7.5122e+16	2.0000e+17	4.0000e-01	6.6000e-01	1.7200e+02	3.7561e-01
41	1.3001e+02	1.1915e+01	5.7119e-05	1.3171e+02	7.5122e+16	2.0000e+17	4.0000e-01	6.6000e-01	1.7200e+02	3.7561e-01
42	1.4313e+02	1.3121e+01	5.7119e-05	1.7579e+02	7.5122e+16	2.0000e+17	4.0000e-01	6.6000e-01	1.7200e+02	3.7561e-01
43	1.5758e+02	1.4449e+01	5.7119e-05	2.3463e+02	7.5122e+16	2.0000e+17	4.0000e-01	6.6000e-01	1.7200e+02	3.7561e-01
44	1.7349e+02	1.5910e+01	5.7119e-05	3.1317e+02	7.5122e+16	2.0000e+17	4.0000e-01	6.6000e-01	1.7200e+02	3.7561e-01
45	1.9101e+02	1.7519e+01	5.7119e-05	4.1799e+02	7.5122e+16	2.0000e+17	4.0000e-01	6.6000e-01	1.7200e+02	3.7561e-01
46	2.1030e+02	1.9290e+01	5.7119e-05	5.5789e+02	7.5122e+16	2.0000e+17	4.0000e-01	6.6000e-01	1.7200e+02	3.7561e-01
47	2.3154e+02	2.1240e+01	5.7119e-05	7.4463e+02	7.5122e+16	2.0000e+17	4.0000e-01	6.6000e-01	1.7200e+02	3.7561e-01
48	2.5492e+02	2.3387e+01	5.7119e-05	9.9387e+02	7.5122e+16	2.0000e+17	4.0000e-01	6.6000e-01	1.7200e+02	3.7561e-01
49	2.8067e+02	2.5750e+01	5.7119e-05	1.3265e+03	7.5122e+16	2.0000e+17	4.0000e-01	6.6000e-01	1.7200e+02	3.7561e-01
50	3.0903e+02	2.8352e+01	5.7119e-05	1.7706e+03	7.5122e+16	2.0000e+17	4.0000e-01	6.6000e-01	1.7200e+02	3.7561e-01
51	3.4024e+02	3.1217e+01	5.7119e-05	2.3632e+03	7.5122e+16	2.0000e+17	4.0000e-01	6.6000e-01	1.7200e+02	3.7561e-01
52	3.7461e+02	3.4371e+01	5.7119e-05	3.1542e+03	7.5122e+16	2.0000e+17	4.0000e-01	6.6000e-01	1.7200e+02	3.7561e-01
53	4.1246e+02	3.7843e+01	5.7119e-05	4.2100e+03	7.5122e+16	2.0000e+17	4.0000e-01	6.6000e-01	1.7200e+02	3.7561e-01
54	4.5412e+02	4.1667e+01	5.7119e-05	5.6192e+03	7.5122e+16	2.0000e+17	4.0000e-01	6.6000e-01	1.7200e+02	3.7561e-01
55	5.0000e+02	4.5876e+01	5.7119e-05	7.5000e+03	7.5122e+16	2.0000e+17	4.0000e-01	6.6000e-01	1.7200e+02	3.7561e-01
				2.9907e+04						

#	r press (j/cm3)	ion press (j/cm3)	r int ene (j/)	ion int ene (j/)	velocity (cm/s)
0	1.1693e-07	2.8836e-02	3.4275e-04	4.2275e+01	0.
1	1.1693e-07	2.8836e-02	4.5535e-04	5.6160e+01	0.
2	1.1693e-07	2.8836e-02	6.0493e-04	7.4608e+01	0.
3	1.1693e-07	2.8836e-02	8.0365e-04	9.9117e+01	0.
4	1.1693e-07	2.8836e-02	1.0676e-03	1.3168e+02	0.
5	1.1693e-07	2.8836e-02	3.3103e-05	1.3310e+01	0.
6	1.1693e-07	2.9089e-02	4.4184e-05	1.7766e+01	0.
7	1.1693e-07	2.9089e-02	5.8974e-05	2.3713e+01	0.
8	1.1693e-07	2.9089e-02	7.8714e-05	3.1650e+01	0.
9	1.1693e-07	2.9089e-02	1.0506e-04	4.2244e+01	0.
10	1.1693e-07	2.9089e-02	1.4023e-04	5.6383e+01	0.
11	1.1693e-07	2.9089e-02	1.8716e-04	7.5254e+01	0.
12	1.1693e-07	2.9089e-02	2.4980e-04	1.0044e+02	0.
13	1.1693e-07	2.9089e-02	3.3340e-04	1.3406e+02	0.
14	1.1693e-07	2.9089e-02	4.4498e-04	1.7892e+02	0.
15	1.1693e-07	2.9089e-02	5.9389e-04	2.3879e+02	0.
16	1.1693e-07	2.9089e-02	7.9263e-04	3.1870e+02	0.
17	1.1693e-07	2.9089e-02	1.0579e-03	4.2535e+02	0.
18	1.1693e-07	2.9089e-02	1.4119e-03	5.6768e+02	0.
19	1.1693e-07	2.9089e-02	1.8843e-03	7.5763e+02	0.
20	1.1693e-07	2.9089e-02	2.5148e-03	1.0111e+03	0.
21	1.1693e-07	2.9089e-02	3.3562e-03	1.3495e+03	0.
22	1.1693e-07	2.9089e-02	4.4792e-03	1.8010e+03	0.
23	1.1693e-07	2.9089e-02	5.9780e-03	2.4037e+03	0.
24	1.1693e-07	2.9089e-02	7.9784e-03	3.2080e+03	0.
25	1.1693e-07	2.9089e-02	1.0648e-02	4.2814e+03	0.
26	1.1693e-07	2.9089e-02	1.4211e-02	5.7141e+03	0.
27	1.1693e-07	2.9089e-02	1.8967e-02	7.6263e+03	0.
28	1.1693e-07	2.9089e-02	2.5314e-02	1.0178e+04	0.
29	1.1693e-07	2.9089e-02	3.3785e-02	1.3585e+04	0.
30	1.1693e-07	2.9089e-02	4.5092e-02	1.8131e+04	0.
31	1.1693e-07	2.9089e-02	6.0183e-02	2.4198e+04	0.
32	1.1693e-07	2.9089e-02	8.0324e-02	3.2297e+04	0.
33	1.1693e-07	2.9089e-02	1.0721e-01	4.3106e+04	0.
34	1.1693e-07	2.9089e-02	1.4309e-01	5.7532e+04	0.
35	1.1693e-07	2.9089e-02	1.9097e-01	7.6788e+04	0.
36	1.1693e-07	2.9089e-02	2.5489e-01	1.0249e+05	0.
37	1.1693e-07	2.9089e-02	3.4020e-01	1.3679e+05	0.
38	1.1693e-07	2.9089e-02	4.5407e-01	1.8257e+05	0.
39	1.1693e-07	2.9089e-02	6.0604e-01	2.4368e+05	0.
40	1.1693e-07	2.9089e-02	8.0888e-01	3.2524e+05	0.
41	1.1693e-07	2.9089e-02	1.0796e+00	4.3410e+05	0.
42	1.1693e-07	2.9089e-02	1.4410e+00	5.7939e+05	0.
43	1.1693e-07	2.9089e-02	1.9233e+00	7.7332e+05	0.
44	1.1693e-07	2.9089e-02	2.5670e+00	1.0322e+06	0.
45	1.1693e-07	2.9089e-02	3.4263e+00	1.3776e+06	0.
46	1.1693e-07	2.9089e-02	4.5731e+00	1.8388e+06	0.
47	1.1693e-07	2.9089e-02	6.1038e+00	2.4542e+06	0.
48	1.1693e-07	2.9089e-02	8.1468e+00	3.2757e+06	0.
49	1.1693e-07	2.9089e-02	1.0874e+01	4.3721e+06	0.
50	1.1693e-07	2.9089e-02	1.4513e+01	5.8356e+06	0.
51	1.1693e-07	2.9089e-02	1.9371e+01	7.7889e+06	0.
52	1.1693e-07	2.9089e-02	2.5855e+01	1.0396e+07	0.
53	1.1693e-07	2.9089e-02	3.4510e+01	1.3876e+07	0.
54	1.1693e-07	2.9089e-02	4.6061e+01	1.8520e+07	0.
55	1.1693e-07	2.9089e-02	1.8367e+02	7.3851e+07	0.

Initial properties of the condensed region

zone index	radius (cm)	zone width (cm)	mass (grams)	integrated mass (g)	temperature (ev)
56	5.0000033e+02	3.337e-04	1.001e+04	1.001e+04	6.660e-02
57	5.0000078e+02	4.454e-04	1.336e+04	2.337e+04	6.660e-02
58	5.0000137e+02	5.945e-04	1.784e+04	4.121e+04	6.660e-02
59	5.0000217e+02	7.935e-04	2.381e+04	6.501e+04	6.660e-02
60	5.0000323e+02	1.059e-03	3.177e+04	9.679e+04	6.660e-02
61	5.0000464e+02	1.414e-03	4.241e+04	1.392e+05	6.660e-02
62	5.0000653e+02	1.887e-03	5.661e+04	1.958e+05	6.660e-02
63	5.0000904e+02	2.518e-03	7.555e+04	2.714e+05	6.660e-02
64	5.0001241e+02	3.361e-03	1.008e+05	3.722e+05	6.660e-02
65	5.0001689e+02	4.486e-03	1.346e+05	5.068e+05	6.660e-02
66	5.0002288e+02	5.988e-03	1.797e+05	6.865e+05	6.660e-02
67	5.0003087e+02	7.992e-03	2.398e+05	9.262e+05	6.660e-02
68	5.0004154e+02	1.067e-02	3.201e+05	1.246e+06	6.660e-02
69	5.0005577e+02	1.424e-02	4.272e+05	1.674e+06	6.660e-02
70	5.0007477e+02	1.900e-02	5.702e+05	2.244e+06	6.660e-02
71	5.0010013e+02	2.536e-02	7.611e+05	3.005e+06	6.660e-02
72	5.0013398e+02	3.384e-02	1.016e+06	4.021e+06	6.660e-02
73	5.0017914e+02	4.517e-02	1.356e+06	5.377e+06	6.660e-02
74	5.0023941e+02	6.027e-02	1.810e+06	7.186e+06	6.660e-02
75	5.0031984e+02	8.043e-02	2.416e+06	9.602e+06	6.660e-02

Total mass of condensed region (grams) = 9.602e+06

coefficients used in conrad = con

ion thermal cond.........(1)	1.2175e+02	2-t r thermal cond......(2)	1.0000e+10
rad. eq. cond............(3)	1.0000e-01	flux limit epsilon term.(4)	1.0000e-30
const log lambda.........(5)	0.	4*sigma/c...............(6)	1.3713e-05
2-t plasma emiss. coef...(7)	4.1138e+05	2-t plasma absorp. coef.(8)	3.0000e+10
ion press(i.gas).........(9)	1.6020e-19	r flux limit...........(10)	3.0000e+10
(11)	0.	ion press deriv(i.gas).(12)	1.6020e-19
ion int energy(i.gas)...(13)	0.	ion sp heat(i.gas).....(14)	2.4030e-19
up-stream ave parameter.(15)	2.4030e-19	rad sp. energy coef....(16)	1.3713e-05
(17)	0.	ion shock heating......(18)	1.0000e+00
(19)	0.	(20)	
artificial viscosity....(21)	1.4140e+00	multi-freq rad absorption(22)	3.0000e+10
multi-freq rad emission.(23)	6.3349e+04	multi-freq rad conduct.(24)	1.0000e+10
multi-freq rad flux lim.(25)	3.0000e+10	min init m-f rad energy.(26)	1.0000e-20
(27)	0.	(28)	
vap. rate multiplier....(29)	0.	Boltzman const (MJ/K)...(30)	1.3810e-29
vap/cond flux term......(31)	1.0000e+00	condensation rate mult.(32)	1.0000e+00
chrg exch x-section mult.(33)	0.	non-condensable gas term.(34)	3.1200e+01
(35)	1.0000e+00	mass factor auto zoning.(36)	3.2850e-01
(37)	0.	(38)	0.
x-ray flux multiplier...(39)	0.	(40)	0.
ion thermal vel term....(41)	0.	(42)	0.
rel debris ion vel term.(43)	1.0000e+00	debris ion flux mult...(44)	1.0000e+00
(45)	2.0000e+00	(46)	0.
(47)	1.0000e+00	(48)	0.
(49)	0.	(50)	0.

```
          calculation options used in conrad - isw

radiation temperature op.( 1)    0        no. of const time steps..( 2)   10
                         ( 3)    0        automatic zoning.........( 4)   13
freq of wall output......( 5)  500        hydrodynamic motion......( 6)    0
                         ( 7)    0        ion deposition source....( 8)    0
                         ( 9)    0        freq. of dtb calculation.(10)    1
automatic xray deposition(11)    1        eqn of state option......(12)    0
no. freq. gr. sub-divns..(13)    0        arbitrary radiation opc..(14)    0
arbitrary rosseland opc..(15)    0        allow flowtrace..........(16)    0
dynamic rezoning.........(17)    0                                 (18)    0
                         (19)    0        mass trans calc..........(20)    2
momentum exch w film.....(21)    0        energy exch with film....(22)    0
                         (23)    0        adjust temp in rezoning..(24)    0
ablation model choice....(25)    0        kinetic vapor model......(26)    0
eos and opacity data.....(27)    1        eos interpolation........(28)    0
                         (29)    0        variable film properties.(30)    0
t-dep debris ion calc....(31)    0        add db ion mass to vap...(32)    0
                         (33)    0                                 (34)    0
                         (35)    0                                 (36)    0
                         (37)    0                                 (38)    0
                         (39)    0                                 (40)    0
                         (41)    0                                 (42)    0
                         (43)    0                                 (44)    0
                         (45)    0                                 (46)    0
                         (47)    0                                 (48)    0
                         (49)    0                                 (50)    0


          equation of state table indices

          density slope........   1.0000e+00
          density base.........   1.4000e+01
          temperature slope....   2.5000e-01
          temperature base.....  -3.9794e-01
          min density(1/cm3)...   1.0000e+14
          max density(1/cm3)...   1.0000e+23
          min temperature(ev)..   4.0000e-01
          max temperature(ev)..   2.2494e+04


          header records from equation of state files:

material # 1
          IONMIX calculation performed on date  03/29/88   at time   21:01:09
atomic #s of gases:      2
relative fractions:   1.00e+00

material # 2
          IONMIX calculation performed on date  02/01/88   at time   18:09:35
atomic #s of gases:      3    82
relative fractions:   1.70e-01  8.30e-01

material #s for zones:
 1 1 1 1 1 2 2 2 2 2 2 2 2 2 2 2 2 2 2 2 2 2 2 2 2 2 2 2 2 2 2 2 2 2 2 2 2 2 2 2
 2 2 2 2 2 2 2 2 2 2 2 2 2 2 2 2 2 2 2 2 2 2 2 2 2 2 2 2 2 2 2 2 2 2 2 2 2 2

          radiation group structure

    0

    0
```

#	lower bd (ev)	upper bd (ev)	ave (ev)
1	1.0000e-01	3.1600e-01	2.0800e-01
2	3.1600e-01	1.0000e+00	6.5800e-01
3	1.0000e+00	1.5800e+00	1.2900e+00
4	1.5800e+00	2.5100e+00	2.0450e+00
5	2.5100e+00	3.9700e+00	3.2400e+00
6	3.9700e+00	6.2900e+00	5.1300e+00
7	6.2900e+00	1.0000e+01	8.1450e+00
8	1.0000e+01	1.5800e+01	1.2900e+01
9	1.5800e+01	2.5100e+01	2.0450e+01
10	2.5100e+01	3.9700e+01	3.2400e+01
11	3.9700e+01	6.2900e+01	5.1300e+01
12	6.2900e+01	1.0000e+02	8.1450e+01
13	1.0000e+02	1.7800e+02	1.3900e+02
14	1.7800e+02	3.1600e+02	2.4700e+02
15	3.1600e+02	5.6200e+02	4.3900e+02
16	5.6200e+02	1.0000e+03	7.8100e+02
17	1.0000e+03	3.1600e+03	2.0800e+03
18	3.1600e+03	1.0000e+04	6.5800e+03
19	1.0000e+04	1.0000e+05	5.5000e+04
20	1.0000e+05	1.0000e+06	5.5000e+05

0

#	rad temp (ev)	rad energy (j/g)	rad press (j/cm3)
1	4.0000e-01	3.5079e-07	1.1693e-07
2	4.0000e-01	3.5079e-07	1.1693e-07
3	4.0000e-01	3.5079e-07	1.1693e-07
4	4.0000e-01	3.5079e-07	1.1693e-07
5	4.0000e-01	3.5079e-07	1.1693e-07
6	4.0000e-01	3.5079e-07	1.1693e-07
7	4.0000e-01	3.5079e-07	1.1693e-07
8	4.0000e-01	3.5079e-07	1.1693e-07
9	4.0000e-01	3.5079e-07	1.1693e-07
10	4.0000e-01	3.5079e-07	1.1693e-07
11	4.0000e-01	3.5079e-07	1.1693e-07
12	4.0000e-01	3.5079e-07	1.1693e-07
13	4.0000e-01	3.5079e-07	1.1693e-07
14	4.0000e-01	3.5079e-07	1.1693e-07
15	4.0000e-01	3.5079e-07	1.1693e-07
16	4.0000e-01	3.5079e-07	1.1693e-07
17	4.0000e-01	3.5079e-07	1.1693e-07
18	4.0000e-01	3.5079e-07	1.1693e-07
19	4.0000e-01	3.5079e-07	1.1693e-07
20	4.0000e-01	3.5079e-07	1.1693e-07
21	4.0000e-01	3.5079e-07	1.1693e-07
22	4.0000e-01	3.5079e-07	1.1693e-07
23	4.0000e-01	3.5079e-07	1.1693e-07
24	4.0000e-01	3.5079e-07	1.1693e-07
25	4.0000e-01	3.5079e-07	1.1693e-07
26	4.0000e-01	3.5079e-07	1.1693e-07
27	4.0000e-01	3.5079e-07	1.1693e-07
28	4.0000e-01	3.5079e-07	1.1693e-07
29	4.0000e-01	3.5079e-07	1.1693e-07
30	4.0000e-01	3.5079e-07	1.1693e-07
31	4.0000e-01	3.5079e-07	1.1693e-07
32	4.0000e-01	3.5079e-07	1.1693e-07
33	4.0000e-01	3.5079e-07	1.1693e-07
34	4.0000e-01	3.5079e-07	1.1693e-07

#	radius (cm)	zone width (cm)	mass dens (g/cm3)	compression (vθ/v)	velocity (cm/s)	r temp (ev)	ion temp (ev)	r press (j/cm3)	ion press (j/cm3)	art visc (j/cm3)
0	0.				0.					
1	6.2180e+00	6.2180e+00	1.2888e-06	9.7026e-01	1.4166e+04	6.3699e-01	8.8496e-01	7.5255e-07	2.7513e-02	0.
2	8.2391e+00	2.0211e+00	1.2909e-06	9.7178e-01	-1.1115e+03	6.3699e-01	8.8752e-01	7.5255e-07	2.7636e-02	6.0222e-05
3	9.9262e+00	1.6871e+00	1.3060e-06	9.8319e-01	6.6884e+03	6.3699e-01	8.9319e-01	7.5255e-07	2.8139e-02	0.
4	1.1517e+01	1.5912e+00	1.3214e-06	9.9479e-01	5.9513e+03	6.3699e-01	8.9952e-01	7.5255e-07	2.8673e-02	0.
5	1.3119e+01	1.6014e+00	1.3221e-06	9.9529e-01	-1.7207e+04	6.3699e-01	9.0642e-01	7.5255e-07	2.8907e-02	1.4167e-04
6	1.3188e+01	6.8906e-02	3.5980e-05	6.2991e-01	3.8112e+03	6.3699e-01	6.3556e-01	7.5255e-07	1.7285e-02	0.
7	1.3239e+01	5.0853e-02	6.4484e-05	1.1289e+00	6.4157e+03	6.3699e-01	3.1743e-01	7.5256e-07	3.1743e-02	0.
8	1.3313e+01	7.3991e-02	5.8599e-05	1.0259e+00	-4.8534e+01	6.3699e-01	6.5382e-01	7.5257e-07	2.8867e-02	4.8768e-04
9	1.3411e+01	9.8489e-02	5.8003e-05	1.0155e+00	-3.7880e+02	6.3700e-01	6.5203e-01	7.5258e-07	2.8449e-02	1.2648e-06
10	1.3544e+01	1.3290e-01	5.6393e-05	9.8729e-01	1.7926e+03	6.3700e-01	6.5070e-01	7.5259e-07	2.7667e-02	0.
11	1.3718e+01	1.7433e-01	5.6092e-05	9.8201e-01	1.4188e+03	6.3700e-01	6.5019e-01	7.5261e-07	2.7577e-02	1.5672e-06
12	1.3933e+01	2.1497e-01	5.9014e-05	1.0332e+00	2.0032e+01	6.3700e-01	6.5061e-01	7.5263e-07	2.8919e-02	2.3079e-05
13	1.4226e+01	2.9233e-01	5.5853e-05	9.7784e-01	-1.0422e+03	6.3701e-01	6.5082e-01	7.5264e-07	2.7480e-02	1.2598e-05
14	1.4591e+01	3.6482e-01	5.7040e-05	9.9861e-01	1.7026e+01	6.3701e-01	6.5072e-01	7.5266e-07	2.7988e-02	0.
15	1.5046e+01	4.5538e-01	5.7659e-05	1.0094e+00	3.2940e+02	6.3701e-01	6.5045e-01	7.5269e-07	2.8296e-02	2.1736e-05
16	1.5613e+01	5.6662e-01	5.7790e-05	1.0117e+00	4.4145e+02	6.3702e-01	6.5072e-01	7.5271e-07	2.8348e-02	0.
17	1.6317e+01	7.0499e-01	5.7149e-05	1.0005e+00	6.4442e+02	6.3703e-01	6.5065e-01	7.5274e-07	2.8059e-02	0.
18	1.7169e+01	8.5184e-01	5.7387e-05	1.0047e+00	2.7846e+02	6.3703e-01	6.5066e-01	7.5276e-07	2.8170e-02	1.5366e-06
19	1.8188e+01	1.0189e+00	5.7431e-05	1.0055e+00	4.7339e+02	6.3704e-01	6.5068e-01	7.5276e-07	2.8188e-02	0.
20	1.9394e+01	1.2059e+00	5.7276e-05	1.0035e+00	2.3150e+02	6.3704e-01	6.5067e-01	7.5277e-07	2.8138e-02	6.7053e-07
21	2.0802e+01	1.4079e+00	5.7197e-05	1.0160e+00	2.1160e+02	6.3703e-01	6.5068e-01	7.5275e-07	2.8119e-02	0.
22	2.2429e+01	1.6266e+00	5.7170e-05	1.0014e+00	8.2291e+01	6.3703e-01	6.5068e-01	7.5273e-07	2.8083e-02	1.9121e-07
23	2.4288e+01	1.8597e+00	5.7180e-05	1.0009e+00	1.0854e+02	6.3702e-01	6.5067e-01	7.5270e-07	2.8069e-02	0.
24	2.6396e+01	2.1081e+00	5.7134e-05	1.0011e+00	6.4956e+01	6.3701e-01	6.5066e-01	7.5265e-07	2.8073e-02	2.1720e-08
25	2.8773e+01	2.3765e+00	5.7116e-05	1.0003e+00	2.2284e+01	6.3700e-01	6.5065e-01	7.5258e-07	2.8051e-02	2.0800e-08
26	3.1437e+01	2.6637e+00	5.7115e-05	9.9996e-01	1.5356e+01	6.3698e-01	6.5063e-01	7.5249e-07	2.8042e-02	5.4915e-10
27	3.4409e+01	2.9725e+00	5.7115e-05	9.9993e-01	1.5729e+01	6.3696e-01	6.5061e-01	7.5239e-07	2.8039e-02	0.
28	3.7715e+01	3.3064e+00	5.7114e-05	9.9992e-01	1.6617e+01	6.3689e-01	6.5059e-01	7.5225e-07	2.8037e-02	0.
29	4.1384e+01	3.6689e+00		9.9993e-01	1.7760e+01	6.3685e-01	6.5056e-01	7.5208e-07	2.8033e-02	0.
30	4.5448e+01	4.0634e+00		9.9992e-01	1.9190e+01	6.3685e-01	6.5053e-01	7.5188e-07	2.8030e-02	0.
31	4.9942e+01	4.4938e+00		9.9992e-01	2.0911e+01	6.3679e-01	6.5049e-01	7.5163e-07	2.8025e-02	0.

#			
35	4.0000e-01	3.5079e-07	1.1693e-07
36	4.0000e-01	3.5079e-07	1.1693e-07
37	4.0000e-01	3.5079e-07	1.1693e-07
38	4.0000e-01	3.5079e-07	1.1693e-07
39	4.0000e-01	3.5079e-07	1.1693e-07
40	4.0000e-01	3.5079e-07	1.1693e-07
41	4.0000e-01	3.5079e-07	1.1693e-07
42	4.0000e-01	3.5079e-07	1.1693e-07
43	4.0000e-01	3.5079e-07	1.1693e-07
44	4.0000e-01	3.5079e-07	1.1693e-07
45	4.0000e-01	3.5079e-07	1.1693e-07
46	4.0000e-01	3.5079e-07	1.1693e-07
47	4.0000e-01	3.5079e-07	1.1693e-07
48	4.0000e-01	3.5079e-07	1.1693e-07
49	4.0000e-01	3.5079e-07	1.1693e-07
50	4.0000e-01	3.5079e-07	1.1693e-07
51	4.0000e-01	3.5079e-07	1.1693e-07
52	4.0000e-01	3.5079e-07	1.1693e-07
53	4.0000e-01	3.5079e-07	1.1693e-07
54	4.0000e-01	3.5079e-07	1.1693e-07
55	4.0000e-01	3.5079e-07	1.1693e-07

Note: This page is a rotated (landscape) numerical data listing. The upper block is a continuation data table (rows 32–54) whose column headers are not printed on this page; the lower block carries the column headers.

Upper table (rows 32–54)

#										
32	5.4906e+01	4.9644e+00	5.7114e-05	9.9992e-01	2.2956e+01	6.3673e-01	6.5043e-01	7.5131e-07	2.8019e-02	0.
33	6.0386e+01	5.4797e+00	5.7114e-05	9.9992e-01	2.5291e+01	6.3665e-01	6.5037e-01	7.5093e-07	2.8012e-02	0.
34	6.6430e+01	6.0448e+00	5.7114e-05	9.9992e-01	2.8012e+01	6.3655e-01	6.5029e-01	7.5046e-07	2.8004e-02	0.
35	7.3095e+01	6.6649e+00	5.7114e-05	9.9991e-01	3.1152e+01	6.3643e-01	6.5020e-01	7.4989e-07	2.7993e-02	0.
36	8.0442e+01	7.3461e+00	5.7114e-05	9.9991e-01	3.4782e+01	6.3628e-01	6.5008e-01	7.4919e-07	2.7980e-02	0.
37	8.8536e+01	8.0948e+00	5.7113e-05	9.9991e-01	3.8996e+01	6.3610e-01	6.4993e-01	7.4833e-07	2.7965e-02	0.
38	9.7454e+01	8.9180e+00	5.7113e-05	9.9990e-01	4.3920e+01	6.3587e-01	6.4976e-01	7.4727e-07	2.7945e-02	0.
39	1.0728e+02	9.8234e+00	5.7113e-05	9.9990e-01	4.9722e+01	6.3559e-01	6.4954e-01	7.4597e-07	2.7922e-02	0.
40	1.1810e+02	1.0819e+01	5.7112e-05	9.9989e-01	5.6626e+01	6.3525e-01	6.4927e-01	7.4435e-07	2.7892e-02	0.
41	1.3001e+02	1.1916e+01	5.7112e-05	9.9988e-01	6.4940e+01	6.3482e-01	6.4893e-01	7.4236e-07	2.7856e-02	0.
42	1.4313e+02	1.3122e+01	5.7111e-05	9.9987e-01	7.5091e+01	6.3429e-01	6.4851e-01	7.3987e-07	2.7811e-02	0.
43	1.5758e+02	1.4450e+01	5.7110e-05	9.9986e-01	8.7686e+02	6.3362e-01	6.4798e-01	7.3677e-07	2.7754e-02	0.
44	1.7350e+02	1.5912e+01	5.7108e-05	9.9984e-01	1.0360e+02	6.3278e-01	6.4731e-01	7.3287e-07	2.7682e-02	0.
45	1.9102e+02	1.7521e+01	5.7107e-05	9.9982e-01	1.2414e+02	6.3171e-01	6.4646e-01	7.2792e-07	2.7591e-02	0.
46	2.1031e+02	1.9292e+01	5.7104e-05	9.9978e-01	1.5132e+02	6.3034e-01	6.4536e-01	7.2162e-07	2.7475e-02	0.
47	2.3155e+02	2.1243e+01	5.7100e-05	9.9973e-01	1.8836e+02	6.2856e-01	6.4393e-01	7.1349e-07	2.7323e-02	0.
48	2.5494e+02	2.3391e+01	5.7093e-05	9.9966e-01	2.4075e+02	6.2620e-01	6.4202e-01	7.0285e-07	2.7125e-02	0.
49	2.8070e+02	2.5757e+01	5.7082e-05	9.9955e-01	3.1858e+02	6.2303e-01	6.3943e-01	6.8871e-07	2.6858e-02	0.
50	3.0906e+02	2.8364e+01	5.7060e-05	9.9936e-01	4.4279e+02	6.1863e-01	6.3581e-01	6.6945e-07	2.6491e-02	0.
51	3.4030e+02	3.1239e+01	5.6953e-05	9.9897e-01	6.7176e+02	6.1225e-01	6.3049e-01	6.4226e-07	2.5966e-02	0.
52	3.7476e+02	3.4451e+01	5.4184e-05	9.9709e-01	1.6108e+03	6.0227e-01	6.2203e-01	6.0142e-07	2.5134e-02	0.
53	4.1443e+02	3.9676e+01	5.4184e-05	9.4862e-01	1.5354e+04	5.8412e-01	6.0616e-01	5.3214e-07	2.2678e-02	0.
54	5.0000e+02	8.5568e+01	2.4925e-05	4.3638e-01	0.	5.3812e-01	5.7219e-01	3.8329e-07	9.6621e-03	1.1748e-03
			0.			0.	6.5994e-01	0.		

Lower table (rows 0–32)

#	r energy (j/)	ion energy (j/)	kin energy (j/)	r source (j/)	ion source (j/)	ion->r ex (j/)	flux lim (j/cm2-s)	heat flux (j/cm2-s)
0	2.2735e-03	4.1566e+01	0.	0.	0.	-3.3106e-05	7.5000e-11	0.
1	3.0157e-03	5.5380e+01	1.5161e-02	0.	0.	-4.4021e-05	7.5000e-11	0.
2	3.9598e-03	7.4043e+01	1.2401e-04	0.	0.	-5.8873e-05	7.5000e-11	0.
3	5.1992e-03	9.9064e+01	5.9652e-03	0.	0.	-7.8695e-05	7.5000e-11	0.
4	6.9037e-03	1.3262e+02	6.2744e-03	0.	0.	-1.0476e-04	7.5000e-11	0.
5	3.3822e-04	1.2621e+02	4.5698e-03	0.	0.	-2.0887e-01	7.5000e-11	0.
6	2.5189e-04	1.6798e+02	1.7285e-02	0.	0.	1.0494e-01	7.5000e-11	0.
7	3.6997e-04	2.2598e+02	1.3202e-06	0.	0.	2.6386e-02	7.5000e-11	0.
8	4.9890e-04	2.9998e+02	1.0734e-04	0.	0.	5.4896e-03	7.5000e-11	0.
9	6.8491e-04	4.0133e+02	3.2086e-03	0.	0.	-1.5239e-02	7.5000e-11	0.
10	9.1908e-04	5.3745e+02	2.6826e-03	0.	0.	1.1380e-03	7.5000e-11	0.
11	1.1660e-03	7.1150e+02	7.1378e-07	0.	0.	2.2615e-02	7.5000e-11	0.
12	1.6443e-03	9.5872e+02	2.5786e-03	0.	0.	1.1949e-02	7.5000e-11	0.
13	2.1490e-03	1.2728e+02	9.1853e-03	0.	0.	-1.6986e-02	7.5000e-11	0.
14	2.8376e-03	1.6979e+02	4.5887e-04	0.	0.	2.2381e-02	7.5000e-11	0.
15	3.7787e-03	2.2643e+02	1.0999e-03	0.	0.	1.0265e-02	7.5000e-11	0.
16	5.0999e-03	3.0284e+02	3.1282e-03	0.	0.	1.0848e-02	7.5000e-11	0.
17	6.7783e-03	4.0392e+02	7.7956e-04	0.	0.	1.9953e-02	7.5000e-11	0.
18	9.0398e-03	5.3896e+02	3.0068e-03	0.	0.	1.5072e-02	7.5000e-11	0.
19	1.2089e-02	7.1961e+02	9.5966e-04	0.	0.	2.3606e-02	7.5000e-11	0.
20	1.6145e-02	9.6049e+02	1.0701e-03	0.	0.	2.3424e-02	7.5000e-11	0.
21	2.1576e-02	1.2822e+03	2.1599e-04	0.	0.	3.0091e-02	7.5000e-11	0.
22	2.8808e-02	1.7113e+03	5.0153e-04	0.	0.	3.3602e-02	7.5000e-11	0.
23	3.8437e-02	2.2837e+03	2.3971e-04	0.	0.	4.5258e-02	7.5000e-11	0.
24	5.1337e-02	3.0482e+03	3.7653e-05	0.	0.	5.9588e-02	7.5000e-11	0.
25	6.8528e-02	4.0680e+03	2.3843e-05	0.	0.	7.7768e-02	7.5000e-11	0.
26	9.1449e-02	5.4288e+03	3.3412e-05	0.	0.	1.0324e-01	7.5000e-11	0.
27	1.2203e-01	7.2446e+03	4.9771e-05	0.	0.	1.3755e-01	7.5000e-11	0.
28	1.6283e-01	9.6674e+03	7.5883e-05	0.	0.	1.8333e-01	7.5000e-11	0.
29	2.1726e-01	1.2900e+04	1.1824e-04	0.	0.	2.4451e-01	7.5000e-11	0.
30	2.8987e-01	1.7213e+04	1.8738e-04	0.	0.	3.2636e-01	7.5000e-11	0.
31	3.8672e-01	2.2967e+04	3.0089e-04	0.	0.	4.3601e-01	7.5000e-11	0.

0

33	5.1589e-01	3.0643e+04	4.8828e-04	0.	5.8313e-01	7.5000e-11	0.
34	6.8811e-01	4.0881e+04	7.9947e-04	0.	7.8085e-01	7.5000e-11	0.
35	9.1771e-01	5.4534e+04	1.3197e-03	0.	1.0471e+00	7.5000e-11	0.
36	1.2237e+00	7.2739e+04	2.1957e-03	0.	1.4063e+00	7.5000e-11	0.
37	1.6314e+00	9.7007e+04	3.6838e-03	0.	1.8920e+00	7.5000e-11	0.
38	2.1743e+00	1.2935e+05	6.2369e-03	0.	2.5505e+00	7.5000e-11	0.
39	2.8970e+00	1.7243e+05	1.0669e-02	0.	3.4460e+00	7.5000e-11	0.
40	3.8584e+00	2.2980e+05	1.8468e-02	0.	4.6680e+00	7.5000e-11	0.
41	5.1360e+00	3.0615e+05	3.2420e-02	0.	6.3423e+00	7.5000e-11	0.
42	6.8322e+00	4.0767e+05	5.7857e-02	0.	8.6469e+00	7.5000e-11	0.
43	9.0808e+00	5.4254e+05	1.0530e-01	0.	1.1836e+01	7.5000e-11	0.
44	1.2056e+01	7.2147e+05	1.9619e-01	0.	1.6276e+01	7.5000e-11	0.
45	1.5983e+01	9.5843e+05	3.7598e-01	0.	2.2499e+01	7.5000e-11	0.
46	2.1149e+01	1.2715e+06	7.4558e-01	0.	3.1284e+01	7.5000e-11	0.
47	2.7911e+01	1.6836e+06	1.5419e+00	0.	4.3782e+01	7.5000e-11	0.
48	3.6701e+01	2.2235e+06	3.3622e+00	0.	6.1706e+01	7.5000e-11	0.
49	4.8006e+01	2.9253e+06	7.8582e+00	0.	8.7622e+01	7.5000e-11	0.
50	6.2294e+01	3.8260e+06	2.0262e+01	0.	1.2542e+02	7.5000e-11	0.
51	7.9799e+01	4.9559e+06	6.2244e+01	0.	1.8103e+02	7.5000e-11	0.
52	9.9925e+01	6.3046e+06	4.7771e+02	0.	2.6193e+02	7.5000e-11	0.
53	1.2404e+02	7.7350e+06	5.7926e+04	0.	3.2354e+02	7.5000e-11	0.
54	2.5922e+02	9.3293e+06	0.	0.	6.4978e+02	7.5000e-11	0.

Energy conservation check — units are (J/   )

Initial Energies

ion int E = 7.3851e+07
rad int E = 1.8367e+02
ion kin E = 0.
wall int E=-7.7819e+09

Current Energies

ion int E = 4.4110e+07
rad int E = 8.2361e+02
ion kin E = 5.8501e+04
wall int E=-7.7735e+09

Total Energy Exchanged

ion -> rad   = 8.4933e+06
rad -> wall   = 8.5077e+06
sorc -> ions = 0.
outr wal loss=-8.4682e-06
tot rad->wall= 8.5077e+06
wall E->vap E=-1.0569e+06
ph trans work=-2.0033e+06
ph trans heat=-1.5174e+06

E. Exchanged last time step

ion -> rad   = 1.8498e+03
rad -> wall   = 2.3486e+03
sorc -> ions = 0.
outr wal loss=-5.9585e-09
tot rad->wall= 2.3486e+03
wall E->vap E=-3.6418e+02
ph trans work=-4.5756e+02
ph trans heat=-5.2349e+02

Totals

Initial Energies

radiation   = 1.8367e+02
ion (int+KE) = 7.3851e+07
total cavity = 7.3851e+07
wall region =-7.7819e+09
wall + cavity=-7.7080e+09

Current Energies

radiation   = 8.2361e+02
ion (int+KE) = 4.4169e+07
total cavity = 4.4170e+07
wall region =-7.7735e+09
wall + cavity=-7.7293e+09

Initial minus Losses

radiation   =-1.4201e+04
ion (int+KE) = 6.4301e+07
total cavity = 6.4287e+07
wall region =-7.7743e+09
w.+c.-ph.tr.w=-7.7100e+09

Properties of wall material

heat capacity (J/g/eV)   = 1.510e+03
mass density (j/cm**3)   = 9.550e+00
heat of vaporization(J/g)   = 9.110e+02
thermal conductivity (J/cm/s/eV) = 3.030e+03

vaporization temperature at 1 bar (eV) = 1.770e-01
current vaporization temperature (eV) = 1.487e-01
temperature at back of wall (eV)   = 6.660e-02
sensible internal energy (J/g)   = -6.865e+02
vaporization internal energy (J/g)   = 2.245e+02

current interface zone index (j-1) = 55
fraction of interface zone vaporized = 0.77792
fraction of interface zone condensed = 0.22208

total mass vaporized (grams) = 2.824e+04
current net vaporization rate (g/s) = -6.385e+06

zone index	radius (cm)	zone width (cm)	temperature (eV)	internal energy (J/g)
55	5.0000000e+02	2.500e-04	9.605e-02	-7.660e+02
56	5.0000033e+02	3.337e-04	9.522e-02	-7.672e+02
57	5.0000078e+02	4.454e-04	9.413e-02	-7.689e+02
58	5.0000137e+02	5.945e-04	9.270e-02	-7.710e+02
59	5.0000217e+02	7.935e-04	9.085e-02	-7.738e+02
60	5.0000323e+02	1.059e-03	8.849e-02	-7.774e+02
61	5.0000464e+02	1.414e-03	8.554e-02	-7.818e+02
62	5.0000653e+02	1.887e-03	8.199e-02	-7.872e+02
63	5.0000904e+02	2.518e-03	7.795e-02	-7.933e+02
64	5.0001241e+02	3.361e-03	7.379e-02	-7.996e+02
65	5.0001689e+02	4.486e-03	7.018e-02	-8.050e+02
66	5.0002288e+02	5.988e-03	6.782e-02	-8.086e+02
67	5.0003087e+02	7.992e-03	6.684e-02	-8.101e+02
68	5.0004154e+02	1.067e-02	6.663e-02	-8.104e+02
69	5.0005577e+02	1.424e-02	6.660e-02	-8.104e+02
70	5.0007477e+02	1.900e-02	6.660e-02	-8.104e+02
71	5.0010013e+02	2.536e-02	6.660e-02	-8.104e+02
72	5.0013398e+02	3.384e-02	6.660e-02	-8.104e+02
73	5.0017914e+02	4.517e-02	6.660e-02	-8.104e+02
74	5.0023941e+02	6.027e-02	6.660e-02	-8.104e+02
75	5.0031984e+02	8.043e-02	6.660e-02	-8.104e+02

1 behind condensed region

0 max over-pressure= 2.9090e-02 (j/cm3)   time= 1.0000e-07 (s)   cycle=   1

0 max heat flux= 1.9288e+04 (j/cm2*s)   time= 1.0000e-07 (s)   cycle=   1

0 instantaneous and integrated values at first wall

0

time(s)	pres(mpa)	e flx(w/cm2)	impulse(mpa-s)	t heat(j/cm2)	surf t(k)
1.1771e-04	1.0809e-02	1.0770e+04	1.3947e-06	1.5047e+00	0.
2.4546e-04	9.6621e-03	8.3070e+03	2.6933e-06	2.7086e+00	0.
0.		0.	0.		0.

time(s) (sec)	vaporized mass (g)	mass vaporization rate (g/s)
1.1771e-04	2.9084e+04	-6.7828e+06
2.4546e-04	2.8244e+04	-6.3852e+06
0.	0.	0.